AD NUMBER

AD102536

NEW LIMITATION CHANGE

TO

Approved for public release, distribution unlimited

FROM

Distribution authorized to U.S. Gov't. agencies and their contractors; Administrative/Operational Use; JUN 1956. Other requests shall be referred to Wright Air Development Center, Wright-Patterson AFB, OH 45433.

AUTHORITY

AFWAL ltr dtd 17 Apr 1980

WADC TECHNICAL REPORT 55-13

A DESIGN MANUAL FOR REGENERATIVE HEAT EXCHANGERS OF THE ROTARY TYPE

HAROLD H. SOGIN
KAMAL-ELDIN HASSAN

ILLINOIS INSTITUTE OF TECHNOLOGY

JUNE 1956

WRIGHT AIR DEVELOPMENT CENTER

PAGES _____

ARE

MISSING

IN

ORIGINAL

DOCUMENT

WADC TECHNICAL REPORT 55-13

A DESIGN MANUAL FOR REGENERATIVE HEAT EXCHANGERS OF THE ROTARY TYPE

HAROLD H. SOGIN
KAMAL-ELDIN HASSAN

ILLINOIS INSTITUTE OF TECHNOLOGY

JUNE 1956

AERONAUTICAL RESEARCH LABORATORY
CONTRACT AF 33(616)-98
PROJECT 3066
TASK 70141

WRIGHT AIR DEVELOPMENT CENTER
AIR RESEARCH AND DEVELOPMENT COMMAND
UNITED STATES AIR FORCE
WRIGHT-PATTERSON AIR FORCE BASE, OHIO

Carpenter Litho & Prtg. Co., Springfield, O.
400 - June 1956

FOREWORD

This report was prepared by Dr. Harold H. Sogin and Mr. Kamal-Eldin Hassan on Contract AF 33(616)-98. They were assisted by Mr. Frederick Salzberg. The work was performed at the Heat Transfer Laboratory, Department of Mechanical Engineering, Illinois Institute of Technology, Chicago, Illinois. The work was administered by Dr. Max Jakob, Director, and, since his demise on January 4, 1955, by Mr. Stothe P. Kezios, Acting Director of the Heat Transfer Laboratory. The contract was issued from the Aeronautical Research Laboratory, Wright Air Development Center - Mr. Erich Soehngen was the task scientist for the laboratory. This work is further identified as Task 70141, "Transient Heat Transfer in Regenerators," under Project 3066, "Gas Turbine Technology."

ABSTRACT

This report deals with the thermal design of rotary type regenerative heat exchangers for aircraft gas turbine power plants. Hausen's regenerator theory is developed in a form directly applicable to the rotary machine, and deviations from some of the underlying assumptions are examined. A numerical method to calculate the performance of unbalanced regenerators is included, but this calculation is not required for application of the theory. Pressure drop and heat transfer data for flame trap and wire screen matrices are assembled. The effect of the regenerator performance on the thermodynamic cycle is discussed. Finally, a sample calculation is presented.

PUBLICATION REVIEW

This report has been reviewed and is approved.

FOR THE COMMANDER:

Aldro Lingard

ALDRO LINGARD
Chief, Aeronautical Research Laboratory
Directorate of Research

TABLE OF CONTENTS

Page

ABSTRACT iii

LIST OF TABLES ix

LIST OF ILLUSTRATIONS x

NOMENCLATURE xii

Chapter 1: INTRODUCTION

1-1 Purpose 1

1-2 Scope 1

1-3 Application of the Thermodynamic Regenerator 1

1-3.1 Thermodynamic Cycle of the Simple Gas Turbine Power Plant 1

1-3.2 Thermodynamic Gas Turbine Cycle with Regeneration 3

1-3.3 Evaluation of the Heat Exchanger Effectiveness in the Thermodynamic Cycle 3

1-4 Some Comparisons of Recuperative and Regenerative Heat Exchangers 5

1-4.1 Limitation of the Recuperator 5

1-4.2 Regenerator Core or Matrix 7

1-5 Regenerator Types 7

1-5.1 Axial or Disk Regenerators 8

1-5.2 Radial or Drum Regenerators 8

1-6 Leakage 8

1-6.1 Air-to-Gas Leakage through Clearance Spaces 10

1-6.2 Air-to-Air or Gas-to-Gas Leakage 10

1-6.3 Air-to-Gas Leakage through Matrix 10

1-6.4 Carry-Over Leakage 10

1-7 Other Design Considerations 10

Chapter 2: THEORY OF THE ROTATING REGENERATIVE HEAT EXCHANGER

2-1 Assumptions 12

2-1.1 Homogeneity 12

Page

2-1.2 Steady-State Operation 12
2-1.3 Uniform Temperatures of the Fluids at Entrances to the Matrix 12
2-1.4 Convection without Conduction 12
2-1.5 Constant Coefficients of Heat Transfer 13
2-1.6 Constant Density 13
2-2 Derivation of the Differential Equations 13
2-2.1 Thermal Energy Conveyed by the Fluid 14
2-2.2 Thermal Energy Conveyed by the Solid Material 14
2-2.3 Thermal Energy in the Carry-Over 16
2-2.4 Balance of the Transported Thermal Energy . . 16
2-2.5 Heat Exchange in the Elemental Volume of Space 16
2-2.6 The Differential Equations in Dimensionless Space Coordinates 17
2-3 Boundary Conditions 18
2-3.1 Difficulty of Formulating Boundary Conditions for the Actual Regenerator 18
2-3.2 Ideal Regenerator 19
2-3.3 Dimensionless Lengths 21
2-3.4 Boundary Conditions of the Ideal Regenerator 22
2-3.5 Comparison of the Ideal and Actual Regenerators 23
2-3.6 Single-Blow Problem 24
2-4 Solutions of the Regenerator Problem 25
2-5 Iliffe's Numerical Method 26
2-5.1 Nusselt's Integral Equations 26
2-5.2 Review of Simpson's Rule for Integration . . . 28
2-5.3 Application of Simpson's Rule to the Solution of the Integral Equations 29
2-5.4 Integration for m Even 31
2-5.5 Integration for m = 1 31
2-5.6 Integration for m = 3 32
2-5.7 Integration for m Odd and Greater than 3 . 33
2-5.8 Final Form of the Simultaneous Linear Albegraic Equations 33

Page

2-5.9 General Remarks regarding the Calculation Procedure 33

2-6 Numerical Calculation of Balanced Regenerators 37

2-7 Regenerator Effectiveness obtained from Numerical Calculations 37

2-8 Results of the Theory of the Balanced Regenerators . . 39

2-9 Unbalanced Regenerators 43

2-9.1 Use of Harmonic Means of Dimensionless Lengths 43

2-9.2 Use of Harmonic Mean of Effectiveness 43

2-10 Effect of Curvature in the Drum Type Matrix 43

2-11 Simplified Theories for Regenerators with Small Reduced Periods 44

2-12 Effect of Conductivity on Regenerator Performance . . 46

2-12.1 Conductivity in the x-Direction 46

2-12.2 Conductivity in the z-Direction 50

2-13 Effect of Leakage on Regenerator Performance 52

Chapter 3: PROPERTIES OF REGENERATOR MATRICES

3-1 Void and Solid Fractions 55

3-1.1 Flame Trap Matrices 55

3-1.2 Wire Screen Matrices 55

3-2 Heat Transfer Surface Area per Unit Volume 56

3-3 Free Area of Fluid Flow 56

3-4 Equivalent Diameter 57

3-5 Matrix Heat Capacity 58

3-6 Pressure Losses 58

3-6.1 Friction Factors for Flame Trap Matrices . . . 59

3-6.2 Friction Factors for Wire Screen Matrices . . 60

3-7 Heat Transfer 63

3-7.1 Coefficients of Heat Transfer for Flame Trap Matrices 64

3-7.2 Coefficients of Heat Transfer for Wire Screen Matrices 68

Page

Chapter 4: EFFECT OF REGENERATOR PERFORMANCE ON THE GAS TURBINE POWER PLANT

4-1 Actual Cycle of the Gas Turbine Power Plant 70
4-1.1 Actual Work of Compressor and Turbine 70
4-1.2 Pressure Losses 70
4-1.3 Leakage 72
4-2 Thermal Efficiency of the Actual Cycle 72
4-3 Evaluation of the Effects of Leakage and Pressure Drop 72
4-3.1 Effect of Leakage 73
4-3.2 Effect of Pressure Drop 73
4-4 Effects of Regenerator Speed, Length, and Mass Velocity 76
4-4.1 Effect of Regenerator Speed 76
4-4.2 Effect of Regenerator Length 76
4-4.3 Effect of Mass Velocity 79

Chapter 5: A DESIGN PROCEDURE

5-1 Preliminary Remarks 81
5-2 Statement of the Problem 81
5-3 Analysis of the Solution 83
5-4 Selection of the Matrix 83
5-5 Calculation of the Mean Inlet and Outlet Temperatures on the Cold and Hot Sides of the Regenerator 84
5-6 Evaluation of the Mean Temperature of Each Fluid . . . 85
5-7 Relationships Derived from the Correlation of Pressure Drop Data 86
5-8 Calculation of the Angle Subtended by the Ducts . . . 87
5-9 Relations Derived from the Correlations of Heat Transfer Data 88
5-10 Determination of the Utilization Factor in Terms of the Carry-Over 89
5-11 Results of the Sample Calculations 90
5-12 Final Remarks 91

REFERENCES. 93

Page

Appendix A: INFLUENCE OF CURVATURE IN DRUM TYPE MATRICES

A-1 General Remarks 97

A-2 Derivation of the Differential Equations 97

A-2.1 Thermal Energy Conveyed by the Fluid 97

A-2.2 Thermal Energy Conveyed by the Solid 97

A-2.3 Thermal Energy in the Carry-Over 99

A-2.4 Balance of the Transported Thermal Energy . . 99

A-2.5 Heat Exchange in the Elemental Volume of Space 99

A-2.6 The Differential Equations in Dimensionless Space Coordinates 100

A-3 Reduced Length and Reduced Period 100

A-4 Interpretation of the Modifications Caused by Curvature 101

Appendix B: WORK AND THERMAL EFFICIENCY OF AN ACTUAL REGENERATIVE GAS TURBINE CYCLE

B-1 General Remarks 104

B-2 Evaluation of Temperatures T_2, T_4, and T_A 104

B-3 Evaluation of the Heat Added to the Cycle 106

B-4 Net Work of the Cycle 106

B-5 Maximum Thermal Efficiency 106

LIST OF TABLES

Table		Page
3-1	Heat Transfer Correlations for Flame Trap Matrices (Ref. 15)	67
3-2	Constant C_2 to be Employed in Eq. 3-21 for Wire Screen Matrices (Ref. 15)	68
5-1	Given Design and Performance Conditions for the Illustrative Problem	82
5-2	Basic Geometric and Thermal Properties of the Assumed Matrix Material	84
5-3	Resume of Temperatures at the Regenerator Inlets and Outlets	85
5-4	Values of the Fluid Properties in the Illustrative Example	86
5-5	Results of the Calculations	91

LIST OF ILLUSTRATIONS

Figure		Page
1-1	Temperature-Entropy Diagram for Simple Gas Turbine Cycle	2
1-2	Regenerative Gas Turbine Power Plant	4
1-3	Efficiencies of Simple and Regenerative Gas Turbine Cycles	6
1-4	Disk Type Regenerator	9
1-5	Drum Type Regenerator	9
2-1	Nomenclature for the Plane Matrix Regenerator	15
2-2	Ideal Regenerator	20
2-3	Division of the Matrix for the Numerical Solution of Equations	30
2-4	Equations 2-55	34
2-5	Equations 2-56	35, 36
2-6	Effectiveness of Balanced Regenerators	40
2-7	Effectiveness of Balanced Regenerators	41
2-8	Performance Chart for Balanced Regenerators	42
2-9	Effect of Matrix Conductivity in Direction of Fluid Flow for Balanced Regenerators **(Deleted - See page 48)**	
2-10	Effect of Conduction along the Matrix on the Effectiveness of Thermally Balanced Regenerators with $\Pi = 0$	49
2-11	Regenerator with Matrix Composed of Ribbons	51
2-12	Effect of Leakage on Regenerator Effectiveness	53
3-1	Dimensions of Flame Trap Material of Reference 15	61
3-2	Friction Factors of Wire Screen Matrices (Ref. 15)	62
3-3	Limiting Nusselt Numbers for Rectangular Tubes with Uniform Heat Input	66
4-1	Temperature-Entropy Plane for a Real Regenerative Gas-Turbine Cycle	71
4-2	Effect of Fractional Leakage on a Gas Turbine Power Plant for Pressure Drop $\Delta p/p = 0.10$	74
4-3	Effect of Pressure Drop on a Gas Turbine Power Plant for Fractional Leakage $\Delta m/m = 0.05$	75

Figure		Page
4-4	Effect of Rotor Speed on Gas Turbine Power Plant Performance at Design-Point Conditions	77
4-5	Effect of Matrix Length on Gas Turbine Power Plant Performance at Design-Point Conditions	78
4-6	Effect of Rate of Mass Flow on Gas Turbine Power Plant Performance at Design-Point Conditions	80
A-1	Nomenclature for the Drum Type Regenerator	98

NOMENCLATURE

Note 1: The symbol F is used for the unit Fahrenheit degree (temperature difference). One Rankine degree is equal to one Fahrenheit degree; hence, the symbol F is also used for a degree on the absolute temperature scale. The symbol °F is used for the temperature, that is, the place on the Fahrenheit temperature scale.

Note 2: The prime (′), the double prime (″), and the triple prime (‴) are used with symbols C, m, q, and S to denote that the quantity refers to a unit of length, a unit of area, or a unit of volume, respectively.

Symbol	Quantity	Unit
A	facial area or cross sectional area of flow in duct	ft^2
C	heat capacity	B/F
C, C_1, C_2, C_3	constants	—
c_p	specific heat	B/lb F
D	wire diameter	in., ft
D_e	equivalent diameter (see Eq. 3-12)	ft
f	friction factor (see Eq. 3-16)	—
f	reduced temperature of the solid at inlet or outlet plane (see Eq. 2-34)	—
G	mass velocity	$lb/sec\ ft^2$
g	acceleration constant	ft/sec^2
g	a function	—
h	coefficient of heat transfer	$B/hr\ ft^2\ F$
$h_1, \ldots, h_4$	enthalpy	B/lb
K	fraction of circle subtended by ducts	—
K	kernel functions (see Eq. 2-39 and -41)	—
k	thermal conductivity	B/hr ft F
L	matrix length	ft
l	drum length	ft
m	rate of flow	lb/hr
m	index	—
N	number of divisions in numerical calculation	—
N	speed of rotation	sec^{-1}
N_{Nu}	Nusselt number, hD_e/k	—

Symbol	Quantity	Unit
N_{Pr}	Prandtl number, $\mu c_p/k$	—
N_{Re}	Reynolds number, $GD_e/(\alpha \cdot \mu)$	—
N_{St}	Stanton number, $\alpha \cdot h/Gc_p$	—
n	exponent	—
n	pitch	$in.^{-1}$, ft^{-1}
p	pressure	lb/ft^2
Q_a	heat added during the thermodynamic cycle	B/lb
q	rate of heat transfer	B/hr
R	gas constant	ft/F
r	radius	ft
r_p	pressure ratio	—
S	area of heat transfer surface	ft^2
T	absolute temperature	°R
t	temperature of solid	°F
U	utilization factor (see Eq. 2-20)	—
u	fluid velocity in x-direction	ft/hr
V	volume, relative volume	ft^3
v	matrix velocity in y-direction	ft/hr
W	work of cycle	B/lb
x	distance from entrance in direction of fluid motion	ft
Y,Y*	duct width (see Fig. 2-2)	ft
y,y*	distance solid particle moves in stream (see Fig. 2-2)	ft
α	ratio of free flow area to facial area	—
β	void fraction	—
γ	specific weight	lb/ft^3
Δ	increment of ξ	—
ϵ	dummy variable of integration	—
η	reduced time (see Eq. 2-17)	—
η_c	compressor efficiency	—
η_{Rec}	recuperator effectiveness	—
η_{Reg}	regenerator effectiveness	—

Symbol	Quantity	Unit
η_t	turbine efficiency	—
θ	temperature of gas	°F
κ	ratio of specific heats	—
Λ	reduced length (see Eq. 2-18)	—
μ	dynamic viscosity	lb/hr ft, lb/sec ft
ξ	reduced distance (see Eq. 2-10)	—
Π	reduced period	—
ρ	density	lb/ft^3
τ	time	hr
Φ	conduction parameter (see Eq. 2-77)	—
ϕ	variable angle	—
ω	speed of rotation	radians/sec

Subscripts

A	state point at air-side regenerator outlet in thermodynamic cycle
a	air side of regenerator
app	apparent
B	state point at gas-side regenerator outlet in thermodynamic cycle
b	bulk mean
g	gas side of regenerator
i	inside
m	mean
o	entrance; outside
opt	optimum
r	reduced; radial
s	solid

Chapter 1: INTRODUCTION

1-1 Purpose

The idea of regeneration to increase the thermal efficiency of a thermodynamic cycle is well known. Because some advantages of space and weight requirements have appeared in favor of the rotating regenerative heat exchanger, many investigators during the past decade have examined the possibilities of its application to gas turbine power plants of aircraft. The purpose of this report is to bring the present theoretical and experimental knowledge to a form which may be useful to designers interested in that application.

1-2 Scope

The report deals mainly with thermal design of the regenerator. The influence of the regenerator performance on the over-all thermodynamic cycle is considered. Heat transfer and pressure drop data are presented. Mechanical design, power plant arrangement, and the still incompletely solved problem of satisfactorily sealing the fluid streams are mentioned only insofar as they may have a bearing on the thermal design or performance calculations.

1-3 Application of the Thermodynamic Regenerator

In the next few sections some characteristics of thermodynamic regeneration are briefly reviewed by outlining the operation of a gas turbine cycle with and without regeneration and by comparing the performances of the two cases.

1-3.1 Thermodynamic Cycle of the Simple Gas Turbine Power Plant

The ideal thermodynamic cycle of a simple, open, gas turbine power plant is shown diagrammatically in the temperature-entropy plane of Fig. 1-1. The air at the atmospheric condition p_1, T_1 is compressed isentropically to state p_2, T_2. Then heat is added at constant pressure by burning fuel in the air until the gas attains the temperature T_3. The air is then expanded isentropically in a turbine to atmospheric pressure $p_4 = p_1$.

Manuscript released by the author in June 1955 for publication as a WADC Technical Report.

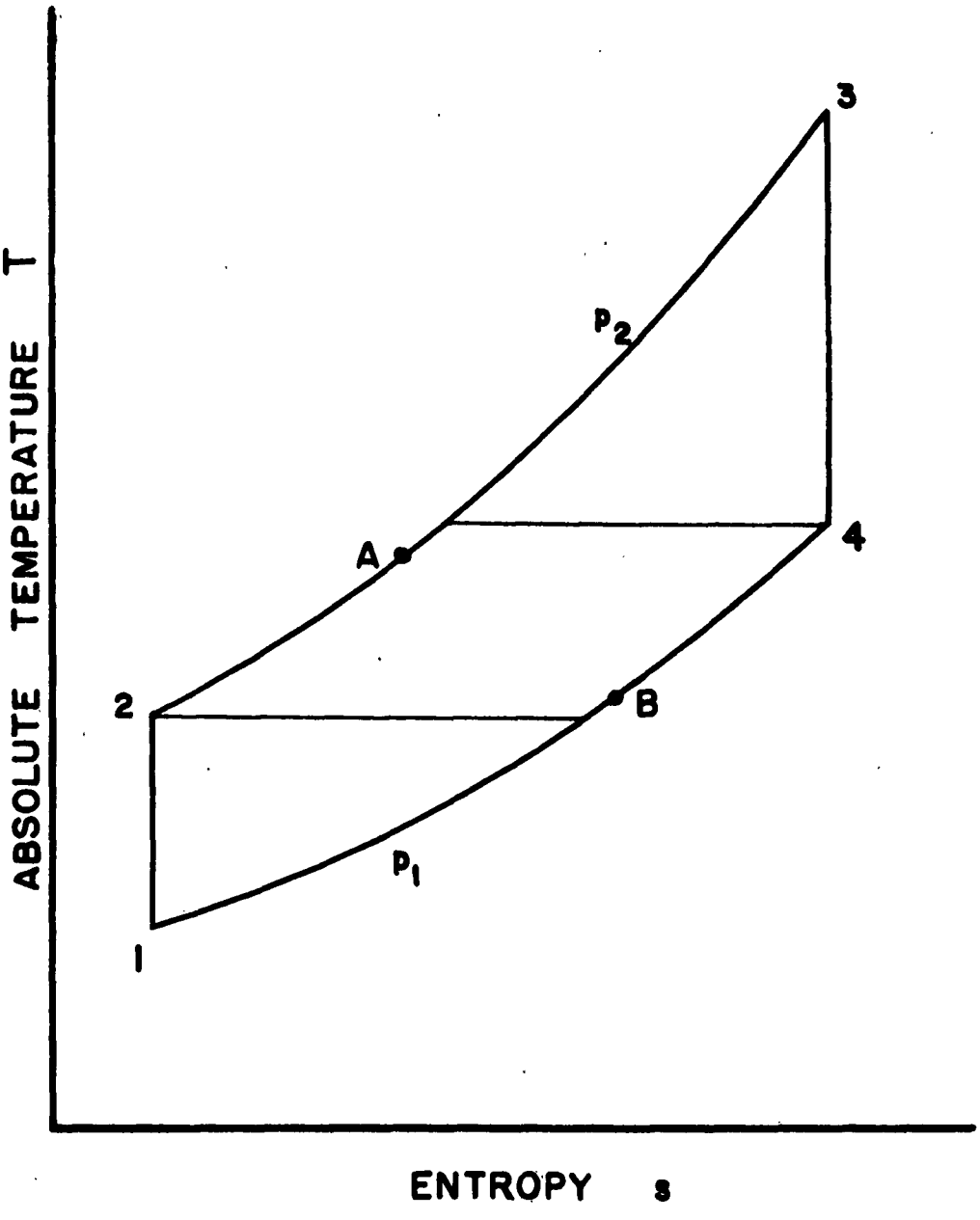

FIG. 1-1 TEMPERATURE – ENTROPY DIAGRAM FOR SIMPLE GAS TURBINE CYCLE

1-3.2 Thermodynamic Gas Turbine Cycle with Regeneration

A heat exchanger is now introduced to transfer some heat from the exhaust gases (Point 4) to the high-pressure air flowing from the compressor to the combustion chamber. This reduces the amount of fuel needed to bring the air to Point 3. A schematic flow diagram of a regenerative gas turbine power plant is shown in Fig. 1-2. The numbers and letters refer to the correspondingly labeled points in Fig. 1-1.

As can be seen in Fig. 1-1, the amount of heat transferred in the exchanger depends upon the difference between the temperatures T_4 and T_2. In the case of high pressure ratios (p_2/p_1), it can happen that $T_4 \leq T_2$ so that a heat exchanger would decrease the thermal efficiency. For this reason regeneration must not be introduced arbitrarily.

Further, with the addition of the heat exchanger to the power plant some inherent disadvantages must be considered. The size and weight of the plant increase, the pressure losses increase, and some compressed air leaks to the exhaust without passing through the turbine. The heat exchanger must do more than just compensate for these deleterious effects if its addition is to be worth while.

1-3.3 Evaluation of the Heat Exchanger Effectiveness in the Thermodynamic Cycle

The ideal amount of thermal energy that could be transferred per unit time from the exhaust gases to the relatively cold air is $m_a c_{p,a}(T_4 - T_2)$, subscript a referring to the cold air side of the heat exchanger, m being the rate of flow in lb/hr, and c_p an average specific heat in B/lb F. For practical reasons, the actual rate of heat transfer is $m_a c_{p,a}(T_A - T_2)$, where T_A is the actual temperature of the cold air leaving the heat exchanger (see Fig. 1-1 and -2). The ratio of the actual to the ideal rate is called the heat exchanger effectiveness. Accordingly,

$$\eta_{ex} = \frac{T_A - T_2}{T_4 - T_2} \qquad (1\text{-}1)$$

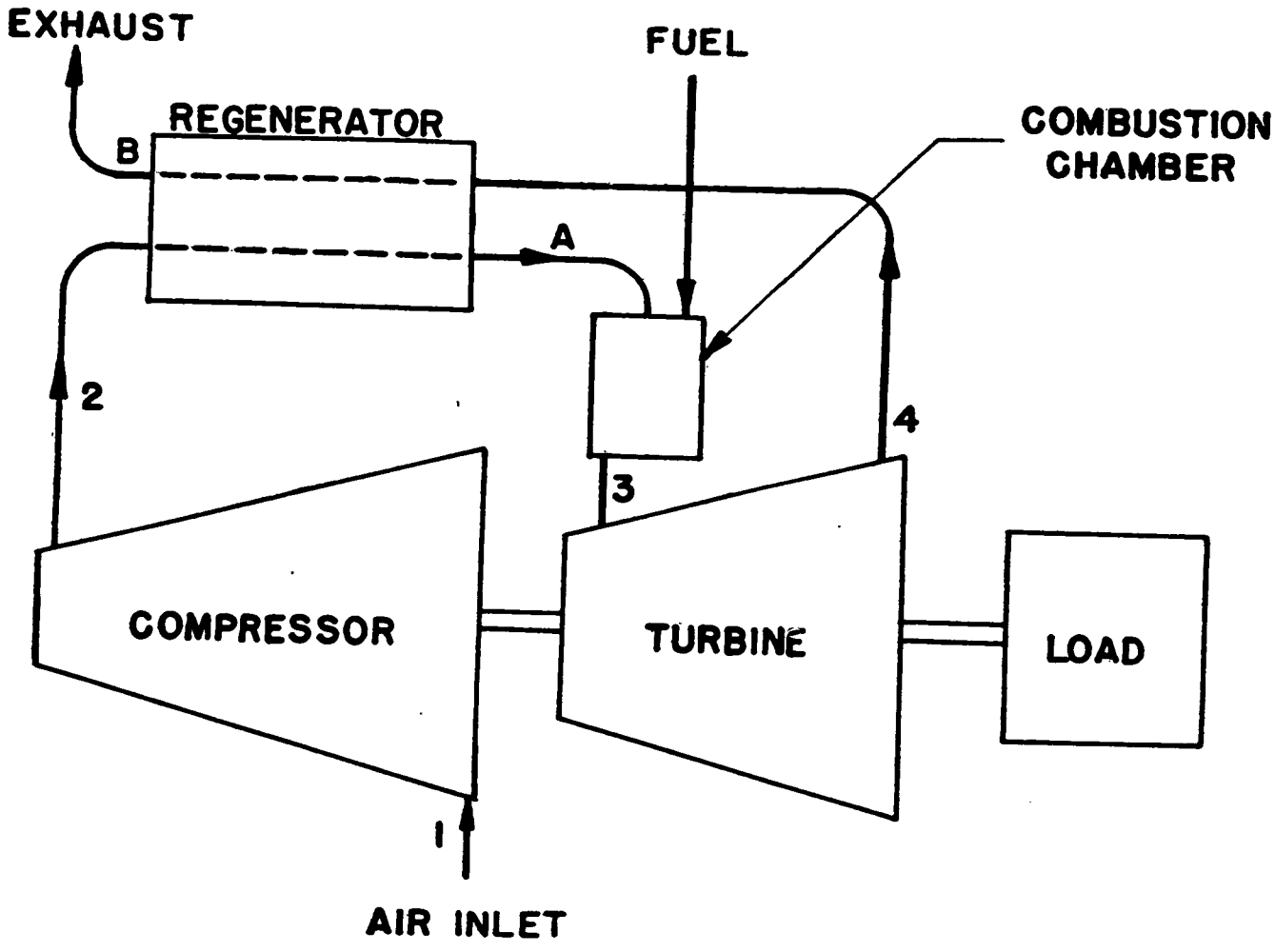

FIG. 1-2 REGENERATIVE GAS TURBINE POWER PLANT

Schmitt (Ref. 26) calculated the influence of regeneration on the thermal efficiency of a gas turbine power plant operating as follows:

Air inlet temperature,	$t_1 = -58°F$ or	$T_1 = 402°R$
Maximum cycle temperature,	$t_3 = 1832°F$ or	$T_3 = 2292°R$
Heat exchanger effectiveness,		$\eta_{ex} = 0.7$
Compressor efficiency,[1]		$\eta_c = 0.85$
Turbine efficiency,[1]		$\eta_t = 0.82$

The results of the calculations are shown graphically in Fig. 1-3. Obviously, regeneration is most practical at low pressure ratios, as has already been mentioned. If the heat exchanger effectiveness would be increased, the maximum thermal efficiency of the cycle would be increased and translated to a lower value of the pressure ratio, as is indicated by the trend of the curves in Fig. 1-3.

One way to increase the heat exchanger effectiveness is to increase its size. However, there is an optimum value of η_{ex} beyond which a gain in cycle efficiency cannot be made without excessive increases of size and weight of the power plant. This optimum depends upon the heat exchanger.

1-4 Some Comparisons of Recuperative and Regenerative Heat Exchangers

In this report the conventional heat exchanger of the shell-and-tube type is called a "recuperator" and the rotating or Ljungstroem type is called a "regenerator". The term, "regenerator", is used here apart from its meaning in the science of thermodynamics. Where ambiguity may arise the longer expression, "regenerative heat exchanger", is employed.

1-4.1 Limitation of the Recuperator

It has been shown that the smallest recuperators to meet a specified performance are obtained by using large numbers of tubes having small diameter (see, for example, Ref. 28). One of the main reasons is that in fine passages the flow becomes laminar, in which case the required

[1] The compressor and turbine efficiencies are defined in Chapter 4.

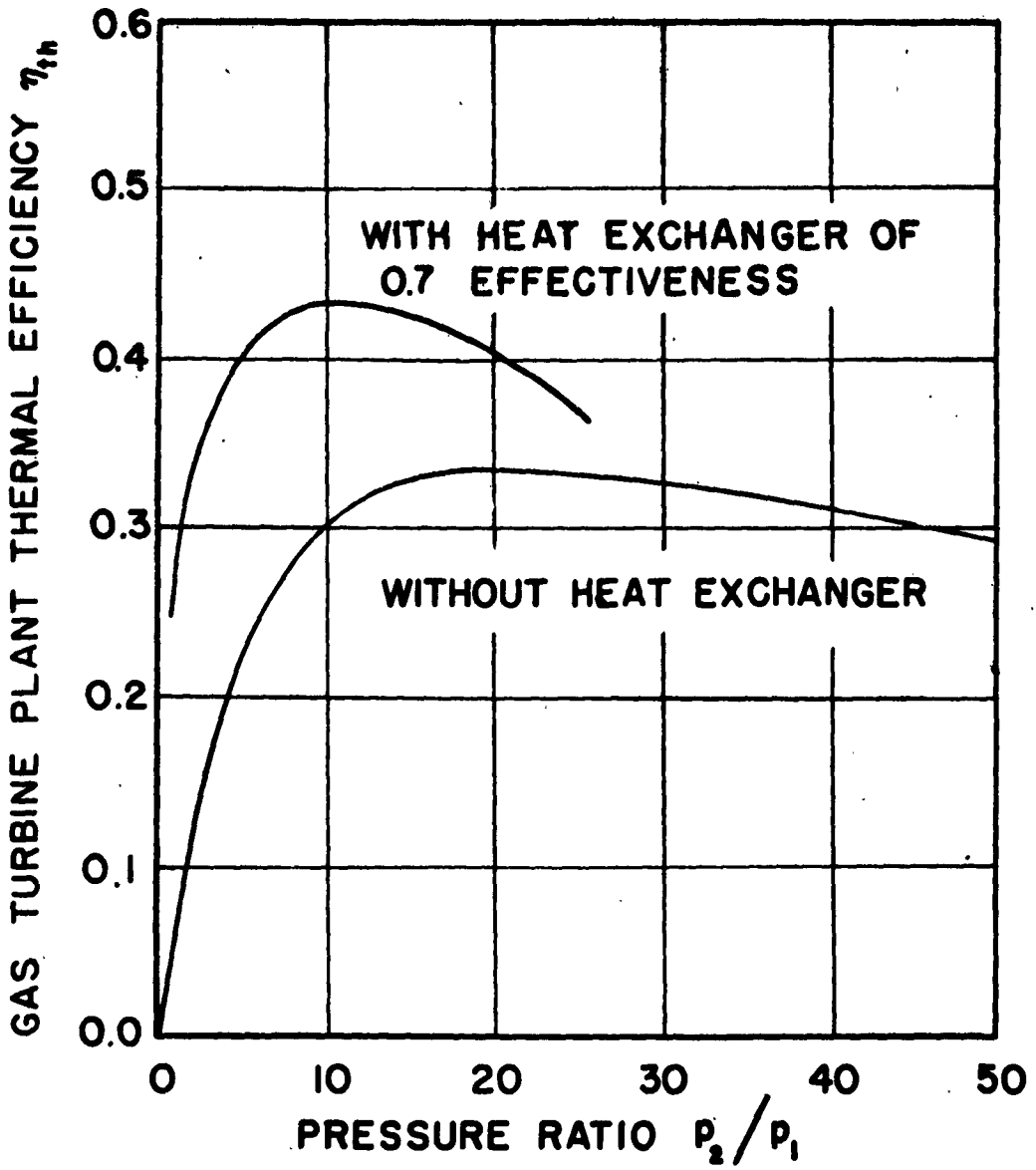

FIG. 1-3 EFFICIENCIES OF SIMPLE AND REGENERATIVE GAS TURBINE CYCLES

core size diminishes much more rapidly with the Reynolds number than in the case of turbulent flow. A practical limit of the tube size is set by constructional difficulties in separating the two fluids inside the recuperator core and in providing headers or tube sheets; also, operational difficulties arise on account of fouling and cleaning.

1-4.2 Regenerator Core or Matrix

In the regenerator core the constructional difficulties can be avoided. Well defined passages are unnecessary, for the two fluids are allowed to occupy the same space at different times. The heat is exchanged primarily by virtue of the matrix capacity for heat storage rather than by its nature to conduct heat. Hence, the size of the passages may be considerably reduced, and a compact and relatively light weight core, or matrix, can be obtained. Since seals within the matrix are unnecessary, any heterogeneously packed, permeable solid can be employed. Thus, the matrix may be constructed from layers of wire gauze or screens, odd shapes of braided wires and ceramic fibers, as well as various types and shapes of crimped ribbons and tubular packings. There is some evidence (Ref. 15) indicating that no appreciable amounts of soot build up inside of the passages of these matrices, and so the above mentioned operational difficulties may be avoided.

1-5 Regenerator Types

The matrix of the regenerator is exposed to the hot fluid for some time during which its temperature rises. Then it is exposed to the cold fluid which takes away the amount of heat that had been stored during the heating period. This process repeats itself in a cyclic way. In applications of the steel and liquefaction industries, the regenerators are built with two matrices which are alternately heated and cooled by switching the fluids with valves. The important theories of regenerators have been developed with those arrangements in view.

It seems that the method most suitable for producing this cyclic change in aircraft power plants is to rotate the matrix so that any part of the matrix is carried alternately through the hot and cold fluid streams.

This method is similar to that of the rotative type air preheaters used in modern steam power plants. In this report one of the main regenerator theories is recast so that it is directly applicable to the rotating regenerator; also, other theories are discussed from that standpoint.

Rotating regenerators may be classified according to whether the fluids flow axially or radially.

1-5.1 Axial or Disk Regenerators

The matrix of the axial regenerator shown in Fig. 1-4 is built in the shape of a disk. The disk is mounted coaxially in a round cylinder divided into two ducts. The two fluids flow in opposite sense, the hot fluid flowing in one duct and the cold fluid in the other. The matrix rotates about its axis and would usually be turned by a positive external drive requiring a very small amount of power. Thus, any point in the matrix passes alternately through the hot and cold streams, carrying the heat from the one to the other.

1-5.2 Radial or Drum Regenerators

Figure 1-5 represents the drum type regenerator. The matrix is built in a cylindrical form through which the fluids flow radially. This drum is mounted coaxially with two round ducts. The inner duct and the annular space are divided in the axial direction into two parts, one for the cold fluid and the other for the hot fluid. As in the previous case, the fluids are in counterflow through the matrix.

1-6 Leakage

One of the practical problems arising in the mechanical design of a regenerator for application to the gas turbine power plant is the prevention of leakage, particularly from the high pressure air to the low pressure gas. The amounts of leakage play an important role in the thermal design and thermodynamic performance. Four types of leakage may possibly occur.

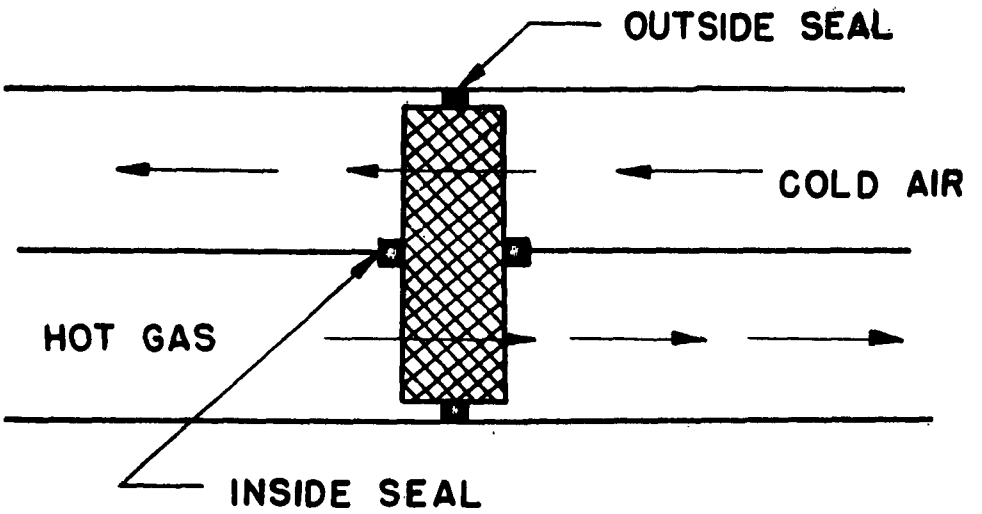

FIG.1-4 DISK TYPE REGENERATOR

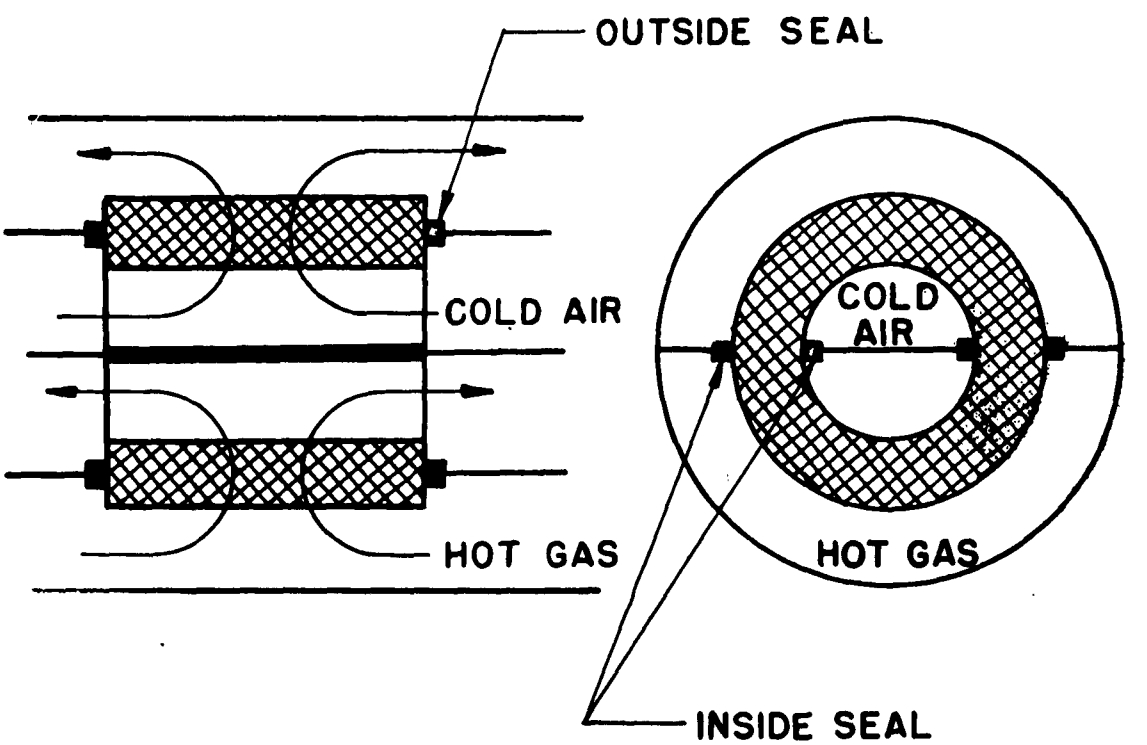

FIG.1-5 DRUM TYPE REGENERATOR

1-6.1 Air-to-Gas Leakage through Clearance Spaces

Leakage from the air side to the gas side occurs through gaps between the moving matrix and the stationary walls separating the two fluids. This type of leakage affects the power plant efficiency adversely, because the compressor must handle air at a higher rate than the turbine. The leakage can be considerably reduced by the inside seals shown in Fig. 1-4 and -5.

1-6.2 Air-to-Air or Gas-to-Gas Leakage

Some air or gas may bypass the matrix through the clearance space between the rotating matrix and the duct walls, because a pressure drop exists across the matrix. Hence, parts of either fluid may not pass through the matrix, and the effectiveness of the regenerator diminishes. This type of leakage is reduced by means of the outside seals indicated in Fig. 1-4 and -5.

1-6.3 Air-to-Gas Leakage through Matrix

In matrices other than the tubular, or flame trap type, the air could leak through the matrix to the exhaust side. This is prevented by dividing the matrix into sectoral compartments and using seals wide enough to cover at least one compartment at a time.

1-6.4 Carry-Over Leakage

Finally, the so-called "carry-over" leakage or "let down" occurs. The fluid trapped in the individual compartments of the matrix are carried from one stream to the other by virtue of the matrix rotation. Because the air has a high density, the carry-over is greater from the air to the gas side than from the gas to the air side of the regenerator. The carry-over is unavoidable; however, it can be kept below a reasonable limit with slow speeds of rotation.

1-7 Other Design Considerations

In addition to the leakage which is a problem unique to the regenerative heat exchanger, the pressure drop, common to all types of heat ex-

changers, must be considered. The effects of the pressure drops on both the air and gas sides is to decrease the expansion ratio of the turbine, thus reducing the thermal efficiency of the power plant. To be worth while, the regenerator must of course augment the net output considerably more than would be needed just to balance the decrease due to pressure drop.

The effect of size and weight should be considered from the viewpoint of the aircraft performance and purpose. As already mentioned, because of its small passages and finely divided structure, the regenerator appears to have an advantage of being lighter than a recuperator meeting the same performance requirements.

Chapter 2: THEORY OF THE ROTATING REGENERATIVE HEAT EXCHANGER

2-1 Assumptions

The assumptions of Hausen's (Ref. 10 and 12) theory are discussed in the next sections. Then his basic differential equations are developed from the standpoint of their application to the rotating regenerator.

2-1.1 Homogeneity

It is assumed that both the solid and the fluids are continuous, homogeneous media. This assumption is essential for the formulation of the differential equations. In practice the matrix may be considered homogeneous if the material is so finely divided that the sizes of the voids and individual solid elements are very small compared to the overall volume of the matrix.

2-1.2 Steady-State Operation

It is assumed that the matrix has been rotating long enough so that the temperature of any point in the matrix solid repeats itself periodically. Thus, any transients of starting and stopping are not considered.

At each point in space through which the matrix passes the temperature is independent of the time. This means that as an element in the matrix reaches a particular position in space, it attains a certain temperature affixed to that position.

2-1.3 Uniform Temperatures of the Fluids at Entrances to the Matrix

The temperature of the fluids at the entrances to the matrix is assumed uniform. Of course, at the exits their temperatures vary from point to point as will be determined by the theory.

2-1.4 Convection without Conduction

Heat is transferred only by convection at the interface of the matrix and the fluids. An infinitesimal elemental subdivision of the matrix material interchanges heat only with the contacting fluid and not

with neighboring subdivisions; within each infinitesimal subdivision of the solid the conductivity is infinite in the direction normal to the direction of fluid flow and zero in the direction parallel to the fluid flow. In other words, no heat is conducted through any finite part of the solid, while the capacity of this part for heat storage is not impaired. Since the matrix is usually made of thin sheets or wires of heat resisting materials which have relatively low conductivity, this assumption is justifiable. Some effects of finite conductivity are discussed in later sections.

As for the fluids, heat is convected by them and is conducted within them only in regions on the interface of each subdivision. This assumption is justified by the low conductivity of the fluids.

2-1.5 Constant Coefficients of Heat Transfer

The coefficient of heat transfer h is assumed constant in either stream. This means that influences of transients in the boundary layers and of variations in the fluid properties are neglected. This assumption may be justified by the facts that the transients are of relatively brief duration and that the thermal properties of the fluids change relatively little with temperature. In practice, the fluid properties are evaluated at certain mean temperatures (see Section 5-6).

2-1.6 Constant Density

The thermal expansion or contraction of the fluid during heating or cooling changes the velocity of the fluid as it passes through the matrix. The influence of these variations are omitted from the theory in order to simplify the mathematics. Calculations by Saunders and Smoleniec (Ref. 25) indicate that this assumption is justifiable.

2-2 Derivation of the Differential Equations

Suppose that the matrix has been stretched out so that its motion is rectilinear. Then the matrix is said to be flat or plane. It is evident that the findings regarding the flat matrix are directly applicable to the disk type regenerator; also, it is shown in Appendix A that after minor modification the results are applicable to the drum type regenerator.

With reference to Fig. 2-1, the matrix has the length L in the main direction of fluid flow. The velocity of the matrix is v, the direction being normal to that of the fluid stream. The fluid flows with a mass velocity of m'' pounds per hour per square foot of facial or frontal area. A heat balance is made on an element of volume in space. The dimensions of the element in the plane of motion are δx by δy; its depth, normal to the plane of motion, is one foot.

Under steady-state conditions (see Section 2-1.2), thermal energy is carried in the x-direction by the fluid and in the y-direction by the solid; also some heat is carried over in the y-direction by the fluid trapped in the interstices of the matrix element.

2-2.1 Thermal Energy Conveyed by the Fluid

The energy transported per unit time by the fluid into the element of space is

$$q_x = m'' (\delta y \cdot 1) \cdot c_p \cdot \theta \qquad (2\text{-}1)$$

where $\theta = \theta(x,y)$ is the fluid temperature; $c_p \cdot \theta$ is the enthalpy of the fluid referred to zero enthalpy at 0°F.

2-2.2 Thermal Energy Conveyed by the Solid Material

Similarly as in Section 2-2.1, the thermal energy transported per unit time by the solid material into the element of space is

$$q_{y,1} = v \cdot (\delta x \cdot 1) \cdot \rho_{s,app} \cdot c_{p,s} \cdot t \qquad (2\text{-}2)$$

where subscript s refers to the solid, $t = t(x,y)$ is the solid temperature, and $c_{p,s} \cdot t$ is the enthalpy of the material referred to zero enthalpy at 0°F. Subscript app means that the apparent density should be employed. Subscript 1 indicates that only one part of the heat conveyed in the y-direction is considered.

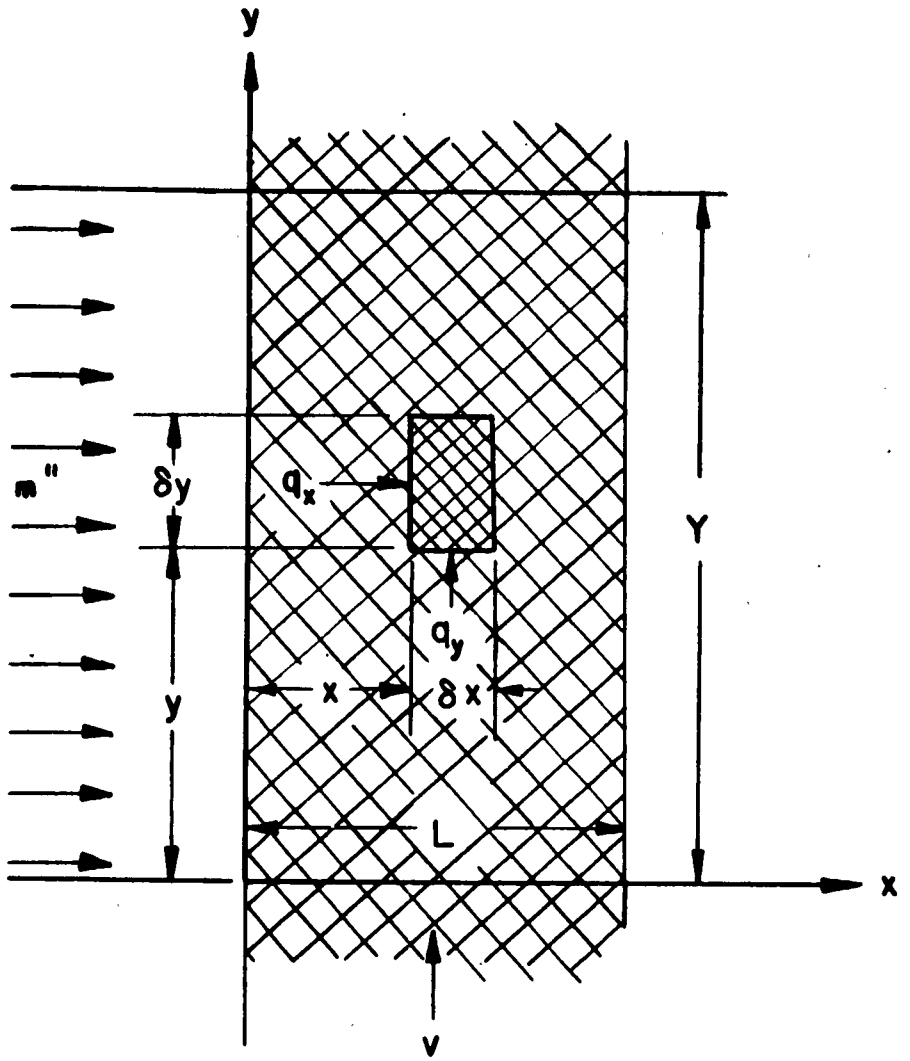

FIG. 2-1 NOMENCLATURE FOR THE PLANE MATRIX REGENERATOR

2-2.3 Thermal Energy in the Carry-Over

A second part of the heat conveyed in the y-direction is the thermal energy of the fluid carried over in unit time by the matrix:

$$q_{y,2} = v(\delta x \cdot 1)\, \rho_{app} \cdot c_p \cdot \theta \qquad (2\text{-}3)$$

2-2.4 Balance of the Transported Thermal Energy

Applying the First Law of Thermodynamics to the elemental volume of space and observing that no heat is stored,

$$\frac{\partial q_x}{\partial x}\,\delta x + \frac{\partial (q_{y,1} + q_{y,2})}{\partial y}\,\delta y = 0 \qquad (2\text{-}4)$$

Substituting for q_x, $q_{y,1}$, and $q_{y,2}$ from Eq. 2-1, -2, and -3 into Eq. 2-4 and simplifying,

$$m'' c_p \frac{\partial \theta}{\partial x} + C''' v \frac{\partial t}{\partial y} + \rho \beta v c_p \frac{\partial \theta}{\partial y} = 0 \qquad (2\text{-}5)$$

where ρ is the actual fluid density, β is the void fraction (the ratio of the volume of voids to the volume of matrix), and

$$C''' \equiv \rho_{s,app} \cdot c_{p,s} \qquad (2\text{-}6)$$

2-2.5 Heat Exchange in the Elemental Volume of Space

As the relatively hot matrix "flows" into the space element it loses heat to the flowing fluid by convection. The rate of change of the enthalpy of the matrix material is equal to the rate of heat transferred by convection in the same space element. Accordingly,

$$\frac{\partial}{\partial y}(v \cdot \delta x \cdot C''' t)\,\delta y = -\, hS'''\,(t - \theta)\,\delta x\,\delta y \qquad (2\text{-}7)$$

The minus sign appears because t decreases in the positive y-direction. The same equation would be obtained if the matrix were considered to be cold and gaining heat from the fluid. Simplifying,

$$\frac{\partial t}{\partial y} = \frac{hS'''}{vC'''} (\theta - t) \qquad (2\text{-}8)$$

Eliminating $\partial t/\partial y$ from Eq. 2-5 and -8 and placing $m'' = u\rho\beta$,

$$\frac{\partial \theta}{\partial x} + \frac{v}{u} \cdot \frac{\partial \theta}{\partial y} = \frac{hS'''}{m''c_p} (t - \theta) \qquad (2\text{-}9)$$

It may be noted that u is the effective axial velocity of the fluid, that is, the distance a fluid particle moves per unit time in the x-direction through the matrix interstices. Equations 2-8 and -9 are the basic differential equations governing the temperatures of the solid and fluids in the flat regenerator. In the next section they are brought to a more convenient form.

2-2.6 The Differential Equations in Dimensionless Space Coordinates

Introducing

$$\xi = \frac{h\ S'''}{m''c_p} x \qquad (2\text{-}10)$$

and

$$\eta = \frac{hS'''}{C'''} \left(\frac{y}{v} - \frac{x}{u}\right) \qquad (2\text{-}11)$$

and substituting for x and y in terms of ξ and η, Eq. 2-8 and -9 become

$$\frac{\partial t}{\partial \eta} = \theta - t \qquad (2\text{-}12)$$

$$\frac{\partial \theta}{\partial \xi} = t - \theta \qquad (2\text{-}13)$$

where t and θ are now regarded as functions of ξ and η.

Equations 2-12 and -13 describe the heat exchange in one of the regenerator streams. Therefore, the problem of the heat exchange in the regenerator is solved using two sets of these equations. In both streams,

x is positive in the direction of the flow and y is positive in the direction of the matrix motion.

2-3 Boundary Conditions

Only counterflow regenerators will be considered.[1] The two streams will be called the "cold air" and the "hot gas", and symbols denoting quantities on corresponding sides of the regenerator will be distinguished by subscripts a and g, respectively. Thus, a plane normal to the flow direction of the cold air is at a distance x_a from the cold-air entrance. The same plane would be at a distance x_g from the hot-gas entrance, so that

$$x_g = L - x_a \tag{2-14}$$

In order to formulate the boundary conditions the "actual" regenerator will be replaced by an "ideal" regenerator. It will be convenient to consider the matrix of fine tubular construction; however, substantially the same analysis would apply to gauze type matrices.

2-3.1 Difficulty of Formulating Boundary Conditions for the Actual Regenerator

As the solid particles in a plane normal to the direction of the matrix motion enter one of the fluid streams, a point at $x_1 \neq 0$ is not immediately affected because the fluid does not reach that point until the time x_1/u has elapsed; meanwhile the point moves to $y_1 = v \cdot (x_1/u)$. Also, at the farther side of the fluid stream, at $x = 0$, there is a distance in the y-direction, namely, $v \cdot (L/u)$, such that fluid particles entering cannot reach all parts of the passages before they are blocked or sealed. Summarizing, in the actual regenerator the duration of time a point in the matrix is affected by a given stream depends upon its distance x from the entrance of the fluid. A point of the matrix at $x = 0$ spends the full heating or cooling period in the fluid stream whereas a point at $x = L$ stays a shorter time. These variable exposure

[1] Hausen (Ref. 10) also considered parallel-flow regenerators. He showed that their maximum effectiveness is limited to a value of 0.5.

times lead to mathematical boundary conditions which are difficult to handle. Therefore, an ideal regenerator is defined which closely approximates the actual regenerator for all practical purposes and simplifies the mathematics.

2-3.2 Ideal Regenerator

An ideal flat regenerator is shown diagrammatically in Fig. 2-2. The walls dividing the two fluid streams are imagined to be permeable, in such a way that they allow the matrix to pass through them but keep the fluids out. Further, the walls of each channel are slanted at the angle $\tan^{-1}(v/u)$ from the main direction of the fluid flow. Hence, the fluid particles move parallel to the walls. As a consequence of this arrangement, any point in the matrix enters the stream at the moment the fluid arrives; the point is immediately affected by the first particle of fluid entering at the near side of the stream. At the far side, the fluid particles leave the matrix, without being replaced by other fluid particles. Thus, in the ideal regenerator, carry-over from one stream to the other is avoided.

With reference to Fig. 2-2,

$$y^* = y - \frac{v}{u} x \tag{2-15}$$

and the distance between the permeable walls is

$$Y^* = Y - \frac{v}{u} x \tag{2-16}$$

Hence, the distances y^* are measured from an axis which is oblique to the direction of flow, and the distance Y^* is uniform, so that all points of the matrix in the ideal regenerator have the same length of effective path in a given stream.

It may be noted that upon eliminating y from Eq. 2-11 and -15,

$$\eta = \frac{hS''}{vC''} y^* \tag{2-17}$$

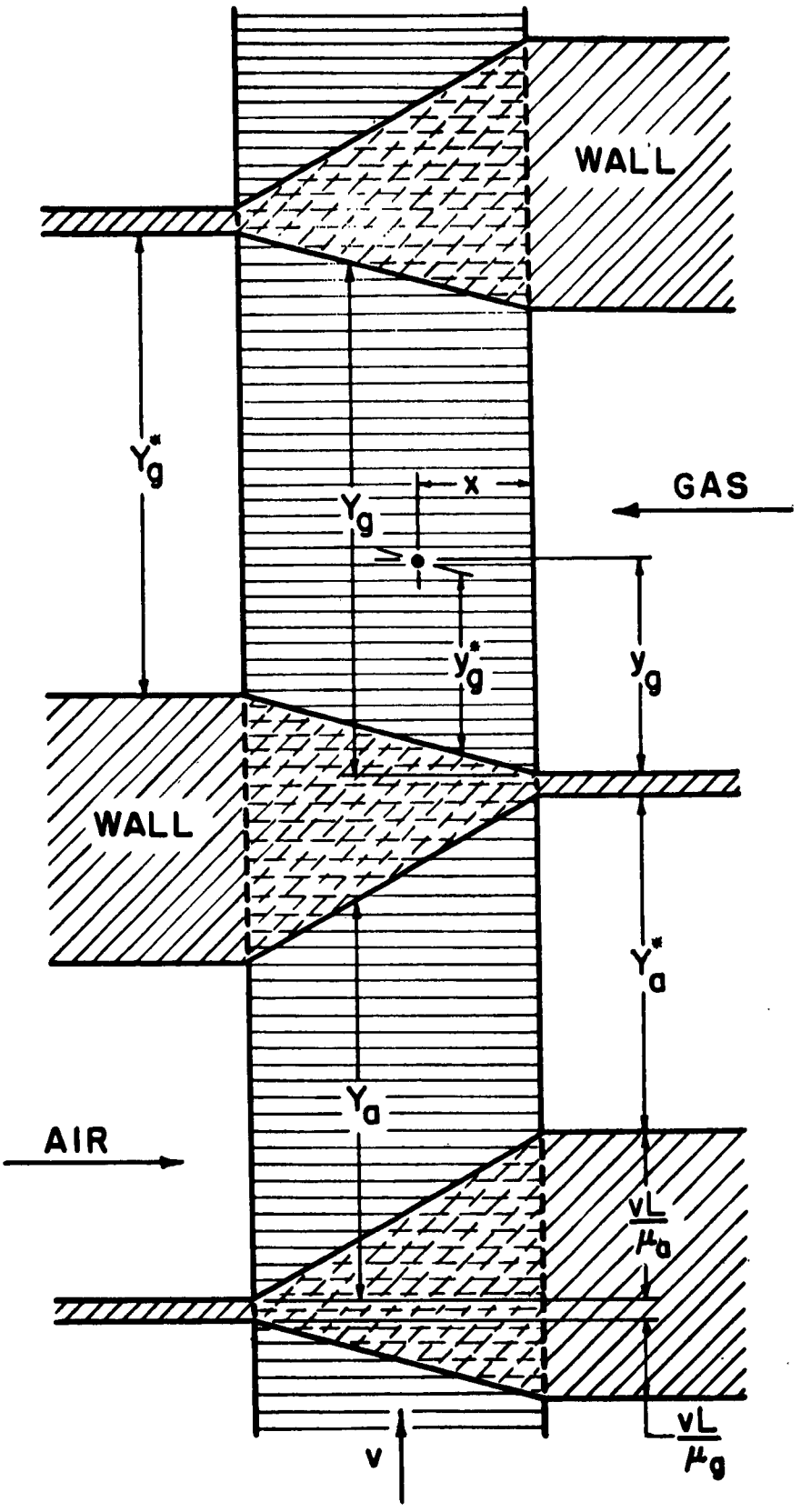

FIG. 2-2 IDEAL REGENERATOR

and that the differential equations in dimensionless space coordinates, namely, Eq. 2-12 and -13, are unaltered.

2-3.3 Dimensionless Lengths

To formulate the boundary conditions of the ideal regenerator, the extreme values of ξ and η will be needed. The value of ξ for $x = L$ will be denoted by Λ and will be called the reduced length. Thus,

$$\Lambda \equiv \frac{h\, S'''}{m'' c_p} L \tag{2-18}$$

The value of η for $y^* = Y^*$ will be denoted by Π and will be called the reduced period.[1] Thus,

$$\Pi \equiv \frac{hS'''}{vC'''} Y^* \tag{2-19}$$

It is of some interest that the ratio

$$U \equiv \frac{\Pi}{\Lambda} = \frac{m'' c_p}{vC'''} \cdot \frac{Y^*}{L} \tag{2-20}$$

which is called the utilization factor, is independent of h and S'''.

It should be noted that values of Λ and Π on the air side of the regenerator are generally not equal to corresponding values on the gas side. Since x is measured from the plane at which the fluid enters the matrix and since $\xi/\Lambda = x/L$, the quantities ξ_a and ξ_g corresponding to the same plane are related by the equation,

$$\frac{\xi_g}{\Lambda_g} + \frac{\xi_a}{\Lambda_a} = 1 \tag{2-21}$$

---

[1] The reason for this bizarre name for a distance is that the theory was originally developed for non-rotary regenerators which operate in a quasi-stationary way, and the term "period" as well as the symbol Π are retained to avoid any confusion in case the reader consults the literature.

Further,

$$\frac{\Lambda_g}{\Lambda_a} = \frac{m''_a\, c_{p,a}}{m''_g\, c_{p,g}} \cdot \frac{h_g}{h_a} \tag{2-22}$$

and

$$\frac{\Pi_g}{\Pi_a} = \frac{Y^*_g}{Y^*_a} \cdot \frac{h_g}{h_a} \tag{2-23}$$

Eliminating the ratio h_g/h_a from Eq. 2-22 and -23,

$$\frac{\Lambda_g}{\Lambda_a} = \frac{\Pi_g}{\Pi_a} \cdot \frac{m''_a\, c_{p,a}\, Y^*_a}{m''_g\, c_{p,g}\, Y^*_g} \tag{2-24}$$

For many practical purposes it may be assumed that $c_{p,a} = c_{p,g}$. Moreover, in the application of the theory to an aircraft gas turbine power plant, if the leakage from one stream to the other is very small compared with the total rate of flow it may also be assumed that $m''_a\, Y^*_a = m''_g\, Y^*_g$, by continuity. Under these circumstances the ratio in the parentheses of Eq. 2-24 takes the value 1, and

$$\frac{\Lambda_g}{\Lambda_a} = \frac{\Pi_g}{\Pi_a} \quad \text{or} \quad U_a = U_g \tag{2-25}$$

This is a useful relationship in dealing with regenerators which have unequal reduced lengths and reduced periods, that is, so-called unbalanced regenerators.

2-3.4 Boundary Conditions of the Ideal Regenerator

In accordance with the assumption in Section 2-1.3 that the temperatures of the fluids at the entrance planes are uniform,

$$\vartheta_a(0, \eta_a) \equiv \vartheta_{a,o} \tag{2-26}$$

and

$$\vartheta_g(0, \eta_g) \equiv \vartheta_{g,o} \tag{2-27}$$

where both $\Theta_{a,o}$ and $\Theta_{g,o}$ are constants.

Since nothing happens to the ideal matrix as it passes through the permeable wall, the temperature at a point in the solid leaving one stream is equal to the temperature at that point entering the second stream. Accordingly, considering that $t_g = t_g(x_g, y_g^*)$ and $t_a = t_a(x_a, y_a^*)$, and focusing our attention on a plane of the matrix which leaves the cold air and on another which enters the hot gas, we may write

$$t_g(x_g, 0) = t_a(L - x_g, Y_a^*) \tag{2-28}$$

Introducing the reduced lengths and reduced periods and considering now that $t_g = t_g(\xi_g, \eta_g)$ and $t_a = t_a(\xi_a, \eta_a)$, we may transform Eq. 2-28 to

$$t_g(\xi_g, 0) = t_a\left(\Lambda_a\left[1 - \frac{\xi_g}{\Lambda_g}\right], \Pi_a\right) \tag{2-29}$$

Similarly, focusing our attention on planes which leave the hot gas and enter the cold air,

$$t_a(\xi_a, 0) = t_g\left(\Lambda_g\left[1 - \frac{\xi_a}{\Lambda_a}\right], \Pi_g\right) \tag{2-30}$$

The problem of the ideal regenerator is now mathematically formulated. A solution is required to satisfy two sets of the linear partial differential Eq. 2-12 and -13, one set for each fluid, and to satisfy the boundary conditions, namely, Eq. 2-26, -27, -29, and -30.

2-3.5 Comparison of the Ideal and Actual Regenerators

The difference lies in the slanted, permeable wall, which is impossible to construct in the actual regenerator. This wall has two features:

First, it has the ability to separate the fluid from the solid, allowing the solid to pass through it. The effect, as already mentioned, is to eliminate the carry-over losses discussed in Section 1-6.4. In

practice this type of leakage may be kept low by employing low speeds of rotation, say, 30 to 40 revolutions per minute. This places a limit on the matrix velocity v.

Second, the permeable wall is slanted at the angle $\tan^{-1}(v/u)$ with respect to the direction of fluid flow, while the wall of the actual regenerator is straight. As $(v/u) \to 0$, the shape of the ideal regenerator approaches the shape of the actual one. Since practical values of v/u would usually be quite small, the approximation is good. It may be noted that the same approximation would be made by omitting the second term in the parentheses of Eq. 2-11, for this term arose by the admittance of a carry-over of thermal energy from one elemental volume of space to another (Section 2-2.3).[1]

2-3.6 Single-Blow Problem

An allied problem, which is of a simpler nature than the one treated above, deals with the "single-blow". Its importance here lies in the fact that its solution may be employed to solve the regenerator problem. Also, it has been employed in several experimental studies to determine the coefficients of heat transfer. See, for example, Ref. 12, 25, and 26.

In the single-blow, a stationary matrix having an arbitrary initial temperature distribution is suddenly subjected to a continuous blow of fluid entering with constant temperature. Mathematically, the problem is to solve one set of the basic differential equations, namely, Eq. 2-12 and -13, with one boundary of the form of Eq. 2-26 or -27 and the condition that

$$t(\xi,0) = f(\xi) \qquad (2\text{-}31)$$

where $f(\xi)$ is a prescribed function. The solution is comprised of expressions for $t(\xi,\eta)$ and $\theta(\xi,\eta)$. Solutions are presented in

[1] The next several sections deal with the mathematical solution of the regenerator problem. The reader who is interested mainly in the results and their application may proceed without loss of continuity to Section 2-8.

Ref. 2, 22, and 27; the last two references deal with the case that $f(\xi)$ = constant.

2-4 Solutions of the Regenerator Problem

Hausen (Ref. 10) developed a purely analytical solution. The main results, presented in Section 2-8, are directly applicable to the balanced regenerator, that is, a regenerator in which $\Lambda_a = \Lambda_g$ and $\Pi_a = \Pi_g$. Nusselt (Ref. 23), working independently, brought the mathematical problem to a form requiring the solution of a set of integral equations. Numerical methods, one of which is based on Nusselt's treatment and is presented in Section 2-5, have since shown that the results for the balanced regenerator may be applied to predict the over-all performance of an unbalanced regenerator, provided a proper averaging procedure is employed. Although quite time consuming, the numerical methods have the advantages of being applicable to both balanced and unbalanced regenerators and of providing the transient histories and the steady-state temperature distributions in both the matrix and the fluids. Even when the temperature distributions of a balanced regenerator are required, a numerical solution appears preferable to direct substitution into the mathematical series comprising the results of Hausen's analytical solution.

Hausen (Ref. 11) devised the first numerical method, the so-called heat-pole method. He divided the matrix into a number of strips or heat poles along the x-axis. Since no conduction occurred, he could treat each pole as though it were an individual bed in the single-blow theory, for which analytical solutions of a closed form were already available.

Saunders and Smoleniec (Ref. 25) solved the single-blow problem numerically by converting the differential equations to difference equations and integrating in a stepwise manner. Starting with a regenerator matrix of uniform temperature, allowing it to cycle successively through the hot and cold fluids, and observing the point in the calculations where the temperatures repeated themselves, they determined the steady-state distributions and, consequently, the regenerator performance. At the same time they could predict the number of revolutions the matrix turned before coming to steady-state conditions. In any practical case

where

$$K_a(\xi_a - \epsilon) \equiv -e^{-\Pi_a - (\xi_a - \epsilon)} \cdot \Pi_a \cdot \frac{iJ_1\left(2i\sqrt{\Pi_a(\xi_a - \epsilon)}\right)}{\sqrt{\Pi_a(\xi_a - \epsilon)}} \qquad (2\text{-}39)$$

In the same way, Eq. 2-35 becomes

$$1 - f_a\,\Lambda_a\left[1 - \frac{\xi_g}{\Lambda_g}\right] = e^{-\Pi_g}\left[1 - f_g(\xi_g)\right] + \int_0^{\xi_g} K_g(\xi_g - \epsilon)\left[1 - f_g(\epsilon)\right] d\epsilon \qquad (2\text{-}40)$$

where

$$K_g(\xi_g - \epsilon) \equiv -e^{-\Pi_g - (\xi_g - \epsilon)} \cdot \Pi_g \cdot \frac{iJ_1\left(2i\sqrt{\Pi_g(\xi_g - \epsilon)}\right)}{\sqrt{\Pi_g(\xi_g - \epsilon)}} \qquad (2\text{-}41)$$

Equations 2-38 and -40 are two simultaneous integral equations giving the temperature distributions in the matrix planes at the entry to the two fluids, namely, f_a and f_g. It will be seen that when these distributions are known, the effectiveness can readily be found. To carry out the calculations, the integrals are to be evaluated by means of Simpson's rule or its equivalent, as shown below.

2-5.2 Review of Simpson's Rule for Integration

To evaluate a definite integral $\int_a^b g(\epsilon)\, d\epsilon$ by Simpson's rule, the interval (a,b) on the ϵ-axis is divided into an even number of parts, each of width Δ. Approximating the function $g(\epsilon)$ with parabolic segments through every group of three successive points, one may write the following equation with an error of the order Δ^2.

$$\int_a^b g(\epsilon)\, d\epsilon = \frac{\Delta}{3}\Big[g(a) + 4g(a+\Delta) + 2g(a+2\Delta) + 4g(a+3\Delta) + 2g(a+4\Delta) + \ldots + 2g(b-2\Delta) + 4g(b-\Delta) + g(b)\Big] \qquad (2\text{-}42)^1$$

[1] The parentheses in this equation and in all remaining equations of this section enclose the functional arguments.

In particular, if the number of intervals is 2,

$$\int_a^b g(\epsilon)\, d\epsilon = \frac{\Delta}{3}\left[g(a) + 4g \cdot \frac{a+b}{2} + g(b)\right] \qquad (2\text{-}43)$$

2-5.3 Application of Simpson's Rule to the Solution of the Integral Equations

In applying Simpson's rule to solve Eq. 2-38 and -40, each of the reduced lengths Λ_a and Λ_g is divided into N equal parts of length Δ_a and Δ_g, respectively, as shown in Fig. 2-3. It is unnecessary that N be an even number. Regarding Eq. 2-38, consider that $\xi_a = m \cdot \Delta_a$ where $m = 0, 1, 2, \ldots, N$. Then

$$f_g(N \cdot \Delta_g [1 - \frac{m}{N}]) = f_a(m \cdot \Delta_a) \cdot e^{-\Pi_a} + \int_0^{m \cdot \Delta_a} K_a(m \cdot \Delta_a - \epsilon) \cdot f_a(\epsilon)\, d\epsilon \qquad (2\text{-}44)$$

With the understanding that a symbol of the type $f_{g,n}$ will henceforth replace the symbol of the type $f_g(n \cdot \Delta_g)$, Eq. 2-44 takes the simpler form,

$$f_{g,N-m} = f_{a,m} \cdot e^{-\Pi_a} + \int_0^{m \cdot \Delta_a} K_a(m \cdot \Delta_a - \epsilon) \cdot f_a(\epsilon)\, d\epsilon \qquad (2\text{-}45)$$

This equation is typical of $N + 1$ equations which will be written by placing $m = 0,1,2,\ldots,$ and N. Equation 2-40 could be written in a similar, typical manner to represent another set of $N + 1$ equations. Employing Simpson's rule or its equivalent to evaluate the integrals, one obtains a total of $2N + 2$ linear algebraic equations in which the unknowns are $f_{g,m}$ and $f_{a,m}$ for $m = 0,1,2,\ldots,N$.

Since Simpson's rule can be used only if m is an even number, equivalent expressions are needed for the cases in which m is odd. In the next four sections, the integrals are developed according to whether m is even, $m = 1$, $m = 3$, and m is an odd number greater than 3.

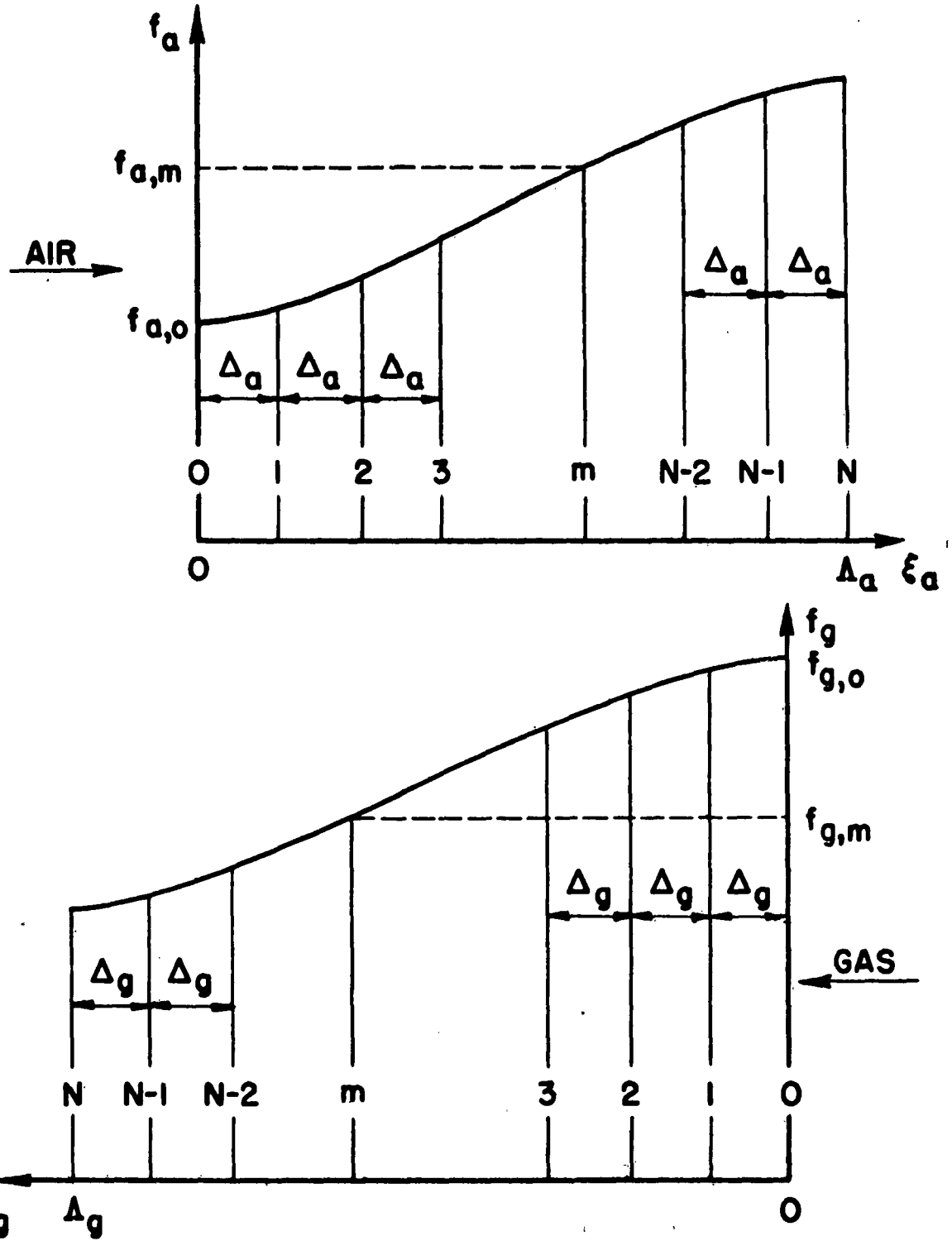

FIG.2-3 DIVISION OF THE MATRIX FOR THE NUMERICAL SOLUTION OF EQUATIONS

2-5.4 Integration for m Even

In this case Simpson's rule is directly applicable and the integral in Eq. 2-45 becomes

$$\int_0^{m\cdot\Delta_a} K_a(m\cdot\Delta_a-\epsilon)\cdot f_a(\epsilon)\,d\epsilon$$

$$=\frac{\Delta_a}{3}\Big\{K_a(m\cdot\Delta_a-0)\cdot f_a(0)+4K_a(m\cdot\Delta_a-\Delta_a)\cdot f_a(\Delta_a)$$

$$+2K_a(m\cdot\Delta_a-2\Delta_a)\cdot f_a(2\Delta_a)+\cdots$$

$$+2K_a(m\cdot\Delta_a-[m-2]\,\Delta_a)\cdot f_a([m-2]\cdot\Delta_a)$$

$$+4K_a(m\cdot\Delta_a-[m-1]\,\Delta_a)\cdot f_a([m-1]\cdot\Delta_a)$$

$$+K_a(m\cdot\Delta_a-m\cdot\Delta_a)\cdot f_a(m\cdot\Delta_a)\Big\} \qquad (2\text{-}46)$$

The symbol $K_{a,n}$ may replace the lengthier notation $K_a(n\cdot\Delta_a)$, a similar change of notation having already been made in regard to f. Then

$$\int_0^{m\cdot\Delta_a} K_a(m\cdot\Delta_a-\epsilon)\cdot f_a(\epsilon)\,d\epsilon$$

$$=\frac{\Delta_a}{3}\Big\{K_{a,m}\cdot f_{a,0}+4K_{a,m-1}\cdot f_{a,1}+2K_{a,m-2}\cdot f_{a,2}$$

$$+4K_{a,m-3}\cdot f_{a,3}+\cdots+2K_{a,2}\cdot f_{a,m-2}$$

$$+4K_{a,1}\cdot f_{a,m-1}+K_{a,0}\cdot f_{a,m}\Big\} \qquad (2\text{-}47)$$

In the special case that $m=0$, the integral is zero.

2-5.5 Integration for m = 1

In this case Iliffe assumed that the temperature distribution can be represented in the range $0\le\epsilon\le 3\Delta_a$ by a polynomial of the third order:

$$f_a(\epsilon)=a_0+a_1\epsilon+a_2\epsilon^2+a_3\epsilon^3 \qquad (2\text{-}48)$$

Substituting $\epsilon = 0$, Δ_a, $2\Delta_a$, and $3\Delta_a$, the values of a_0, a_1, a_2, and a_3 can be determined in terms of $f_{a,0}$, $f_{a,1}$, $f_{a,2}$, and $f_{a,3}$. Then employing Eq. 2-48 to determine $f_{a,1/2} \equiv f_a(\Delta_a/2)$,

$$f_{a,1/2} = \frac{1}{16}\left[5f_{a,0} + 15f_{a,1} - 5f_{a,2} + f_{a,3}\right] \tag{2-49}$$

Thus, the interval $(0, \Delta_a)$ has been subdivided into two equal parts so that Eq. 2-43 is applicable. The result is

$$\int_0^{\Delta_a} K_a(\Delta_a - \epsilon) \cdot f_a(\epsilon)\, d\epsilon$$

$$= \frac{\Delta_a}{6}\left\{K_{a,1} \cdot f_{a,0} + \frac{1}{4} K_{a,1/2} \cdot \left[5f_{a,0} + 15f_{a,1} - f_{a,2} + f_{a,3}\right] + K_{a,0} \cdot f_{a,1}\right\} \tag{2-50}$$

2-5.6 Integration for $m = 3$.

Iliffe assumed that the entire integrand could be represented by another third-order polynomial:

$$K_a(3\Delta_a - \epsilon) \cdot f_a(\epsilon) = A_0 + A_1\epsilon + A_2\epsilon^2 + A_3\epsilon^3 \tag{2-51}$$

Again substituting $\epsilon = 0$, Δ_a, $2\Delta_a$, and $3\Delta_a$, the values of A_0, A_1, A_2, and A_3 can be determined in terms of $K_{a,3} \cdot f_{a,0}$, $K_{a,2} \cdot f_{a,1}$, $K_{a,1} \cdot f_{a,2}$, and $K_{a,0} \cdot f_{a,3}$. After replacing the coefficients in Eq. 2-51 with their newly derived values and integrating with respect to ϵ from 0 to $3\Delta_a$,

$$\int_0^{3\Delta_a} K_a(3\Delta_a - \epsilon) \cdot f_a(\epsilon)\, d\epsilon = \frac{3}{8}\Delta_a\left[K_{a,3} \cdot f_{a,0} + 3K_{a,2} \cdot f_{a,1} + 3K_{a,1} \cdot f_{a,2} + K_{a,0} \cdot f_{a,3}\right] \tag{2-52}$$

2-5.7 Integration for m Odd and Greater than 3

In this case Iliffe employed the relationship

$$\int_0^{m\cdot\Delta_a} g(\epsilon)\,d\epsilon = \int_0^{3\cdot\Delta_a} g(\epsilon)\,d\epsilon + \int_{3\cdot\Delta_a}^{m\cdot\Delta_a} g(\epsilon)\,d\epsilon \qquad (2\text{-}53)$$

Thus, he could use the results from the case that $m = 3$ in conjunction with the result from the case that m is even. With due regard for the actual meaning of the index m in the present case, for example, observing that $m-3$ is even, the final result is

$$\int_0^{m\cdot\Delta_a} K_a(m\cdot\Delta_a - \epsilon)\cdot f_a(\epsilon)\,d\epsilon$$

$$= \Delta_a\left\{\frac{3}{8}K_{a,m}\cdot f_{a,0} + \frac{9}{8}K_{a,m-1}\cdot f_{a,1} + \frac{9}{8}K_{a,m-2}\cdot f_{a,2}\right.$$

$$+\left[\frac{3}{8}+\frac{1}{3}\right]K_{a,m-3}\cdot f_{a,3} + \frac{4}{3}K_{a,m-4}\cdot f_{a,4} + \frac{2}{3}K_{a,m-5}\cdot f_{a,5} + \cdots$$

$$\left. + \frac{2}{3}K_{a,2}\cdot f_{a,m-2} + \frac{4}{3}K_{a,1}\cdot f_{a,m-1} + \frac{1}{3}K_{a,0}\cdot f_{a,m}\right\} \qquad (2\text{-}54)$$

2-5.8 Final Form of the Simultaneous Linear Algebraic Equations

Applying the results of Sections 2-5.4 through 2-5.7 successively in accordance with Eq. 2-45 for $m = 0,1,2,\ldots,N$, one obtains the $N + 1$ equations shown in Fig. 2-4; they are referred to as Eq. 2-55. As already suggested, the other set of $N + 1$ equations may be obtained by replacing $f_{g,N-m}$, Δ_a, $K_{a,m}$, $f_{a,m}$, and Π_a by $1 - f_{a,N-m}$, Δ_g, $K_{g,m}$, $1 - f_{g,m}$, and Π_g, respectively. These equations are shown in Fig. 2-5 and are referred to as Eq. 2-56.

2-5.9 General Remarks regarding the Calculation Procedure

The sets of Eq. 2-55 and -56 are $2N + 2$ linear algebraic equations in $f_{g,m}$ and $f_{a,m}$ for $m = 0,1,2,\ldots,N$. The solution, therefore, represents the temperature distributions in the matrix at the planes of entry to the gas and the air.

$$f_{g,N} = e^{-\Pi_o} f_{o,o}$$

$$f_{g,N-1} = \left(\tfrac{1}{6} K_{o,1} + \tfrac{5}{24} K_{o,\frac{1}{2}}\right) \Delta_o f_{o,o} + \left[\left(\tfrac{5}{24} K_{o,\frac{1}{2}} + \tfrac{1}{6} K_{o,o}\right) \Delta_o + e^{-\Pi_o}\right] f_{o,1} - \tfrac{5}{24} \Delta_o K_{o,\frac{1}{2}} f_{o,2} + \tfrac{1}{24} \Delta_o K_{o,\frac{1}{2}} f_{o,3}$$

$$f_{g,N-2} = \tfrac{1}{3} \Delta_o K_{o,2} f_{o,o} + \tfrac{4}{3} \Delta_o K_{o,1} f_{o,1} + \left(\tfrac{1}{3} \Delta_o K_{o,o} + e^{-\Pi_o}\right) f_{o,2}$$

$$f_{g,N-3} = \tfrac{3}{8} \Delta_o K_{o,3} f_{o,o} + \tfrac{9}{8} \Delta_o K_{o,2} f_{o,1} + \tfrac{9}{8} \Delta_o K_{o,1} f_{o,2} + \left(\tfrac{3}{8} \Delta_o K_{o,o} + e^{-\Pi_o}\right) f_{o,3}$$

$$f_{g,N-4} = \tfrac{1}{3} \Delta_o K_{o,4} f_{o,o} + \tfrac{4}{3} \Delta_o K_{o,3} f_{o,1} + \tfrac{2}{3} \Delta_o K_{o,2} f_{o,2} + \tfrac{4}{3} \Delta_o K_{o,1} f_{o,3} + \left(\tfrac{1}{3} \Delta_o K_{o,o} + e^{-\Pi_o}\right) f_{o,4}$$

$$f_{g,N-5} = \tfrac{3}{8} \Delta_o K_{o,5} f_{o,o} + \tfrac{9}{8} \Delta_o K_{o,4} f_{o,1} + \tfrac{9}{8} \Delta_o K_{o,3} f_{o,2} + \tfrac{17}{24} \Delta_o K_{o,2} f_{o,3} + \tfrac{4}{3} \Delta_o K_{o,1} f_{o,4} + \left(\tfrac{1}{3} \Delta_o K_{o,o} + e^{-\Pi_o}\right) f_{o,5}$$

$$f_{g,N-6} = \tfrac{1}{3} \Delta_o K_{o,6} f_{o,o} + \tfrac{4}{3} \Delta_o K_{o,5} f_{o,1} + \tfrac{2}{3} \Delta_o K_{o,4} f_{o,2} + \tfrac{4}{3} \Delta_o K_{o,3} f_{o,3} + \tfrac{2}{3} \Delta_o K_{o,2} f_{o,4} + \tfrac{4}{3} \Delta_o K_{o,1} f_{o,5} + \left(\tfrac{1}{3} \Delta_o K_{o,o} + e^{-\Pi_o}\right) f_{o,6}$$

$$f_{g,N-7} = \tfrac{3}{8} \Delta_o K_{o,7} f_{o,o} + \tfrac{9}{8} \Delta_o K_{o,6} f_{o,1} + \tfrac{9}{8} \Delta_o K_{o,5} f_{o,2} + \tfrac{17}{24} \Delta_o K_{o,4} f_{o,3} + \tfrac{4}{3} \Delta_o K_{o,3} f_{o,4} + \tfrac{2}{3} \Delta_o K_{o,2} f_{o,5} + \tfrac{4}{3} \Delta_o K_{o,1} f_{o,6}$$
$$+ \left(\tfrac{1}{3} \Delta_o K_{o,o} + e^{-\Pi_o}\right) f_{o,7}$$

GENERALLY FOR ANY EVEN VALUE OF m:

$$f_{g,N-m} = \tfrac{1}{3} \Delta_o K_{o,m} f_{o,o} + \tfrac{4}{3} \Delta_o K_{o,m-1} f_{o,1} + \tfrac{2}{3} \Delta_o K_{o,m-2} f_{o,2} + \tfrac{4}{3} \Delta_o K_{o,m-3} f_{o,3} + \tfrac{2}{3} \Delta_o K_{o,m-4} f_{o,4} + \cdots + \tfrac{2}{3} \Delta_o K_{o,2} f_{o,m-2}$$
$$+ \tfrac{4}{3} \Delta_o K_{o,1} f_{o,m-1} + \left(\tfrac{1}{3} \Delta_o K_{o,o} + e^{-\Pi_o}\right) f_{o,m}$$

AND FOR ANY ODD VALUE OF m LARGER THAN 3:

$$f_{g,N-m} = \tfrac{3}{8} \Delta_o K_{o,m} f_{o,o} + \tfrac{9}{8} \Delta_o K_{o,m-1} f_{o,1} + \tfrac{9}{8} \Delta_o K_{o,m-2} f_{o,2} + \tfrac{17}{24} \Delta_o K_{o,m-3} f_{o,3} + \tfrac{4}{3} \Delta_o K_{o,m-4} f_{o,4} + \tfrac{2}{3} \Delta_o K_{o,m-5} f_{o,5}$$
$$+ \tfrac{4}{3} \Delta_o K_{o,m-6} f_{o,6} + \tfrac{2}{3} \Delta_o K_{o,m-7} f_{o,7} + \cdots + \tfrac{2}{3} \Delta_o K_{o,2} f_{o,m-2} + \tfrac{4}{3} \Delta_o K_{o,1} f_{o,m-1} + \left(\tfrac{1}{3} \Delta_o K_{o,o} + e^{-\Pi_o}\right) f_{o,m}$$

FIG. 2-4 EQUATIONS 2-55

$$f_{\sigma,N} = 1 - e^{-\Pi_\sigma} + e^{-\Pi_\sigma} f_{\sigma,0}$$

$$f_{\sigma,N-1} = 1 - e^{-\Pi_\sigma} - \left(\tfrac{1}{6}K_{\sigma,1} + \tfrac{1}{4}K_{\sigma,\frac{1}{2}} + \tfrac{1}{6}K_{\sigma,0}\right)\Delta_\sigma + \left(\tfrac{1}{6}K_{\sigma,1} + \tfrac{5}{24}K_{\sigma,\frac{1}{2}}\right)\Delta_\sigma f_{\sigma,0} + \left[\left(\tfrac{5}{24}K_{\sigma,\frac{1}{2}} + \tfrac{1}{6}K_{\sigma,0}\right)\Delta_\sigma + e^{-\Pi_\sigma}\right] f_{\sigma,1} - \tfrac{5}{24}\Delta_\sigma K_{\sigma,\frac{1}{2}} f_{\sigma,2} + \tfrac{1}{24}\Delta_\sigma K_{\sigma,\frac{1}{2}} f_{\sigma,3}$$

$$f_{\sigma,N-2} = 1 - e^{-\Pi_\sigma} - \left(\tfrac{1}{3}K_{\sigma,2} + \tfrac{4}{3}K_{\sigma,1} + \tfrac{1}{3}K_{\sigma,0}\right)\Delta_\sigma + \tfrac{1}{3}\Delta_\sigma K_{\sigma,2} f_{\sigma,0} + \tfrac{4}{3}\Delta_\sigma K_{\sigma,1} f_{\sigma,1} + \left(\tfrac{1}{3}\Delta_\sigma K_{\sigma,0} + e^{-\Pi_\sigma}\right) f_{\sigma,2}$$

$$f_{\sigma,N-3} = 1 - e^{-\Pi_\sigma} - \left(\tfrac{3}{8}K_{\sigma,3} + \tfrac{9}{8}K_{\sigma,2} + \tfrac{9}{8}K_{\sigma,1} + \tfrac{3}{8}K_{\sigma,0}\right)\Delta_\sigma + \tfrac{3}{8}\Delta_\sigma K_{\sigma,3} f_{\sigma,0} + \tfrac{9}{8}\Delta_\sigma K_{\sigma,2} f_{\sigma,1} + \tfrac{9}{8}\Delta_\sigma K_{\sigma,1} f_{\sigma,2} + \left(\tfrac{3}{8}\Delta_\sigma K_{\sigma,0} + e^{-\Pi_\sigma}\right) f_{\sigma,3}$$

$$f_{\sigma,N-4} = 1 - e^{-\Pi_\sigma} - \left(\tfrac{1}{3}K_{\sigma,4} + \tfrac{4}{3}K_{\sigma,3} + \tfrac{2}{3}K_{\sigma,2} + \tfrac{4}{3}K_{\sigma,1} + \tfrac{1}{3}K_{\sigma,0}\right)\Delta_\sigma + \tfrac{1}{3}\Delta_\sigma K_{\sigma,4} f_{\sigma,0} + \tfrac{4}{3}\Delta_\sigma K_{\sigma,3} f_{\sigma,1} + \tfrac{2}{3}\Delta_\sigma K_{\sigma,2} f_{\sigma,2} + \tfrac{4}{3}\Delta_\sigma K_{\sigma,1} f_{\sigma,3} + \left(\tfrac{1}{3}\Delta_\sigma K_{\sigma,0} + e^{-\Pi_\sigma}\right) f_{\sigma,4}$$

$$f_{\sigma,N-5} = 1 - e^{-\Pi_\sigma} - \left(\tfrac{3}{8}K_{\sigma,5} + \tfrac{9}{8}K_{\sigma,4} + \tfrac{9}{8}K_{\sigma,3} + \tfrac{17}{24}K_{\sigma,2} + \tfrac{4}{3}K_{\sigma,1} + \tfrac{1}{3}K_{\sigma,0}\right)\Delta_\sigma + \tfrac{3}{8}\Delta_\sigma K_{\sigma,5} f_{\sigma,0} + \tfrac{9}{8}\Delta_\sigma K_{\sigma,4} f_{\sigma,1} + \tfrac{9}{8}\Delta_\sigma K_{\sigma,3} f_{\sigma,2} + \tfrac{17}{24}\Delta_\sigma K_{\sigma,2} f_{\sigma,3} + \tfrac{4}{3}\Delta_\sigma K_{\sigma,1} f_{\sigma,4} + \left(\tfrac{1}{3}\Delta_\sigma K_{\sigma,0} + e^{-\Pi_\sigma}\right) f_{\sigma,5}$$

$$f_{\sigma,N-6} = 1 - e^{-\Pi_\sigma} - \left(\tfrac{1}{3}K_{\sigma,6} + \tfrac{4}{3}K_{\sigma,5} + \tfrac{2}{3}K_{\sigma,4} + \tfrac{4}{3}K_{\sigma,3} + \tfrac{2}{3}K_{\sigma,2} + \tfrac{4}{3}K_{\sigma,1} + \tfrac{1}{3}K_{\sigma,0}\right)\Delta_\sigma + \tfrac{1}{3}\Delta_\sigma K_{\sigma,6} f_{\sigma,0} + \tfrac{4}{3}\Delta_\sigma K_{\sigma,5} f_{\sigma,1} + \tfrac{2}{3}\Delta_\sigma K_{\sigma,4} f_{\sigma,2} + \tfrac{4}{3}\Delta_\sigma K_{\sigma,3} f_{\sigma,3} + \tfrac{2}{3}\Delta_\sigma K_{\sigma,2} f_{\sigma,4} + \tfrac{4}{3}\Delta_\sigma K_{\sigma,1} f_{\sigma,5} + \left(\tfrac{1}{3}\Delta_\sigma K_{\sigma,0} + e^{-\Pi_\sigma}\right) f_{\sigma,6}$$

$$f_{\sigma,N-7} = 1 - e^{-\Pi_\sigma} - \left(\tfrac{3}{8}K_{\sigma,7} + \tfrac{9}{8}K_{\sigma,6} + \tfrac{9}{8}K_{\sigma,5} + \tfrac{17}{24}K_{\sigma,4} + \tfrac{4}{3}K_{\sigma,3} + \tfrac{2}{3}K_{\sigma,2} + \tfrac{4}{3}K_{\sigma,1} + \tfrac{1}{3}K_{\sigma,0}\right)\Delta_\sigma + \tfrac{3}{8}\Delta_\sigma K_{\sigma,7} f_{\sigma,0} + \tfrac{9}{8}\Delta_\sigma K_{\sigma,6} f_{\sigma,1} + \tfrac{9}{8}\Delta_\sigma K_{\sigma,5} f_{\sigma,2} + \tfrac{17}{24}\Delta_\sigma K_{\sigma,4} f_{\sigma,3} + \tfrac{4}{3}\Delta_\sigma K_{\sigma,3} f_{\sigma,4} + \tfrac{2}{3}\Delta_\sigma K_{\sigma,2} f_{\sigma,5} + \tfrac{4}{3}\Delta_\sigma K_{\sigma,1} f_{\sigma,6} + \left(\tfrac{1}{3}\Delta_\sigma K_{\sigma,0} + e^{-\Pi_\sigma}\right) f_{\sigma,7}$$

FIG. 2-5 EQUATIONS 2-56

GENERALLY FOR ANY EVEN VALUE OF m:

$$f_{g,N-m} = 1 - e^{-\Pi_g} - \left(\tfrac{1}{3}K_{g,m} + \tfrac{4}{3}K_{g,m-1} + \tfrac{2}{3}K_{g,m-2} + \tfrac{4}{3}K_{g,m-3} + \tfrac{2}{3}K_{g,m-4} + \cdots + \tfrac{2}{3}K_{g,2} + \tfrac{4}{3}K_{g,1} + \tfrac{1}{3}K_{g,0}\right)\Delta_g + \tfrac{1}{3}\Delta_g K_{g,m} f_{g,0}$$
$$+ \tfrac{4}{3}\Delta_g K_{g,m-1} f_{g,1} + \tfrac{2}{3}\Delta_g K_{g,m-2} f_{g,2} + \tfrac{4}{3}\Delta_g K_{g,m-3} f_{g,3} + \tfrac{2}{3}\Delta_g K_{g,m-4} f_{g,4} + \cdots + \tfrac{2}{3}\Delta_g K_{g,2} f_{g,m-2}$$
$$+ \tfrac{4}{3}\Delta_g K_{g,1} f_{g,m-1} + \left(\tfrac{1}{3}\Delta_g K_{g,0} + e^{-\Pi_g}\right) f_{g,m}$$

FOR ANY ODD VALUE OF m LARGER THAN 3:

$$f_{g,N-m} = 1 - e^{-\Pi_g} - \left(\tfrac{3}{8}K_{g,m} + \tfrac{9}{8}K_{g,m-1} + \tfrac{9}{8}K_{g,m-2} + \tfrac{17}{24}K_{g,m-3} + \tfrac{4}{3}K_{g,m-4} + \tfrac{2}{3}K_{g,m-5} + \tfrac{4}{3}K_{g,m-6} + \tfrac{2}{3}K_{g,m-7} + \cdots + \tfrac{2}{3}K_{g,2}\right.$$
$$\left. + \tfrac{4}{3}K_{g,1} + \tfrac{1}{3}K_{g,0}\right)\Delta_g + \tfrac{3}{8}\Delta_g K_{g,m} f_{g,0} + \tfrac{9}{8}\Delta_g K_{g,m-1} f_{g,1} + \tfrac{9}{8}\Delta_g K_{g,m-2} f_{g,2} + \tfrac{17}{24}\Delta_g K_{g,m-3} f_{g,3}$$
$$+ \tfrac{4}{3}\Delta_g K_{g,m-4} f_{g,4} + \tfrac{2}{3}\Delta_g K_{g,m-5} f_{g,5} + \tfrac{4}{3}\Delta_g K_{g,m-6} f_{g,6} + \tfrac{2}{3}\Delta_g K_{g,m-7} f_{g,7} + \cdots + \tfrac{2}{3}\Delta_g K_{g,2} f_{g,m-2}$$
$$+ \tfrac{4}{3}\Delta_g K_{g,1} f_{g,m-1} + \left(\tfrac{1}{3}\Delta_g K_{g,0} + e^{-\Pi_g}\right) f_{g,m}$$

FIG. 2-5 (CONT.) EQUATIONS 2-56

The functions K defined by Eq. 2-39 and -41 always take positive values and can be evaluated by means of tables of Bessel functions.[1] For values of $2\sqrt{\pi(\xi - \epsilon)}$ greater than 4, the following formula[2] can be used to determine $J_1(ix)$:

$$J_1(ix) = \frac{ie^x}{\sqrt{2\pi x}}\left\{1 - \frac{0.375}{x} - \frac{0.1171875}{x^2} - \frac{0.10253906}{x^3} - \frac{0.1441956}{x^4} - \frac{0.2775764}{x^5} - \ldots\right\} \qquad (2\text{-}57)$$

Once the distributions of f_a and f_g are established the regenerator effectiveness can be calculated as shown in Section 2-7. Also, the temperature at any point in the matrix can be determined by means of Eq. 2-33 and -35. Further, the temperature distributions of the fluids can be calculated by means of Eq. 2-12.

2-6 Numerical Calculation of Balanced Regenerators

In the case that $\Lambda_a = \Lambda_g = \Lambda$ and $\Pi_a = \Pi_g = \Pi$ a symmetry occurs in the two sets of algebraic equations of Section 2-5.8 which makes them identical, namely,

$$f_{g,N-m} = 1 - f_{a,m} \qquad (2\text{-}58)$$

In this case it is sufficient to solve just one set of equations and to employ Eq. 2-58.

2-7 Regenerator Effectiveness obtained from Numerical Calculations

In this section the effectiveness is calculated from the viewpoint of the heat capacity of the matrix. The matrix enters the cold stream with a certain enthalpy and leaves it to enter the hot stream with a lower enthalpy. In steady conditions, the difference between these two enthalpies

---

[1] See, for example, E. Jahnke and F. Emde, Tables of Functions with Formulae and Curves, Dover Publications, New York, 1945; p. 227.

[2] Ibid., pp. 137-138.

is the actual amount of heat energy transferred from the matrix to the cold stream; an equal amount of energy is picked up by the matrix as it traverses the hot stream.

The ideal amount of heat energy transferred is the quantity that the cold air would pick up if its temperature had been raised to that of the incoming hot gas. The ratio of the actual total amount to the ideal total amount is the regenerator effectiveness. The following calculations are made with the above procedure in mind.

For a unit width of matrix, the rate at which heat is carried by the matrix as it moves into the cold stream is

$$\frac{q'_a}{\theta_{g,o} - \theta_{a,o}} = \int_0^L vC''' f_a(\xi_a)\, dx$$

$$= vC''' \cdot \frac{m''_a c_{p,a}}{h_a S'''} \int_0^{\Lambda_a} f_a(\xi_a)\, d\xi_a \qquad (2\text{-}59)$$

Similarly, the rate at which heat is carried by the matrix as it moves out of the cold air is

$$\frac{q'_g}{\theta_{g,o} - \theta_{a,o}} = vC''' \cdot \frac{m''_g c_{p,g}}{h_g S'''} \int_0^{\Lambda_g} f_g(\xi_g)\, d\xi_g \qquad (2\text{-}60)$$

The ideal rate of heat transfer would be obtained if the temperature of the cold air would change from $\theta_{a,o}$ to $\theta_{g,o}$. Accordingly,

$$\frac{q'_i}{\theta_{g,o} - \theta_{a,o}} = m''_a c_{p,a} Y^* \qquad (2\text{-}61)$$

Hence, the regenerator effectiveness is

$$\eta_{Reg} = \frac{q'_a - q'_g}{q'_i}$$

$$= \frac{1}{\Pi_a} \int_0^{\Lambda_a} f_a(\xi_a)\, d\xi_a - \frac{1}{\Pi_g} \cdot \frac{m''_g c_{p,g} Y^*_g}{m''_a c_{p,a} Y^*_a} \int_0^{\Lambda_g} f_g(\xi_g)\, d\xi_g \qquad (2\text{-}62)$$

The integrals in Eq. 2-62 are conveniently evaluated in terms of the numerical values of f_a and f_g obtained from the solution outlined in

Section 2-5. Applying Simpson's rule for the case that the number of intervals N is even,

$$\int_0^{\Lambda} f(\xi)\, d\xi = \frac{\Delta}{3}\left[f_0 + 4f_1 + 2f_2 + 4f_3 + 2f_4 + \cdots + 2f_{N-2} + 4f_{N-1} + f_N\right] \qquad (2\text{-}63)$$

And if N is odd, the technique of Section 2-5.7 may be employed with the result that

$$\int_0^{\Lambda} f(\xi)\, d\xi = \frac{\Delta}{3}\left[\frac{9}{8} f_0 + \frac{27}{8} f_1 + \frac{27}{8} f_2 + \frac{17}{8} f_3 + 4f_4 + 2f_5 + 4f_6 + 2f_7 + \cdots + 2f_{N-2} + 4f_{N-1} + f_N\right] \qquad (2\text{-}64)$$

2-8 Results of the Theory of the Balanced Regenerators

The results of Hausen's analytical solution or of the corresponding numerical calculations are most conveniently represented graphically.

Figures 2-6 and -7 give the effectiveness of balanced regenerators for values of Λ and Π in the range of practical interest. The curves were drawn from data given by Johnson (Ref. 15). In Fig. 2-8 curves of constant utilization factor are presented. The graphs illustrate the following properties of regenerators:

(1) For a given effectiveness there is a minimum reduced length Λ below which that effectiveness cannot be attained.

(2) An increase in the reduced length Λ (or actual length L) is more effective in the case of a regenerator with a small value of Λ than one with a large value of Λ.

(3) For a given value of Λ, the effectiveness decreases as Π increases. This effect is quite large for small values of Λ.

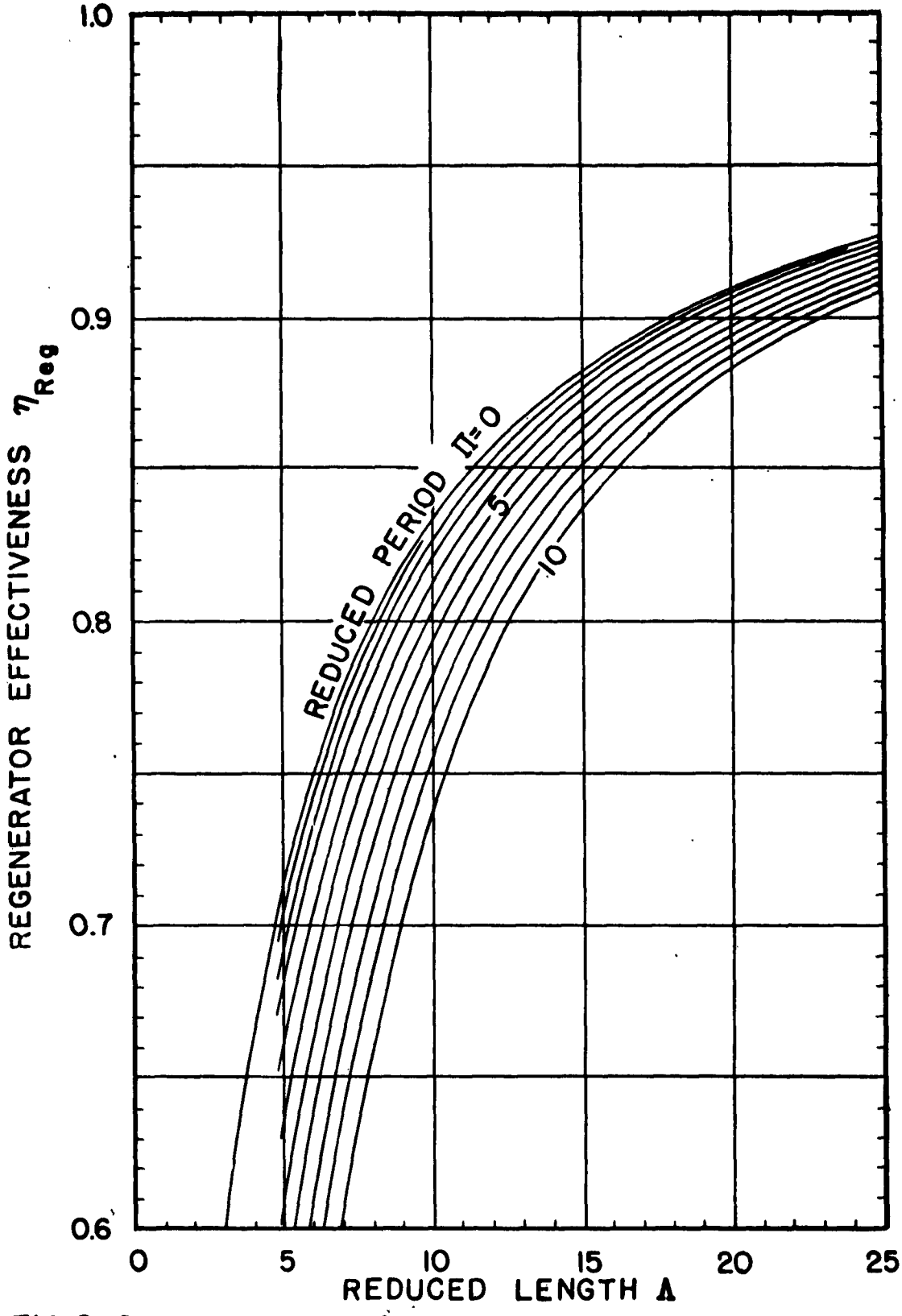

FIG.2-6 EFFECTIVENESS OF BALANCED REGENERATORS

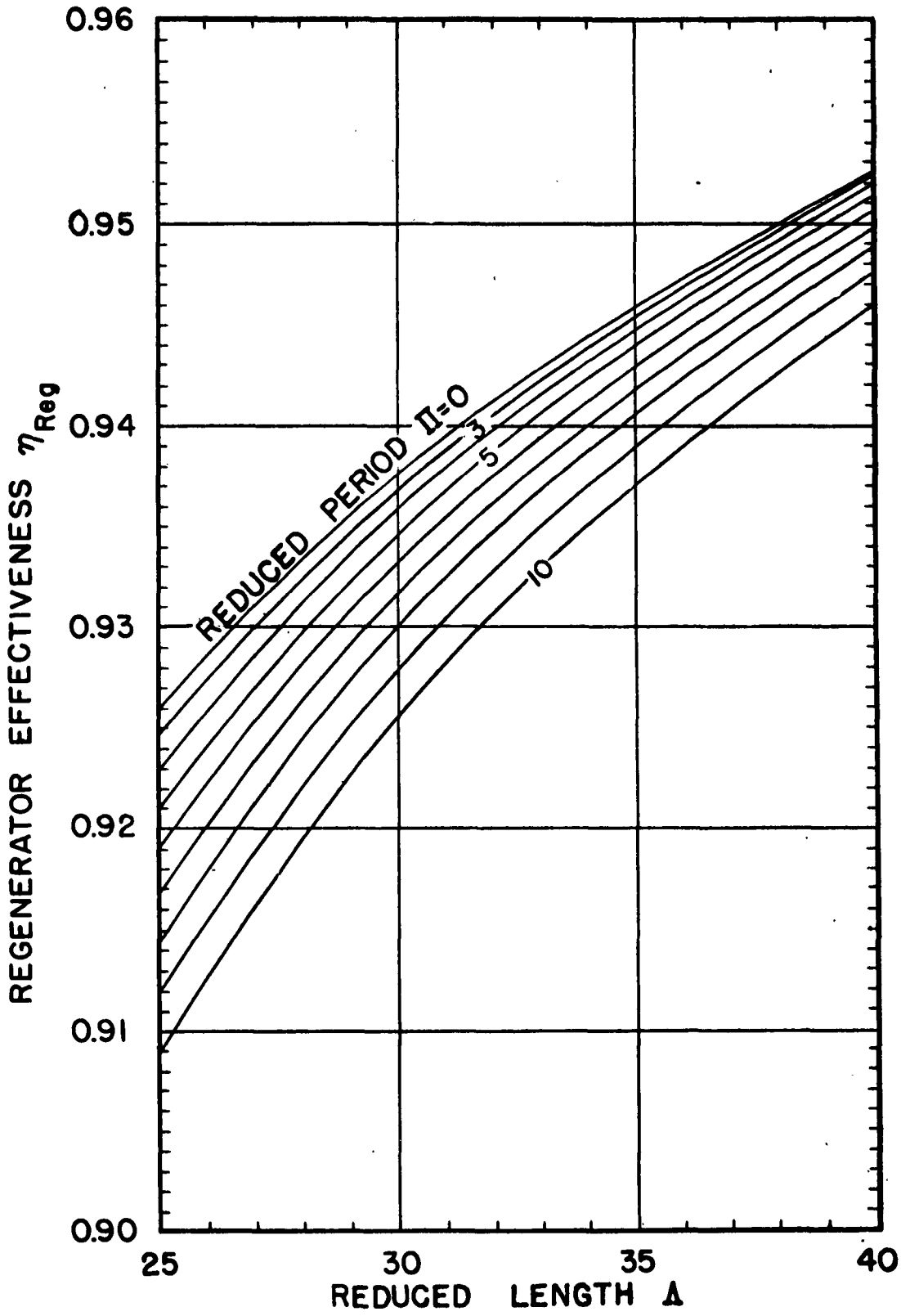

FIG.2-7 EFFECTIVENESS OF BALANCED REGENERATORS

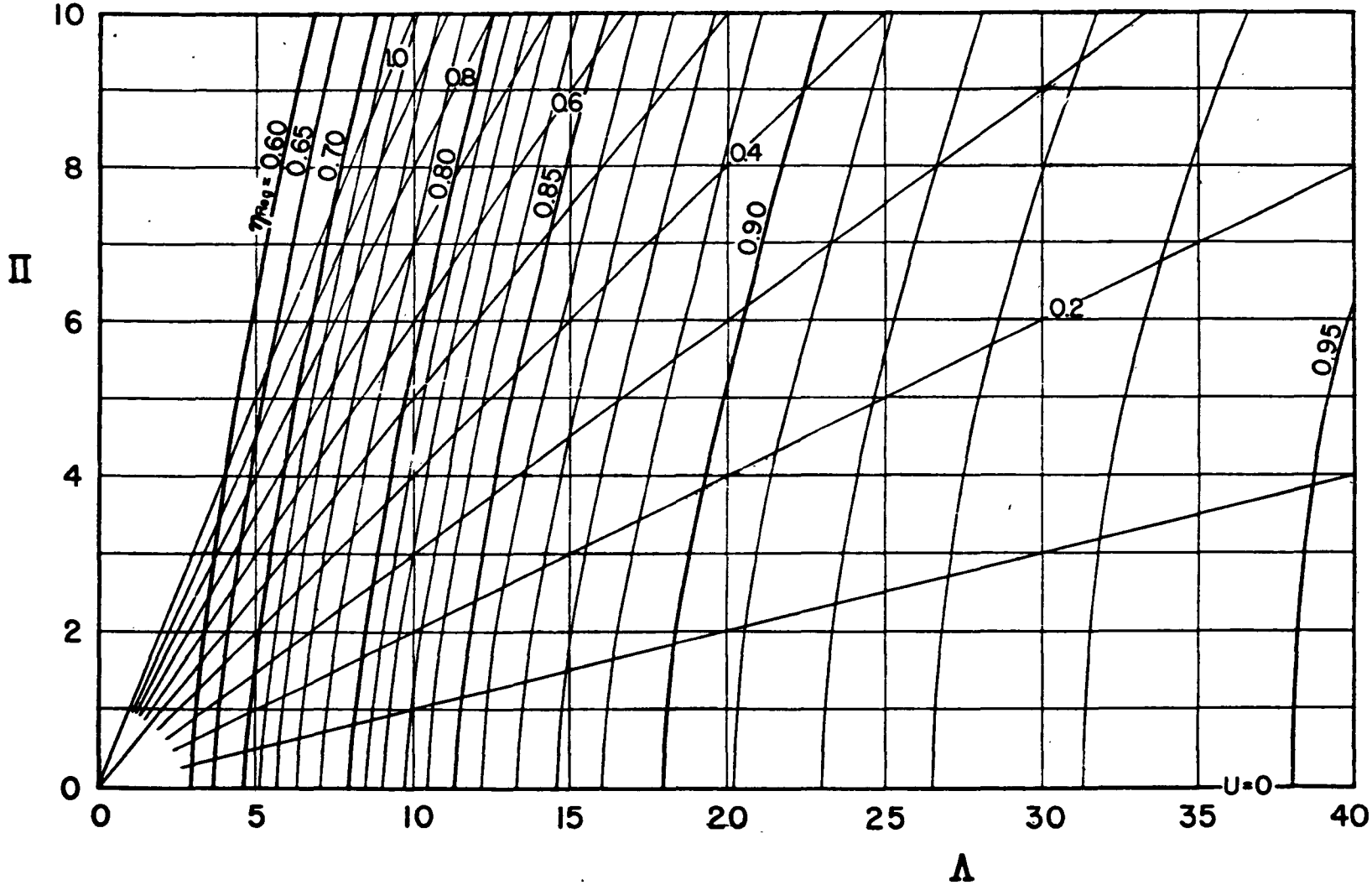

FIG. 2-8 PERFORMANCE CHART FOR BALANCED REGENERATORS

2-9 Unbalanced Regenerators

The results of Section 2-8 can be used to obtain the effectiveness of unbalanced regenerators, at least in the range of practical application. A method of procedure suggested by Saunders and Smoleniec (Ref. 25), namely, to employ a system of arithmetic averages, has been found to yield results which deviate from the exact values. Two methods of procedure, based on harmonic averages, have been found to give virtually equal values and better accuracy when compared with results determined by the much more lengthy procedure described in Sections 2-5 and -7. In the next two sections it is supposed that the parameters Λ and Π on both sides of the regenerator are known.

2-9.1 Use of Harmonic Means of Dimensionless Lengths

First, the harmonic means of Λ_a and Λ_g and of Π_a and Π_g are determined:

$$\frac{2}{\Lambda_m} = \frac{1}{\Lambda_a} + \frac{1}{\Lambda_g}; \qquad \frac{2}{\Pi_m} = \frac{1}{\Pi_a} + \frac{1}{\Pi_g} \tag{2-65}$$

Second, employing charts for the balanced regenerator find $\eta_{Reg,m}$ using the calculated values of Λ_m and Π_m. The effectiveness $\eta_{Reg,m}$ is practically equal to the effectiveness of the given unbalanced regenerator.

2-9.2 Use of Harmonic Mean of Effectiveness

Hausen suggested the following procedure. Determine the effectiveness $\eta_{Reg,a}$ of a balanced regenerator with parameters Λ_a and Π_a and the effectiveness $\eta_{Reg,g}$ of a balanced regenerator with parameters Λ_g and Π_g. Then the effectiveness of the given unbalanced regenerator is practically the harmonic mean. Thus,

$$\frac{2}{\eta_{Reg,m}} = \frac{1}{\eta_{Reg,a}} + \frac{1}{\eta_{Reg,g}} \tag{2-66}$$

2-10 Effect of Curvature in the Drum-Type Matrix

In Appendix A it is shown that a simple transformation allows all results of the calculations for a flat matrix to be employed in dealing with

a drum-type matrix. The major changes occur in the transformations of Section 2-2.6, where ξ and η are defined. The new values of ξ and η are

$$\xi = \frac{hS'''}{m'c_p} \cdot 2\pi K \cdot \frac{r^2 - r_i^2}{2} \tag{2-67}$$

and

$$\eta = \frac{hS'''}{C'''} \frac{\phi}{\omega} - \frac{2\pi K \rho \beta}{m'} \cdot \frac{r^2 - r_i^2}{2} \tag{2-68}$$

In these equations m' is the mass rate of fluid flow per unit length of the regenerator axis; K is the fraction of the circle subtended by the fluid in question; r is a general radial distance; r_i is the inner radius of the drum; ϕ is the angle measured from the plane of entrance; and ω is the angular speed. These coordinates allow for the changes of temperature distributions caused by the curvature of the matrix.

The corresponding new values of Λ and Π are:

$$\Lambda = \frac{hS'''}{m''_m c_p} L \tag{2-69}$$

and

$$\Pi = \frac{hS'''}{C'''} \cdot \frac{2\pi K}{\omega} \tag{2-70}$$

where L is the thickness of the drum and m''_m is the mass velocity of the fluid at the mean radius of the drum.

2-11 Simplified Theories for Regenerators with Small Reduced Periods

In aircraft applications, the reduced periods for the regenerators are rather short, of the order of magnitude of 5. The short reduced periods can be due either to high matrix speed v or to the small ratio of the water equivalents of the flowing fluids to that of the "flowing" matrix.

For infinitely short periods, i.e., for $\Pi_a = \Pi_g = 0$, Nusselt (Ref. 22) showed that the regenerator would have the same thermal characteristics as a recuperator. Under this condition, the matrix temperature depends only on x (or ξ), is independent of y^* (or η), and is the same in the two streams. Also, the temperatures of the two fluids are functions of x only. For this problem, Nusselt considered both the balanced and unbalanced cases.

Iliffe (Ref. 13) further showed that for unbalanced regenerators with infinitely short periods, if $m''_a c_{p,a} Y^*_a = m''_g c_{p,g} Y^*_g$, then the effectiveness would be that of an unbalanced recuperator, namely,

$$\eta_{Rec} = \frac{1}{1 + \frac{1}{\Lambda_a} + \frac{1}{\Lambda_g}} \tag{2-71}$$

For balanced regenerators this reduces to the balanced recuperator effectiveness,

$$\eta_{Rec} = \frac{\Lambda}{\Lambda + 2} \tag{2-72}$$

According to Tipler (Ref. 29), the problem of the high-speed regenerator with linear temperature distributions of the matrix was solved by Lubbock and Bowen (Ref. 19). The general assumptions of Hausen's theory are the basis of the solution. Tipler represents the results as follows:

$$\frac{\Lambda_a}{\Pi_a} \cdot \frac{2}{\eta_{Reg}} = \coth \frac{\Pi_a}{2 + \Lambda_a} + \coth \frac{\Pi_g}{2 + \Lambda_g} \tag{2-73}$$

Tipler compared values of η_{Reg} thus obtained with those from Hausen's theory for balanced regenerators. He found that for $\Pi = 0$ the agreement is good and that for other values the effectiveness derived by this method is less than Hausen's values. For values of Π up to 10 the error is within 4 per cent. Up to $\Pi = 5$, which covers a large range of practical interest, the maximum error is 1 per cent.

Corbitt (see discussion of Ref. 13) presents the simple equation,

$$\eta_{Reg} = \eta_{Rec} \left(1 - \frac{U^2}{9}\right) \qquad (2\text{-}74)$$

where η_{Rec} is the value obtained from Eq. 2-71 or -72. This relation appears to be accurate within 1 per cent in the range of η_{Reg} from 0.8 to 0.98 and of U from 0 to 0.6.

2-12 Effect of Conductivity on Regenerator Performance

The assumption of Section 2-1.4, which specifies that the matrix be made of a certain type of thermally non-isotropic solid, cannot be exactly fulfilled in practice. In the next sections the influences of conduction in the matrix are considered.

2-12.1 Conductivity in the x-Direction

When the general procedure of Section 2-2 is followed and the conductivity in the x-direction is admitted to the problem, Eq. 2-5 appears with another term:

$$m''c_p \frac{\partial \theta}{\partial x} + C''' v \frac{\partial t}{\partial y} + \rho \beta v c_p \frac{\partial \theta}{\partial y} - k(1 - \beta) \frac{\partial^2 t}{\partial x^2} = 0 \qquad (2\text{-}75)$$

where k is the effective conductivity of the matrix in the x-direction. Also, Eq. 2-7 would be replaced by

$$vC''' \frac{\partial t}{\partial y} = - hS''' (t - \theta) + k(1 - \beta) \frac{\partial^2 t}{\partial y^2} \qquad (2\text{-}76)$$

Equation 2-9 would, therefore, remain unchanged and together with Eq. 2-76 would determine the rate of heat transfer in the regenerator. It appears that this general problem has never been solved analytically.

However, the case of infinitely large conductivity in the x-direction was solved by Nusselt (Ref. 22). In this case the matrix temperature is independent of x and the maximum effectiveness is 0.5. This theory could possibly be applied to very short matrices.

Also, Hahnemann (Ref. 8) solved the special problem of the case that $\Pi_a = \Pi_g = 0$. Here the heat capacity is not a criterion of performance; it may take any value without affecting values of Π or Λ. Hahnemann found that to represent the results he could use the parameter,

$$\Phi \equiv \frac{hS''L}{\frac{k(1-\beta)}{L}} \qquad (2\text{-}77)$$

which represents the ratio between the heat transfer by convection and that by conduction. It may be observed that Φ increases as k decreases, so that for a matrix with zero conduction in the x-direction, as assumed by Hausen, $\Phi = \infty$.

The essential results of Hahnemann's work are shown in Fig. 2-9.* Hausen's matrix is represented by the straight, diagonal line for $\Phi = \infty$. It is observed that as Φ decreases (i.e., k increases), the regenerator effectiveness decreases. For a given value of Φ, there is an optimum value of Λ, at which the regenerator effectiveness is a maximum.

The last observation may be explained as follows: The general tendency, as shown in Fig. 2-9, is that η_{Reg} rises with increasing Λ. However, if Λ is already large, then the rate of change of η_{Reg} with respect to Λ is rather small. Now, suppose that Λ is already large and is increased by diminishing m'', say, by increasing the superficial cross-sectional area of flow. This change would have no influence on Φ. However, the heat conduction per unit rate of flow would increase, and at a certain value of Λ, namely, the optimum value, this loss due to the increase of conduction offsets the gain due to the increase of Λ. As Λ is increased further, the conduction losses become excessive and η_{Reg} diminishes.

Another parameter used in Fig. 2-9 is the quantity, $\Lambda/\Phi \equiv k(1-\beta) / (m'' c_p L)$. It may be considered as the ratio of the rate of heat conduction along the matrix to the rate at which heat is carried by the fluid. Cox and Stevens (Ref. 5) used Hahnemann's results for balanced regenerators to plot Fig. 2-10, which covers the range of interest in regenerator design. Again, the parameter is Λ/Φ. This

* This figure was deleted from this report. It is available in the literature cited as Reference 8.

NOTE

This figure has been deleted from this technical report, but is available in the literature cited as Reference 8 of this report.

FIG. 2-10 EFFECT OF CONDUCTION ALONG THE MATRIX ON THE EFFECTIVENESS OF THERMALLY BALANCED REGENERATORS WITH $\Pi = 0$

parameter would seldom be more than 0.02, which in the usual range of operation reduces the regenerator effectiveness by less than 0.015. For most design purposes the effect of conductivity in the matrix could be neglected. It is advisable to check this effect when dealing with very short matrices.

2-12.2 Conductivity in the z-Direction

In the main theory the matrix was assumed homogeneous (see Section 2-1.1). This implies that solid particles, as well as voids, have infinitesimal volumes. Under such conditions, each solid particle would be affected directly by the flowing fluids while neighboring solid particles would not affect each other. A real matrix, however, consists of solid elements of finite size, and some solid particles do not come in direct contact with the fluids but exchange heat by conduction through neighboring particles. For example, if one considers a matrix built of solid strips as shown in Fig. 2-11, then the particles at the center of a strip are heated and cooled by virtue of the heat conduction through particles lying between the center and the surface. If those strips are of infinitesimal thickness, then each solid particle would exchange heat directly with the flowing fluids and the original assumptions would still be satisfied. Also, if the conduction of the strip in the z-direction is infinitely large (while that in the x- and y-directions are zero), then the original assumptions are also satisfied, because there would be no resistance to heat flow between the flowing fluids and the inner solid particles.

The case of a matrix with finite conductivity in the z-direction and zero conductivity in the x- and y-directions was considered by Nusselt (Ref. 22). He gave a graphical method of solution. Ackermann (Ref. 1), a student of Nusselt, undertook an analytical solution and developed an iterative method which is very tedious.

The effect of finite conductivity in the z-direction was estimated by Tipler (Ref. 29) in the following manner: He considered the case of a slab whose surface temperatures change sinusoidally. He calculated the heat stored in the slab at the peak surface temperature and

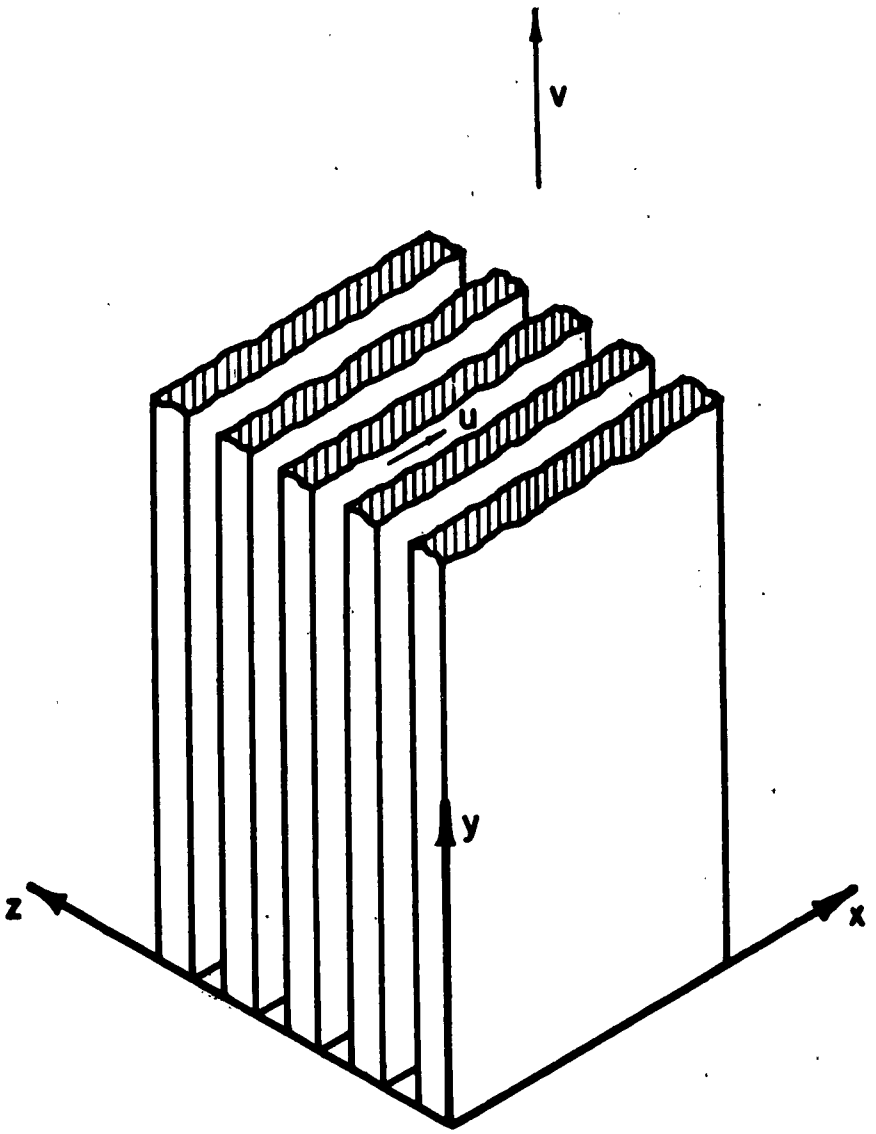

FIG.2-11 REGENERATOR WITH MATRIX COMPOSED OF RIBBONS

compared it with the heat that would be stored in the slab had it been of infinite conductivity. He found that the ratio of the two amounts would be 0.99 or more for practical regenerators. Hence, for all practical purposes, the effect of finite conductivity in the z-direction can be neglected.

Nusselt (Ref. 22) also gave a solution for the case of a strip matrix with infinitely large conductivity in the x-direction, zero conductivity in the y-direction, and finite conductivity in the z-direction. The solution was given as expressions of t and θ in Fourier series in terms of y and z.

2-12.3 Conductivity in the y-Direction

In the main theory the effective conductivity in the y-direction is assumed to be zero. The case of finite conductivity in that direction seems never to have been considered in the literature. However, the case of infinitely large effective conductivity in the y-direction is equivalent to that of infinitely high matrix speed v, which has been discussed in Section 2-11.

2-13 Effect of Leakage on Regenerator Performance

The theoretical treatments are based on the assumption that no leakage occurs. In practice the leakage diminishes the effectiveness by cooling the hot gas before its heat capacity can be most fully utilized in the matrix.

Harper and Rohsenow (Ref. 9) calculated the reduction in the regenerator effectiveness assuming that half the leakage occurs at either side of the matrix. Their results are shown in Fig. 2-12 for several values of fractional leakage $\Delta m/m$. One may employ this chart to obtain the effectiveness η^*_{Reg} of a regenerator with leakage. If it were assumed that all leakage occurs at the downstream air-side of the matrix (i.e., leakage into the gas at the upstream end of the gas-side) the correction would be nearly doubled, with further reduction of the effectiveness. However, it is more probable that the leakage would be less on the

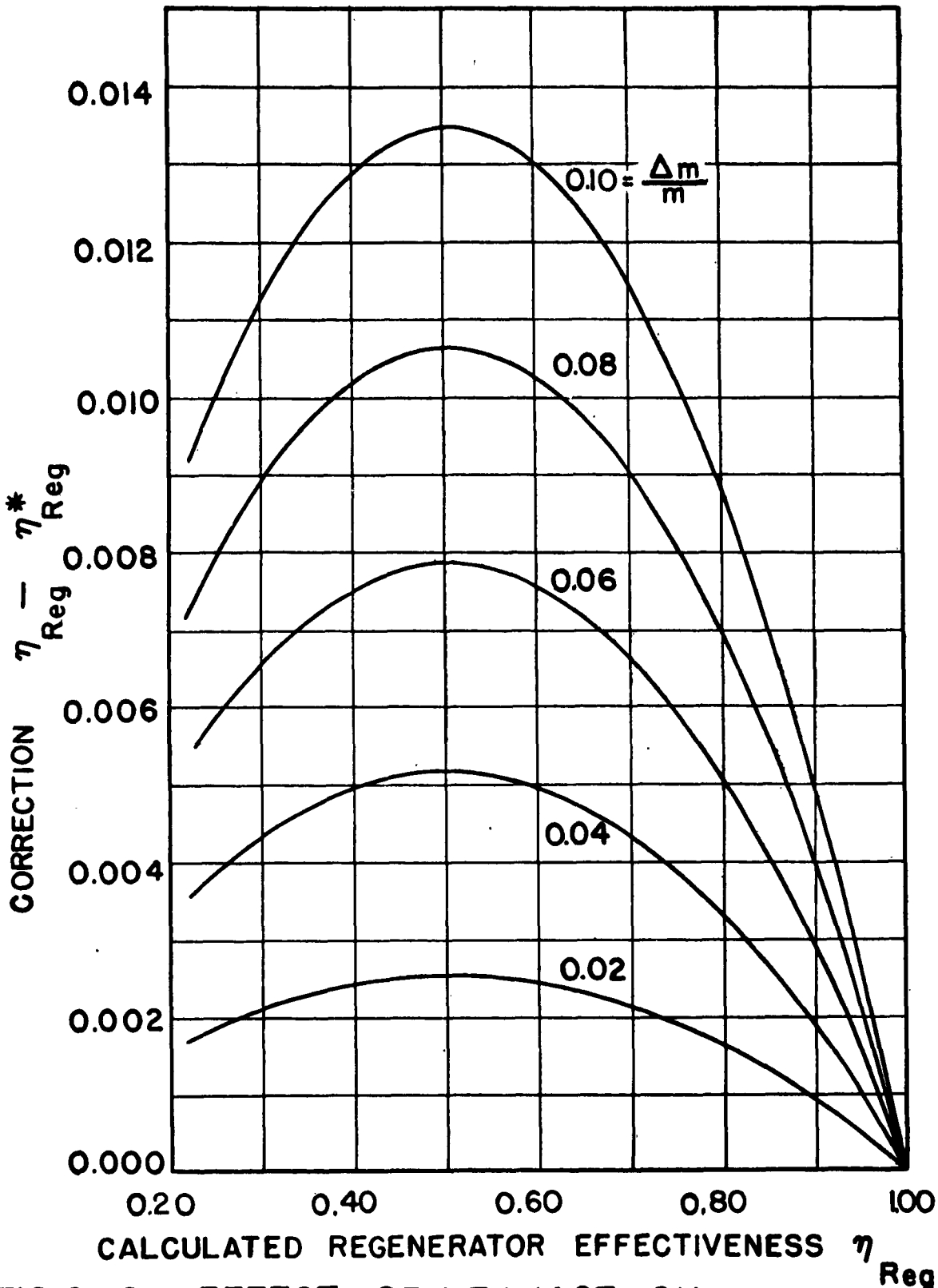

FIG. 2-12 EFFECT OF LEAKAGE ON REGENERATOR EFFECTIVENESS

downstream air-side than on the upstream side. Consequently, an effectiveness calculated by means of the chart in Fig. 2-12 would be slightly low.

For the practical range of effectiveness and for tolerable values of the leakage, the correction is about 0.01, which is not serious. However, the effect of leakage on the thermal efficiency of the entire gas turbine power plant is a serious matter. This subject receives detailed attention in Chapter 4.

Chapter 3: PROPERTIES OF REGENERATOR MATRICES

3-1 Void and Solid Fractions

Several geometric properties and some of the mechanical and thermal properties of matrices are readily expressed in terms of the void fraction, which is denoted by β. The co-value, the solid fraction $(1 - \beta)$, of a given matrix of mass m_s and corresponding total volume V_{tot} is the ratio of the apparent density to the true density of the solid:

$$(1 - \beta) = \frac{m_s}{V_{tot}\,\rho_s} = \frac{\rho_{s,app}}{\rho_s} \qquad (3\text{-}1)$$

It is recommended that Eq. 3-1 be employed as the operational definition of a rather simple laboratory procedure to determine β for matrices of heterogeneous construction having unknown packability.

3-1.1 Flame Trap Matrices

The void fraction of flame trap matrices is equal to the ratio of through area to facial area. This ratio is easily calculated if the passages repeat themselves in any uniform way.

3-1.2 Wire Screen Matrices

Consider screens made of wires having uniform diameter D expressed in feet. The number of wires per foot in one direction is n_1 and in the other n_2; the screens are stacked so that the number of layers per foot of length is n_3; then neglecting any bends of the wire, the solid fraction is

$$(1 - \beta) = \frac{\pi}{4} D^2 (n_1 + n_2)\, n_3 \qquad (3\text{-}2)$$

If the screens are closely packed, $n_3 \approx 1/(2D)$ and

$$(1 - \beta) = \frac{\pi}{8} D(n_1 + n_2) \qquad (3\text{-}3)$$

Further, if $n_1 = n_2 = n$, then

$$(1 - \beta) = \frac{\pi}{4} D \cdot n \qquad (3\text{-}4)$$

3-2 Heat Transfer Surface Area per Unit Volume

The effective heat transfer surface per unit volume of matrix is

$$S''' = \frac{S}{V_{tot}} = \frac{S(1-\beta)}{(m_s/\rho_s)} \tag{3-5}$$

The last expression allows S''' to be evaluated in terms of the mass of the solid material used to build the matrix, if it can be assumed that the contact areas are negligible compared with the areas exposed to the fluids.

For example, consider a matrix made of any metal strips of uniform rectangular cross section; let a be the thickness and b the breadth of the strips. If the total length of the strip is l, the total surface area is $2(a + b)\,l$, and its mass is $ab \cdot l \cdot \rho_s$. Consequently, for such a matrix Eq. 3-5 yields

$$S''' = \frac{2(1-\beta)}{a}\left(1 + \frac{a}{b}\right) \tag{3-6}$$

And if the strip is very thin, so that $a \ll b$,

$$S''' = \frac{2(1-\beta)}{a} \tag{3-7}$$

In a similar way, if wire of diameter D is used to construct the matrix, Eq. 3-5 becomes

$$S''' = \frac{4(1-\beta)}{D} \tag{3-8}$$

In particular, if the wires are in the form of closely packed screens of square mesh (n by n wires per foot),

$$S''' = \pi n \tag{3-9}$$

3-3 Free Area of Fluid Flow

The free flow area is needed to evaluate the velocity through the matrix interstices, which is of interest in determining the pressure drop

and heat transfer characteristics of the matrix. In the following discussion it will be convenient to denote the ratio of the free flow area to the facial area by the symbol α.

In a flame trap matrix $\alpha = \beta$. However, in matrices of heterogeneous construction and even in orderly wire-screen matrices, the free flow area becomes a rather nebulous quantity. In the special case of closely packed wire screens the following approximation has been employed:

$$\alpha = (1 - n_1 D)(1 - n_2 D) \tag{3-10}$$

Further, if $n_1 = n_2 = n$,

$$\alpha = (1 - nD)^2 \tag{3-11}$$

Notice that the free flow area obtained by using α lies in a plane normal to the main direction of flow. However, as in the case of tube banks it may be desirable to employ the absolute minimum cross-sectional area when dealing with the pressure drop and heat transfer properties of matrices; this minimum may be in an oblique plane.

3-4 Equivalent Diameter

In the case of turbulent flow inside tubes, it has been found that both pressure drop and heat transfer data obtained with passages of many different shapes are well correlated if the so-called equivalent diameter is employed as characteristic length in the dimensionless groups. The equivalent diameter is

$$D_e \equiv \frac{4 \cdot (\text{cross-sectional area})}{\text{wetted perimeter}} \tag{3-12}$$

In the case of laminar flow, the use of the equivalent diameter has not been quite so satisfactory and a separate correlation is needed for each shape. Nevertheless, much data are often presented in terms of D_e.

For a wire screen matrix, Eq. 3-12 yields

$$D_e = \frac{4\alpha A}{(S/L)} = \frac{4\alpha}{S^m} \tag{3-13}$$

It follows that if the screens are of uniform mesh and closely packed,

$$D_e = \frac{4(1 - Dn)^2}{\pi n} \tag{3-14}$$

3-5 Matrix Heat Capacity

The heat capacity of a matrix is equal to the product of its mass and the specific heat of the material. It follows that the heat capacity per unit volume of the matrix is

$$C^m = (1 - \beta)\, \rho_s\, c_{p,s} \tag{3-15}$$

3-6 Pressure Losses

The static pressure drop from the inlet duct to the outlet duct on either side of the regenerator may be treated as though the matrix were a recuperator, particularly if the matrix is of the flame trap type. Thus, the pressure drop is comprised of three parts: the entrance or contraction loss, the core or frictional loss, and the exit or expansion loss. From an equation used by Kays (Ref. 16) and by Kays and London (Ref. 17), we may write

$$p_1 - p_2 = \frac{G^2}{\alpha^2 \cdot 2g\gamma_1}\left[(K_c + \frac{T_2}{T_1} K_{ex}) + (1 + \alpha^2)(\frac{T_2}{T_1} - 1) + f \cdot \frac{L}{D_e} \cdot \frac{T_b}{T_1}\right] \tag{3-16}$$

where K_c and K_{ex} are respectively the contraction and expansion coefficients based on the dynamic pressure inside the core; T is the absolute temperature, subscripts 1 and 2 corresponding to the inlet and exit conditions, respectively; f is the friction factor of the core, also based on the dynamic pressure in the core; D_e is the equivalent diameter of the core passages; T_b is the bulk mean temperature of the

fluid; $[p] = lb/ft^2$; $[\gamma_1] = lb/ft^3$; and[1] $[G] = lb/sec\ ft^2$.

In most cases, the effects of the entrance and exit are relatively small compared with the frictional losses. Therefore, it usually is unnecessary to evaluate K_c and K_{ex} with great accuracy; values in the literature for reasonably similar situations may be employed. For example, Kays (Ref. 16) has given values for some tubular constructions. In the case of wire screen matrices of reasonable length only the last two terms in the brackets of Eq. 3-16 need be considered because the other is, relatively, rather small.

The friction coefficients f for laminar flow in matrices have been correlated by means of the typical expression,

$$f = \frac{C}{N_{Re}^n} \tag{3-17}$$

where

$$N_{Re} = \frac{G\,D_e}{\alpha \cdot \mu} \tag{3-18}$$

3-6.1 Friction Factors for Flame Trap Matrices

Locke (Ref. 18) found that the friction coefficient for smooth flame trap regenerators composed of round tubes lies within 2 per cent of the theoretical values obtained using $C = 64$.

Romie et al (Ref. 24) performed pressure drop tests on two flame trap matrices, one made of flat plates and one of cylindrical tubes. After taking the entrance and exit losses into account, the authors found that the corresponding theoretical values, namely, $C = 96$ for the flat plates and $C = 64$ for the tubes, were in fair agreement with the experimental values, particularly if $N_{Re} < 1000$.

---

[1] The mass velocity G is based on the facial or superficial area. This is to be distinguished from a mass velocity based on the free or through area of flow. In our symbols the mass velocity based on the free area is G/α. A bracketed expression [...] is to be read, "the units of ... are".

Johnson (Ref. 15) performed single-blow tests on matrix materials of two shapes shown in Fig. 3-1. The lengths were varied from 0.073 to 0.292 ft by employing one, two, or four elements in series. The range of the Reynolds number was 25 to 200. His experimental results were correlated by means of Eq. 3-17 with $C = 17.7$ and $n = 0.78$ for the matrix material of 0.030-in. spacing and $C = 29.8$ and $n = 0.87$ for the material of 0.021-in. spacing. The maximum deviation of the experimental points from the mean correlating lines was about 25 per cent, but on the average it was about $\pm$ 15 per cent.

Cox and Lamb (Ref. 4) employed six flame trap matrices on a model rotary disk type regenerator. The matrices were made with triangular passages of a type similar to the ones used by Johnson. The ratio L/D_e took values from 31.2 to 82.5, and the Reynolds number varied from about 50 to 400. The authors' correlation can be represented by Eq. 3-17 if $n = 1$ and

$$C = 44 + (1.66 - \alpha^2) \frac{N_{Re}}{(L/D_e)} \qquad (3\text{-}19)$$

In their work, α lay between 0.7 and 0.83.

3-6.2 Friction Factors for Wire Screen Matrices

Johnson (Ref. 15) performed tests on four wire screen matrices. Results of the work and a description of the matrices are presented in Fig. 3-2. It may be noticed that the constructions of Matrices A and B apparently differ only in the total number of layers. The results from Matrices C and D, which have the same void fraction, have been correlated with a single curve. The dotted line may be represented by Eq. 3-17 with $C = 25$ and $n = 0.5$.

Jakob, Kezios, and Sogin (Ref. 14) performed steady-state tests on a wire screen matrix of 0.0075-in. diameter wire and 35 mesh; there were 79 layers, and the matrix length was 1 inch. The authors found a virtually uniform value for f, namely, 4.8, in the range of N_{Re} from about 900 to 1200.

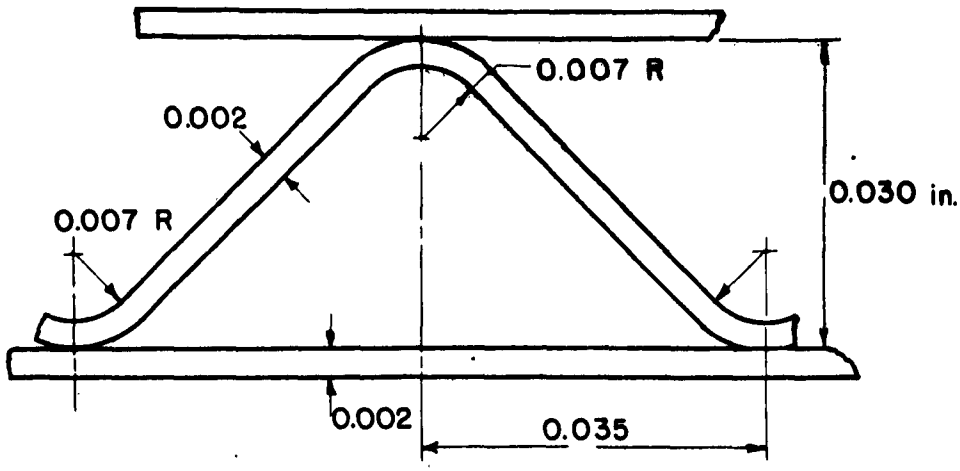

$\alpha = 0.039$

$D_e = 0.00198$ ft

0.030 spacing.

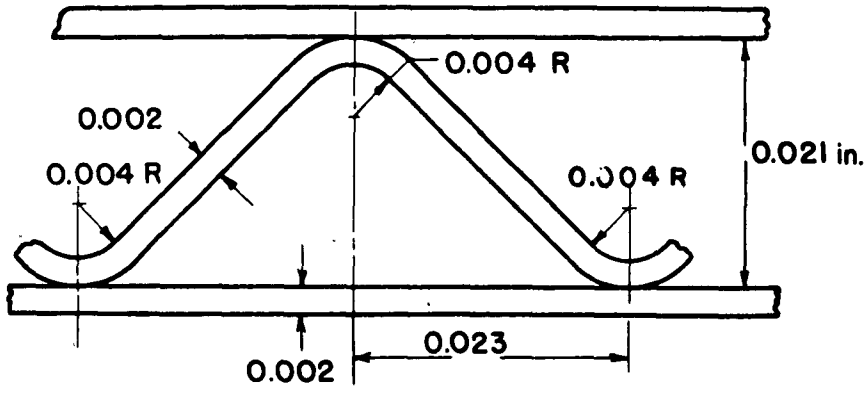

$\alpha = 0.800$

$D_e = 0.001324$ ft

0.021 spacing

FIG. 3-1 DIMENSIONS OF FLAME TRAP MATERIAL OF REFERENCE 15

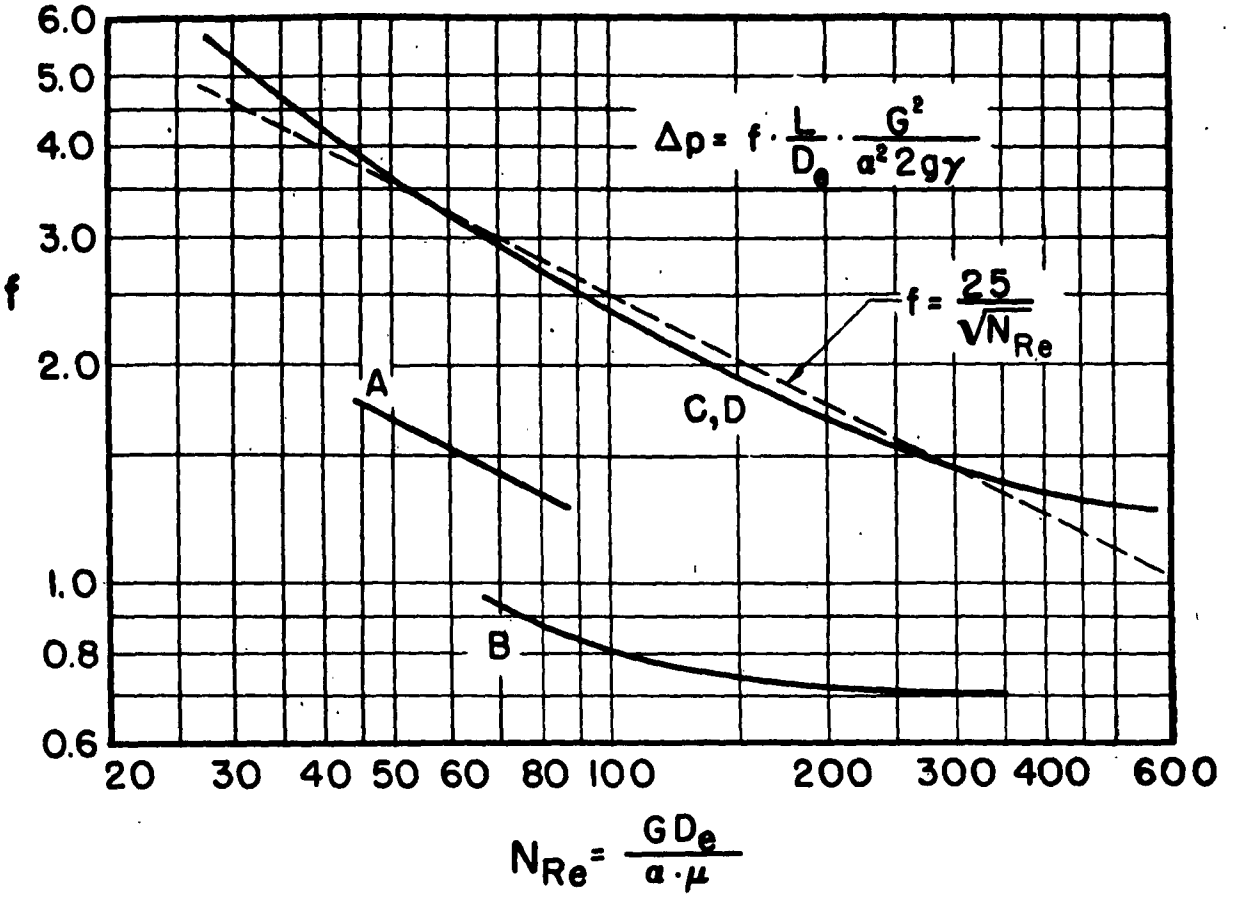

MATRIX	MESH	D (in.)	Nbr. Layers	L (ft)	$10^3 \cdot D_e$ (ft)	a
A	30	0.0105	100	0.175	1.66	0.469
B	30	0.0105	150	0.262	3.57	0.469
C	20	0.009	100	0.150	1.78	0.672
D	40	0.0045	98	0.094	1.65	0.672

FIG. 3-2 FRICTION FACTORS OF WIRE SCREEN MATRICES (REF. 15)

Romie et al (Ref. 24) observed that the pressure-loss coefficient, in addition to depending upon the Reynolds number, depends upon the following three items:

(1) The area ratio α. For example, the pressure-loss coefficient was found to double its value when α was reduced by half.

(2) The spacing between screens, that is, the number of screens per unit length. For example, the pressure-loss coefficient for an assembly of unspaced screens decreased 15 per cent when the screens were separated by a free space of 1/32 inch.

(3) The total number of screens in the assembly. The pressure-loss coefficient decreased or increased as the number of screens increased depending, respectively, upon whether the screens were closely or widely spaced.

More experimentation on configurations of wire screens are needed.

3-7 Heat Transfer

The coefficient of heat transfer h, which must be employed in evaluating Λ and Π (see Eq. 2-18 and -19), has been found by experiments based on the single-blow technique (e.g., Ref. 15, 18, and 24) and on results from periodic regenerators (e.g., Ref. 4 and 20). Also, coefficients obtained from tests on certain recuperator cores may be useful (e.g., Ref. 17).

It has been customary to correlate the coefficients by means of the following two typical equations:

$$N_{Nu} = C_1 N_{Re}^{n} \tag{3-20}$$

and

$$N_{St} = \frac{C_2}{N_{Re}^{1-n}} \tag{3-21}$$

where

$$N_{Nu} = \frac{hD_e}{k} \tag{3-22}$$

$$N_{St} = \frac{\alpha \cdot h}{Gc_p} \tag{3-23}$$

and the Reynolds number is defined by Eq. 3-18; k is the conductivity of the fluid evaluated at a mean temperature. Since the Stanton number is the ratio of the Nusselt number to the product of the Reynolds number and the Prandtl number ($N_{Pr} = c_p \mu/k$), the relationship between C_1 and C_2 is

$$C_1 = N_{Pr} \cdot C_2 \tag{3-24}$$

For air the value of N_{Pr} is 0.689 ± 0.005 in the range of temperature from 200 to 800°F.

In the next two sections, data for flame trap and wire screen matrices are presented. Regarding the relative merit of the two types of matrices, Johnson remarks that the lowest weight for a given performance is obtained with a fine wire screen matrix, but the pressure drop is higher than for a smooth flame trap matrix. The saving in weight is more marked than the increase in pressure drop; however, when the partitions required in constructing the screen matrices are considered, the advantage in weight may be reduced.

3-7.1 Coefficients of Heat Transfer for Flame Trap Matrices

Because the passages of regenerator matrices are small, the flow is expected to be laminar. Glaser (Ref. 7) has shown that for a circular tube with linear temperature distribution (uniform heating) in the axial direction along the wall and with constant fluid properties, the limiting[1]

[1] The limiting value of the Nusselt number is the value toward which the Nusselt number approaches, by virtue of pure conduction, as the Reynolds number approaches zero. Also, this is the value that would occur in a very long passage or in a passage where the velocity and temperature profile are everywhere fully developed (cf. Eq. 3-25).

value of the Nusselt number $N_{Nu,\infty} = 4.36$. Norris and Streid (Ref. 21) assumed constant wall temperature and obtained $N_{Nu,\infty} = 3.66$. The experimental results on cylindrical passages by Locke (Ref. 18) fall between the values obtained by Glaser and by Norris and Streid. The experimental results of Romie et al (Ref. 24) on a circular-tube matrix deviate about 10 per cent from Glaser's theoretical line in the range of $N_{Re}N_{Pr}/(L/D_e)$ from 7 to 30. Below this range, down to about 3.5, the experimental data are about 20 per cent higher than the theoretical values.

Clark and Kays (Ref. 3) performed calculations and steady-state experiments to study the laminar heat transfer in small rectangular passages of various aspect ratios. They correlated their results by means of the typical equation,

$$N_{Nu} = N_{Nu,\infty}\left[1 + C_3 \cdot \frac{N_{Re} \cdot N_{Pr}}{(L/D_e)}\right] \qquad (3\text{-}25)$$

Both $N_{Nu,\infty}$ and C_3 depend upon the aspect ratio[1] Y/X and how the tube wall is heated.

For a good approximation to the regenerator matrix, it may be assumed that the temperature distribution is practically linear. Accordingly, the recommended values of $N_{Nu,\infty}$ and C_3 are those for the case of uniform heat input. The authors' values of $N_{Nu,\infty}$ for this case are shown in Fig. 3-3, and their suggested values for C_3 may be represented by the equation,

$$C_3 = 0.0025 + 0.020\,\frac{X}{Y} \qquad (3\text{-}26)$$

The experimental results of Romie et al (Ref. 24) on the flat plate matrix (infinite aspect ratio) deviate about $\pm$ 10 per cent from the values given by Clark and Kays.

Cox and Lamb (Ref. 4) tested six matrices with triangular passages in a model rotary regenerator. Their results for all the matrices

---

[1] See the inset in the graph of Fig. 3-3.

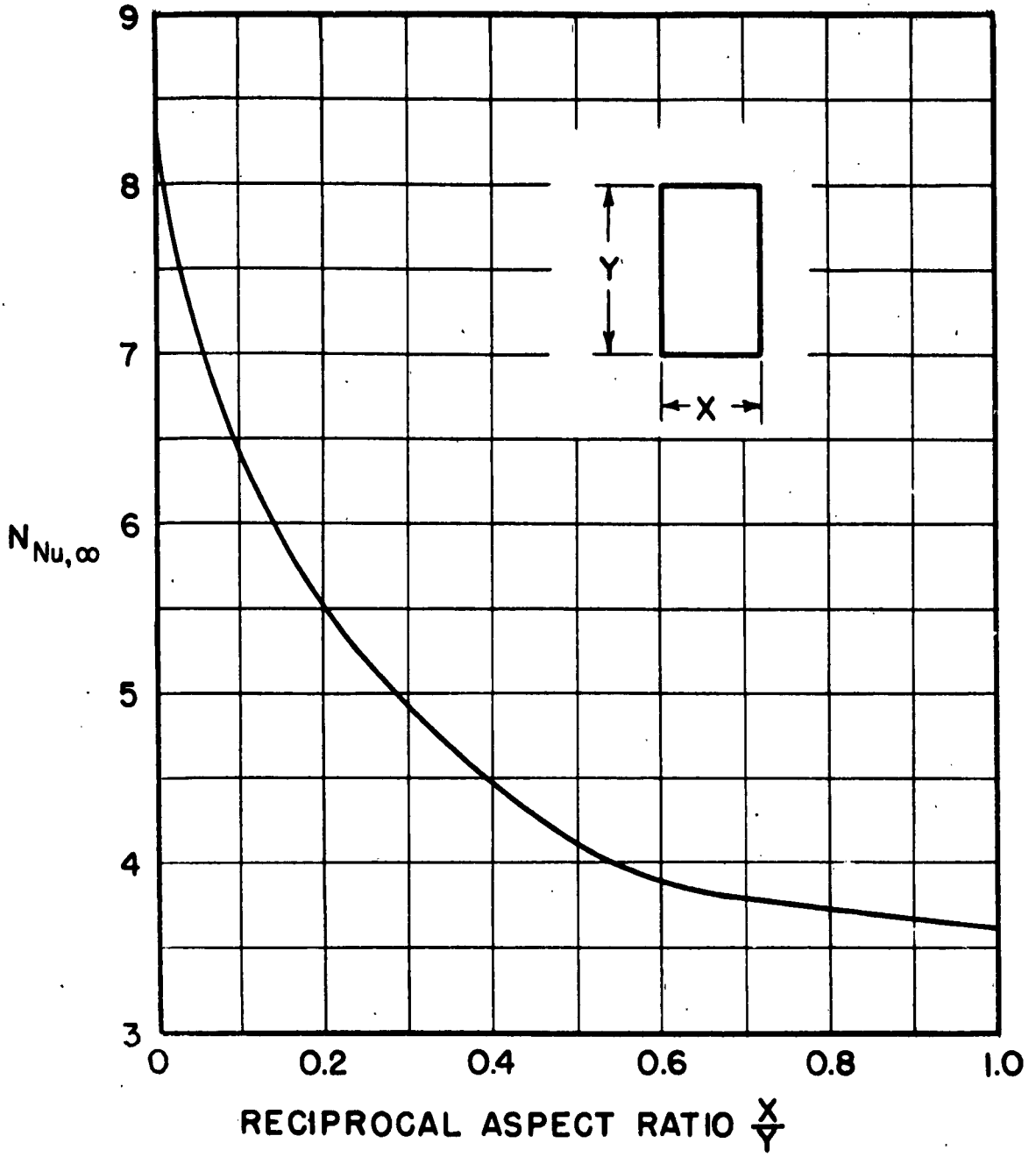

FIG. 3-3 LIMITING NUSSELT NUMBERS FOR RECTANGULAR TUBES WITH UNIFORM HEAT INPUT

deviated by about 10 per cent from the correlating line represented by Eq. 3-25 with $N_{Nu,\infty} = 2.4$ and $C_3 = 0.0735$. The materials were like those used by Johnson (Ref. 15). With reference to Fig. 3-1, it may be observed that the passages were approximately isosceles triangles with included right angles. For the equilateral triangle with uniform heating at the wall $N_{Nu,\infty} = 3.00$ (Ref. 3).

It has been found impossible to fit Eq. 3-25 to all of Johnson's data for the matrices of Fig. 3-1, and it is believed that the correlation of Ref. 4 is the more reliable one for flame trap matrices with triangular passages. The author's original correlations, which appear in the form of Eq. 3-21, are tabulated below. The correlations represent the data in the range of N_{Re} from about 50 to 200. For $N_{Re} < 50$, the Stanton numbers appear to reach limiting values. Average values of the Stanton number in this range are denoted by $N_{St,av}$ and are presented in the next to last column of Table 3-1.

Table 3-1. Heat Transfer Correlations for Flame Trap Matrices (Ref. 15)

Matrix Spacing (in.)	L (ft)	C_2	1 - n	$N_{St,av}$	$N_{Nu,c}$
0.030	0.0729	-	-	0.045	-
0.030	0.146	2.7	1.0	0.037	1.96
0.030	0.292	0.845	0.81	-	1.6
0.021	0.0729	-	-	0.032	-
0.021	0.292	0.205	0.55	0.024	1.5

Further, Johnson remarks that at high Reynolds numbers his Nusselt numbers tend to become constant. Average values of the Nusselt numbers in this region are denoted by $N_{Nu,c}$ and are presented in the last column of Table 3-1.

In the so-called Fraenkl packing, two ribbons having corrugations at 45° to the ribbon edge are put together so that their corrugations are at right angles to each other. Then the two ribbons are wound

in a spiral to form a disk of desired diameter and of a height equal to the ribbon width. One or more such disks are placed in series to form a matrix of desired length. Sometimes spacers are used to separate the packings. These packings have been employed mainly in regenerators for liquefaction of gases. The heat transfer characteristics of Fraenkl packings have been investigated by Glaser (Ref. 6) and by Lund and Dodge (Ref. 20). Glaser correlated his results with the equation,

$$N_{Nu} = \frac{N_{Re}^{0.007(L/D_e)} + 0.65}{10^{0.024(L/D_e)} + 0.60} \qquad (3\text{-}27)$$

3-7.2 Coefficients of Heat Transfer for Wire Screen Matrices

Values for h obtained by Johnson (Ref. 15) are in general higher than corresponding values for flame trap matrices. Of course, the pressure losses are correspondingly higher. Johnson's correlations can be represented by means of Eq. 3-21. In each case $n = 0.5$. Values of the constant C_2 are presented in Table 3-2. The range of the Reynolds number is about 25 to 400. Since some question has been raised regarding Johnson's data for flame trap matrices, the same question arises concerning his data for wire screen matrices. However, there are no other data available on closely packed screens for comparison.

Table 3-2. Constant C_2 to be Employed in Eq. 3-21 for Wire Screen Matrices (Ref. 15)

Matrix (cf. Fig. 3-2)	Description			C_2
	Mesh ($in.^{-1}$)	Wire Diameter (in.)	No. Layers	
A	30	0.0105	100	0.515
B	30	0.0105	150	0.515
C	20	0.009	100	1.00
D	40	0.0045	98	0.74

Romie et al (Ref. 24) employed two wire screen matrices. One consisted of 36 layers of 24 mesh screen made of 0.0075-in. diameter wire and the other of 28 layers of 16 mesh screens made of 0.013-in. diameter wire. The layers were spaced 1/32 in. apart. Their Reynolds number, based on wire diameter as characteristic length, varied from about 20 to 500. The authors' most reliable results are in surprisingly good agreement with data for flow normal to single wires, namely,

$$\frac{hD}{k} = 0.32 + 0.43 \left(\frac{G\,D}{\alpha \cdot \mu}\right)^{0.52} \qquad (3\text{-}28)$$

Chapter 4: EFFECT OF REGENERATOR PERFORMANCE ON THE GAS TURBINE POWER PLANT

4-1 Actual Cycle of the Gas Turbine Power Plant

The actual gas turbine cycle differs from the ideal cycle in several ways. With reference to Fig. 4-1, which is a temperature-entropy diagram of an actual cycle, two importance differences may be observed:

4-1.1 Actual Work of Compressor and Turbine

First, the compression and expansion processes are isentropic in the ideal compressor and turbine but not in the actual ones. Increases of entropy occur in the actual processes. These increases are represented in the T,s-diagram by the amounts of shifting of the Points 2' and 4', the ideal states, to Points 2 and 4, the actual states. These changes of entropy manifest themselves as an increase of the power input to the compressor and a decrease of the power output from the turbine. The net effect may be regarded as either a decrease of the output of a given plant or an increase of plant size for a given output.

It is customary to express the deviations between the actual and ideal units in terms of the compressor efficiency,

$$\eta_c = \frac{h_{2'} - h_1}{h_2 - h_1} \tag{4-1}$$

and the turbine efficiency,

$$\eta_t = \frac{h_3 - h_4}{h_3 - h_{4'}} \tag{4-2}$$

4-1.2 Pressure Losses

Second, there are pressure drops in the low- and high-pressure sides of the cycle on account of ducting and any heat exchanger that may be present. Hence, $p_3 < p_2$ and $p_4 > p_1$. The effect is to decrease the power output and the power plant thermal efficiency.

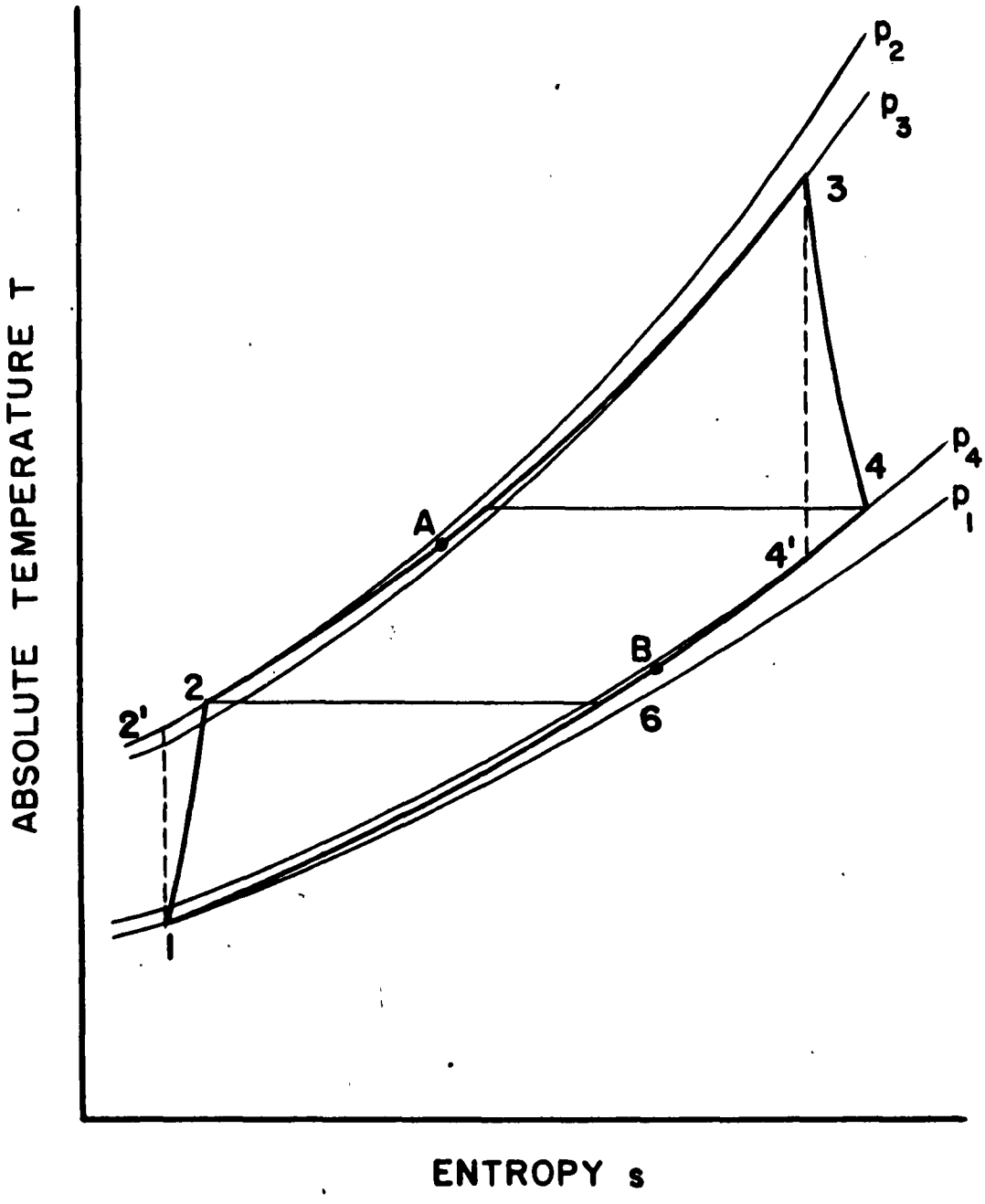

FIG. 4-1 TEMPERATURE-ENTROPY PLANE FOR A REAL REGENERATIVE GAS-TURBINE CYCLE

4-1.3 Leakage

A third difference between the ideal and actual regenerative cycle is the leakage from the high-pressure air to the low-pressure exhaust gas. Some is passed by the seals, and some is carried over by the rotation. On account of this leakage, the amount of fluid passing through the compressor is greater than that passing through the turbine. Hence, a larger and more powerful compressor is required for a given turbine output. The net result is a decrease in the thermal efficiency of the power plant.

4-2 Thermal Efficiency of the Actual Cycle

The power output of the plant and the thermal efficiency of an actual gas turbine cycle operating with practical compression and expansion units, with pressure drop in the intermediate ducting and regenerator, and with leakage from the air side to the gas side are developed in Appendix B. The calculations are based on the assumptions that the fluid is thermally and calorically perfect and that the fuel has negligible influence on the thermodynamic properties.

4-3 Evaluation of the Effects of Leakage and Pressure Drop

Harper and Rohsenow (Ref. 9) employed the results of Appendix B or their equivalents, to calculate and demonstrate the effects of leakage and pressure drop for the following operating conditions:

Air inlet temperature,	60°F, or	$T_1 = 520°R$
Maximum temperature,	1500°F, or	$T_3 = 1960°R$
Compressor efficiency,		$\eta_c = 0.85$
Turbine efficiency,		$\eta_t = 0.88$

The authors expressed their assumed values of leakage and pressure loss, respectively, in terms of the leakage fraction $\Delta m/m$ and the sum of the pressure drop ratios $\sum (\Delta p/p)$. The quantity m is the mass rate of flow through the compressor; and with reference to Fig. 4-1,

$$\sum \frac{\Delta p}{p} = \frac{p_2 - p_3}{p_2} + \frac{p_4 - p_1}{p_1} \qquad (4\text{-}3)$$

The ratio of the first term of Eq. 4-3 to the second, which would be denoted by α_2/α_1 in Appendix B, was not given by Harper and Rohsenow but appears to have been taken as 3/7 in one part of their calculations.

The authors calculated the maximum thermal efficiency $\eta_{th,max}$ and the corresponding (optimum) pressure ratios for the cases that $\Delta m/m = 0$, 0.05, and 0.10 and that $\sum (\Delta p/p) = 0.05$, 0.10, and 0.15. Results of their study are discussed in the next two sections.

4-3.1 Effect of Leakage

As has already been remarked in Section 2-13, the influence of leakage on the effectiveness of the heat exchanger is small. The influence of leakage on the power plant performance is shown in Fig. 4-2a and -2b. With regard to increasing values of $\Delta m/m$, the following changes may be observed:

(1) The maximum attainable thermal efficiency decreases. This is mainly due to the decrease in turbine output, for the mass flow in the turbine is less than the mass flow at the intake of the power plant.

(2) The optimum pressure ratio $r_{p,opt}$ decreases. The effect is most pronounced at lowest values of the regenerator effectiveness.

(3) The work output per pound of air entering the power plant decreases. This is due to the decrease of both the mass flow in the turbine and the optimum compression ratio.

4-3.2 Effect of Pressure Drop

The effect of pressure drop is shown in Fig. 4-3a and -3b. With regard to increasing values of $\sum (\Delta p/p)$, the following changes may be observed:

(1) The maximum attainable thermal efficiency decreases. This is due to the increase in the turbine expansion ratio.

(2) The optimum pressure ratio increases.

(3) The work output per pound of air decreases.

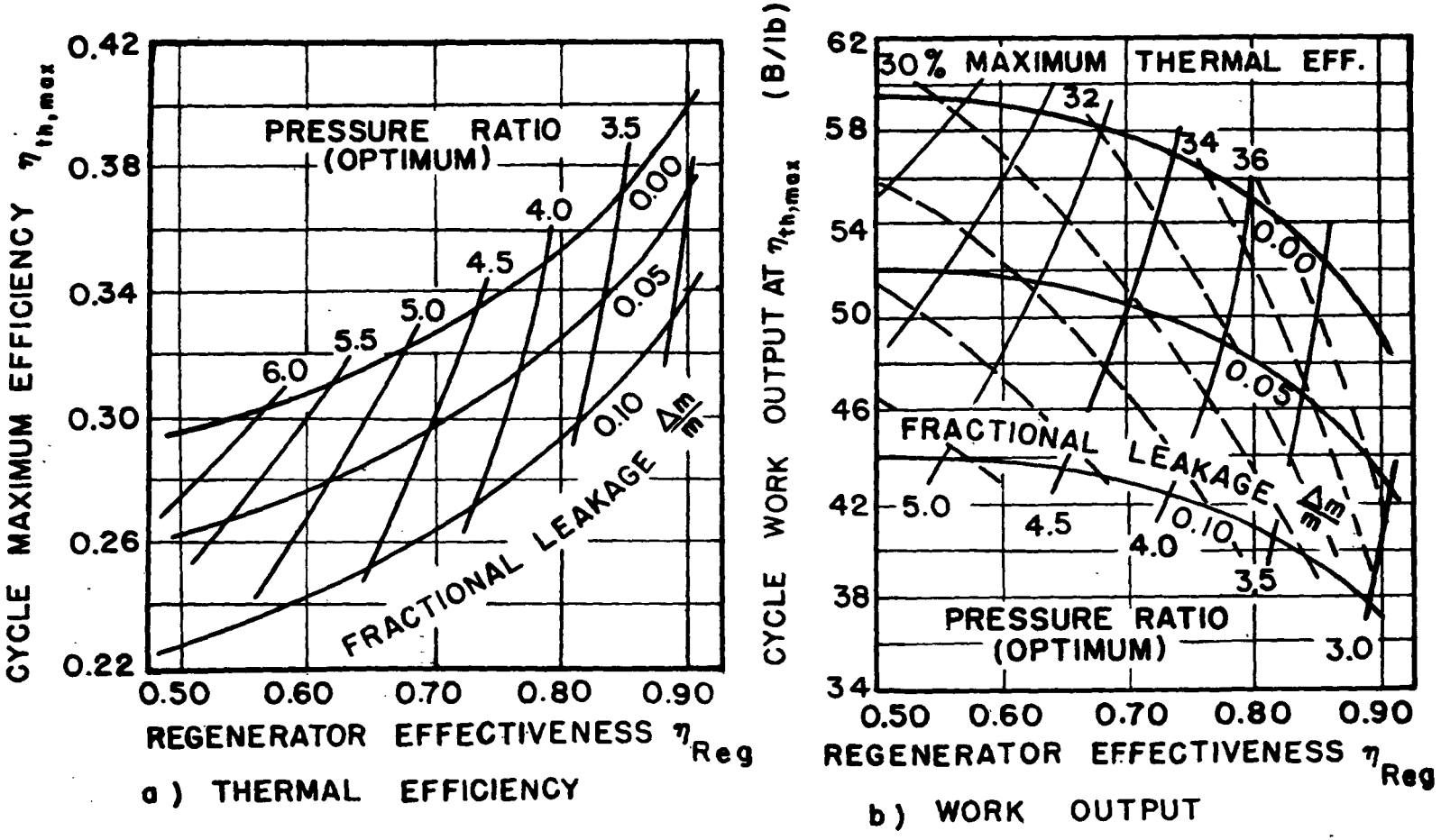

FIG. 4-2 EFFECT OF FRACTIONAL LEAKAGE ON A GAS TURBINE POWER PLANT FOR PRESSURE DROP $\Delta_{P/P}$ =0.10

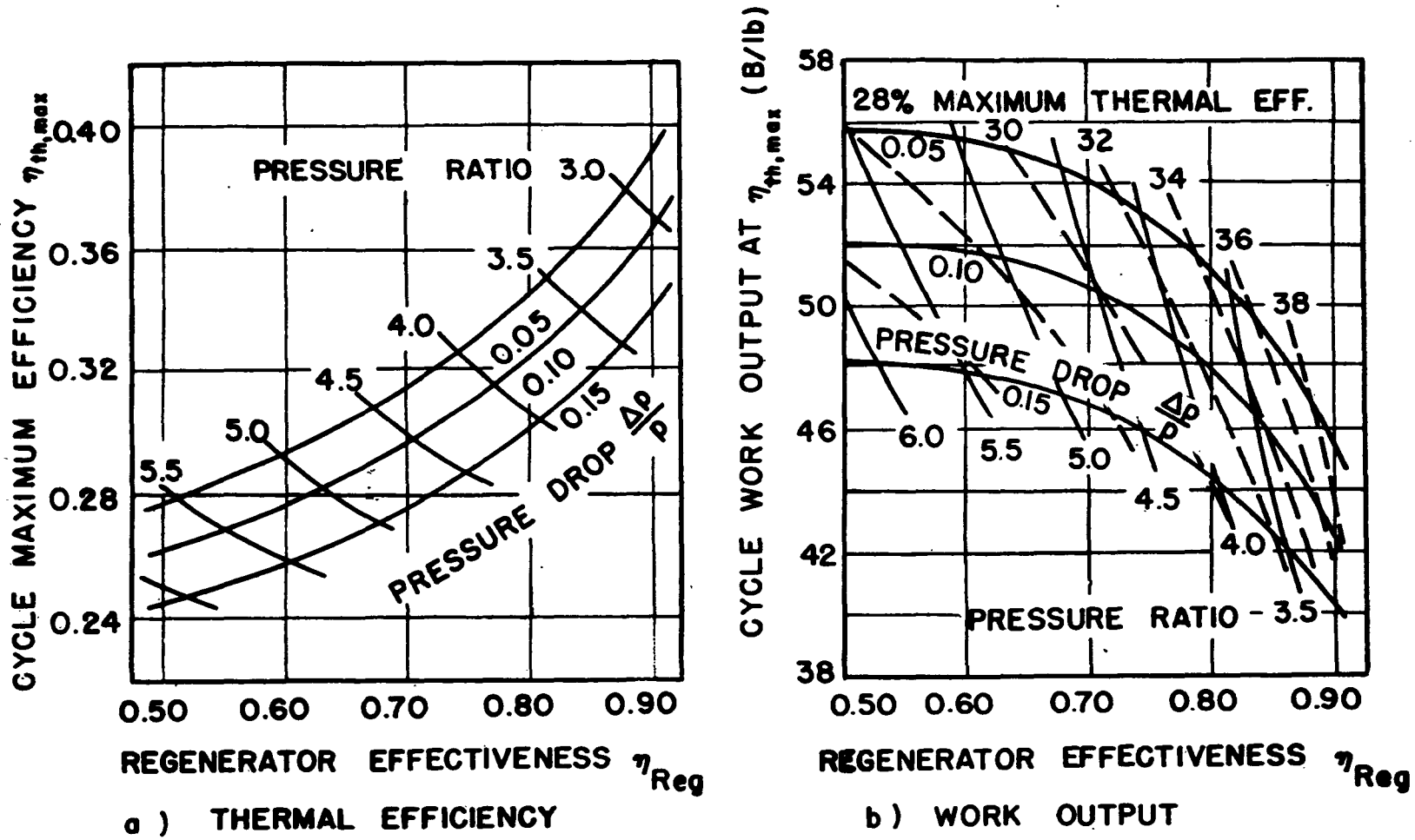

FIG. 4-3 EFFECT OF PRESSURE DROP ON A GAS TURBINE POWER PLANT FOR FRACTIONAL LEAKAGE $\Delta m/m = 0.05$

4-4 Effects of Regenerator Speed, Length, and Mass Velocity

Harper and Rohsenow (Ref. 9), employing the results of Saunders and Smoleniec (Ref. 25), also showed how the rotational speed N, regenerator length L, and the mass velocity m'' affect the power plant. In considering any one of these three variables, the other two were regarded as constant. Also, the net output of the gas turbine power plant was maintained constant under the conditions specified in Section 4-3. A balanced regenerator with $\Lambda = 5$ and $\Pi = 4$ was taken as a basis for reference. The results of the authors' discussion are summarized in the next three sections.

4-4.1 Effect of Regenerator Speed

An increase of regenerator speed decreases Π proportionately but leaves Λ unaltered. The increase of speed increases the carry-over losses. It also influences the leakage through the seals insofar as the regenerator speed affects the optimum pressure ratio. Regarding the pressure losses, Harper and Rohsenow took $\sum (\Delta p/p)$ to be a fixed value.

The results of their calculations are shown in Fig. 4-4. It may be observed that the maximum cycle efficiency reaches a maximum at a certain speed; then it decreases on account of the increasing carry-over losses. The matrix relative volume V increases since the work per pound of air W decreases while total power output remains constant. The optimum pressure ratio $r_{p,opt}$ decreases as the speed increases.

4-4.2 Effect of Regenerator Length

In this case the reduced length Λ changes while the reduced period Π remains constant. The results of calculations for a fixed value of $\Delta m/m$ are shown in Fig. 4-5.

The pressure drop $\sum (\Delta p/p)$ increases with the matrix length. Again, the maximum thermal efficiency reaches an optimum value; then it decreases on account of the rising pressure drop. Since the work per pound of air entering the turbine (denoted by W) decreases as the matrix length increases, the matrix facial area as well as length increase to

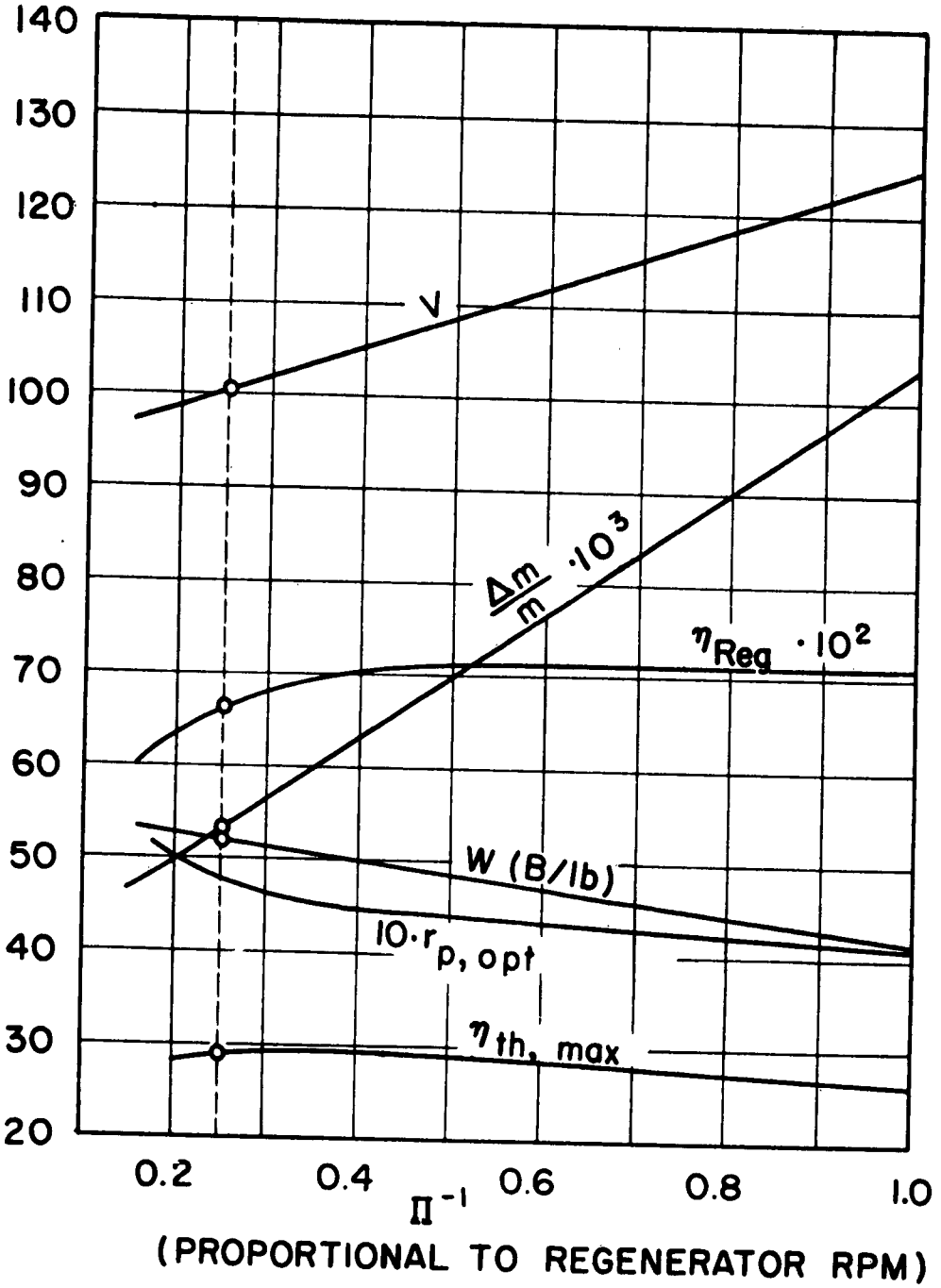

FIG. 4-4 EFFECT OF ROTOR SPEED ON GAS TURBINE POWER PLANT PERFORMANCE AT DESIGN-POINT CONDITIONS

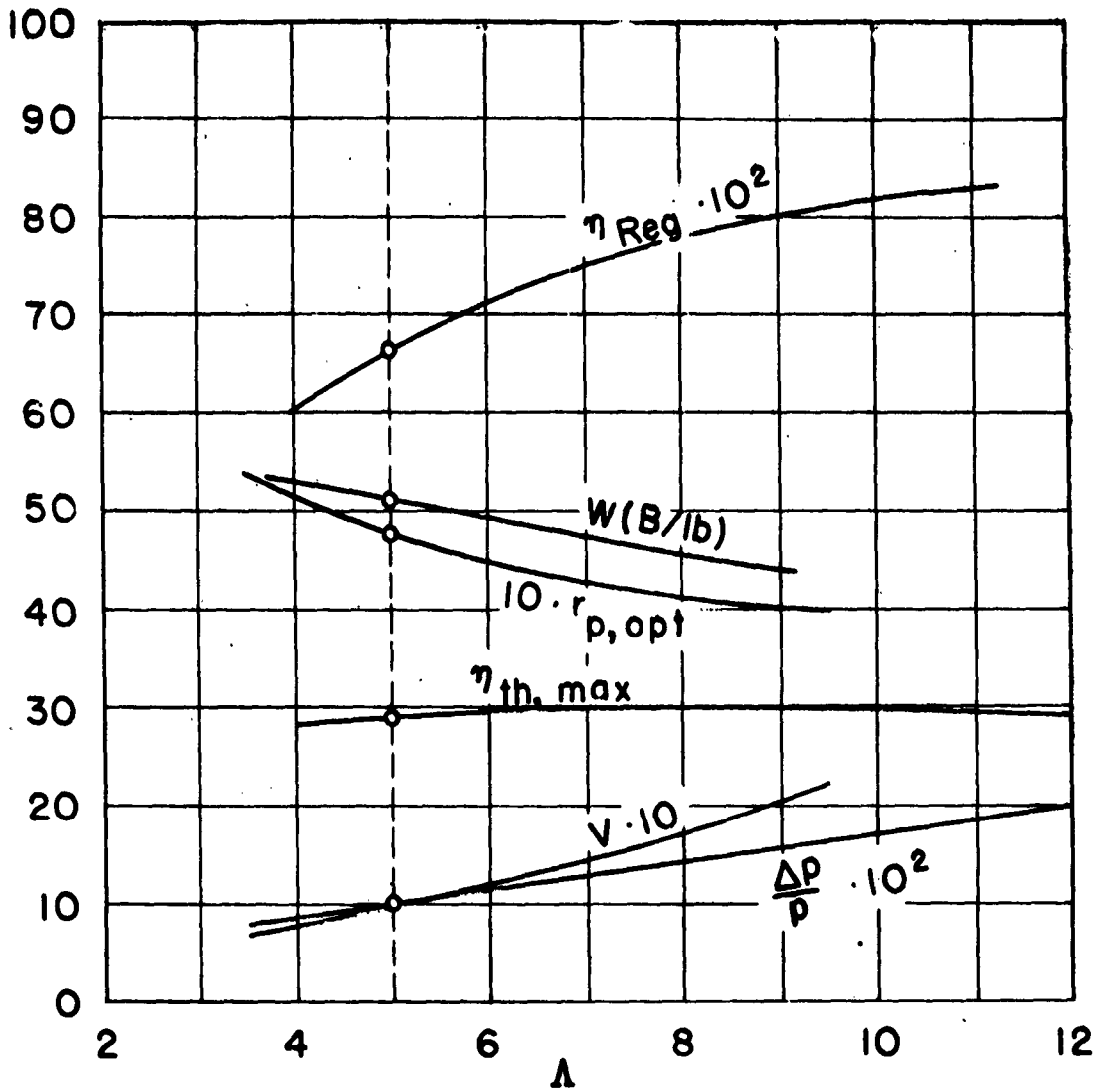

FIG. 4-5 EFFECT OF MATRIX LENGTH ON GAS TURBINE POWER PLANT PERFORMANCE AT DESIGN-POINT CONDITIONS

provide a given fixed total power output. For this reason the relative volume V increases more rapidly than just linearly.

4-4.3 Effect of Mass Velocity

A change of the rate of flow may affect both the reduced length and the reduced period, because it may be accompanied by a change in the value of the coefficient of heat transfer h. For example, if it is assumed that the flow through the matrix is such that

$$h \sim (m'')^{1/2} \tag{4-4}$$

then

$$\Lambda^2 \sim (m'')^{-1} \tag{4-5}$$

and

$$\Pi^2 \sim m'' \tag{4-6}$$

Assuming that the pressure drop increases linearly with m'' and that $\Delta m/m$ remains constant, Harper and Rohsenow presented the results shown in Fig. 4-6. It can be seen that W reaches a maximum value after which it decreases on account of the rising pressure loss.

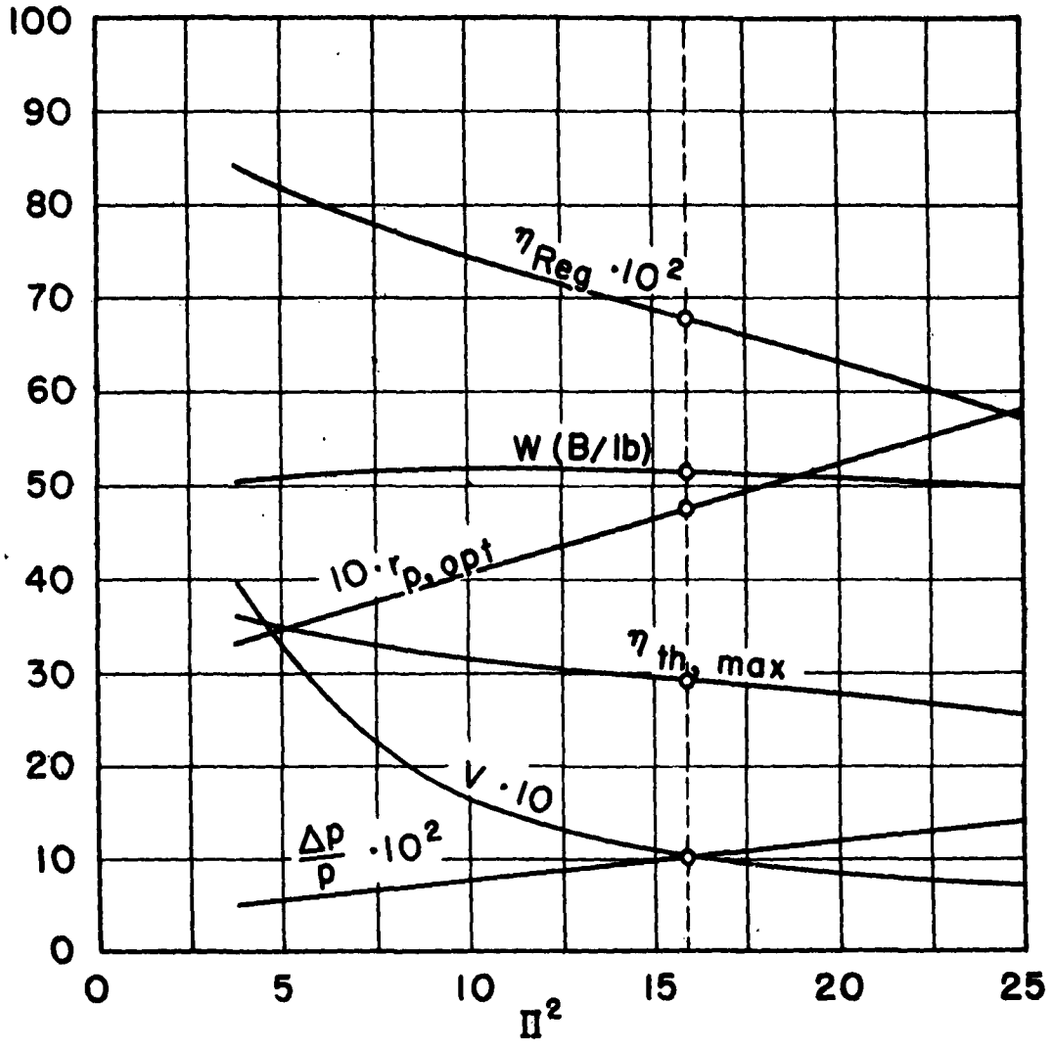

FIG. 4-6 EFFECT OF RATE OF MASS FLOW ON GAS TURBINE POWER PLANT PERFORMANCE AT DESIGN-POINT CONDITIONS

Chapter 5: A DESIGN PROCEDURE

5-1 Preliminary Remarks

As mentioned in the introductory chapter, this manual deals mainly with the thermal design. However, many features of the mechanical design dictate the thermal performance; and limitations of weight, space, and location, in contributing to the over-all problem, may very well determine whether the heat exchanger is a practicable matter in a given application.

The designer must use his science and art to build a regenerator that lies within the allowable mechanical limitations and that provides a satisfactory over-all performance of the power plant. He faces this task with a system or group of quantities whose values are given. Some of these values have had to be determined from the performance requirements, some by auxiliary calculations, and others by judgment, which improves with experience. Generally, his design procedure depends upon the particular group of values he has to start with.

In the following sections a rather special problem is treated. A statement of the problem appears in the next section. Then the analysis is briefly discussed. This is followed by a solution with some sample calculations. The solution illustrates the application of much of the material in Chapters 2 and 3. The results are not intended, however, to be definitive without further development and experimentation, particularly with regard to the pressure drop and heat transfer characteristics of the type of matrix selected. It is hoped that the procedure presented here may suggest how other groups of starting quantities may be handled and, consequently, how other design procedures may be devised.

5-2 Statement of the Problem

We suppose that the designer has been given the quantities in Table 5-1. As can be seen, his regenerator is to achieve an effectiveness of 90 per cent. We suppose that a drum type regenerator is to be designed. For any matrix construction that he selects the designer must calculate the quantities listed below:

L	the matrix length, that is, the thickness of the drum; ft
D_d	the mean or pitch diameter of the drum; ft
l	the axial length of the drum; ft
$2\pi K_a$	the angle subtended by the air side
$2\pi K_g$	the angle subtended by the gas side
N	the speed of rotation; revolutions per second

Table 5-1. Given Design and Performance Conditions for the Illustrative Problem

Symbol*	Quantity	Value	Units
P	power at the shaft	2500	hp
η_c	compressor efficiency	0.85	—
η_{comb}	combustion efficiency	0.95	—
η_t	turbine efficiency	0.85	—
η_{Reg}	required regenerator effectiveness	0.90	—
T_1	temperature at compressor intake	520	°R
T_2	temperature at regenerator inlet (air side)	815	°R
T_3	temperature at throttle	1810	°R
T_4	temperature at regenerator inlet (gas side)	1376	°R
p_2	pressure at regenerator inlet (air side)	58.8	lb/sq in.
p_4	pressure at regenerator inlet (gas side)	15.45	lb/sq in.
Δp_a	allowable pressure drop on air side	0.88	lb/sq in.
Δp_g	allowable pressure drop on gas side	0.75	lb/sq in.
m_a	rate of flow on air side	140,000	lb/hr
m_g	rate of flow on gas side	141,000	lb/hr

*Subscripts 1, ..., 4 refer to the statepoints in the cycle diagram of Fig. 4-1. All temperatures and pressures are absolute.

5-3 Analysis of the Solution

After a matrix is selected the basic geometric and thermal properties can be evaluated in accordance with Sections 3-1 to -5. General relationships regarding pressure drop and heat transfer data can be selected from Sections 3-6 and -7.

The pressure drop depends upon the matrix length L and the mass velocities[1] G_a and G_g. This gives two relations, one between L and G_a and the other between L and G_g.

The heat transfer coefficients h_a and h_g depend, respectively, upon G_a and G_g. Therefore, the reduced lengths Λ_a and Λ_g can be expressed in terms of G_a, G_g, and L. Employing the first two relations, we may eliminate G_a and G_g to express Λ_a and Λ_g in terms of L. Consequently, the harmonic mean reduced length Λ_m can be expressed in terms of L.

The allowable carry-over losses Δm_a from the cold-air side depends upon the speed of rotation and the volume of the matrix. It will be seen that a known value of $\Delta m_a/m_a$ provides a relation among the quantities N, G_a, and L. Also, the utilization factor depends upon N, G_a, and L. Observing that the fractions K_a and K_g are simply related to G_a and G_g, we can calculate a unique value of the utilization factor U. Hence, Λ_m can be found from Fig. 2-8, and all required quantities can be calculated.

5-4 Selection of the Matrix

The matrix of our regenerator is to be made of wire screen. It has been suggested that the material forming the matrix is limited by burnout due to fuel left in the exhaust gases and that the lower limit in the size of wires (or plates) may be in the order of 0.008 inch.[2]

---

[1] It has been found convenient to let $[m'']$ = lb/hr ft^2 and $[G]$ = lb/sec ft^2; hence, $G = 3600\ m''$. The brackets $[...]$ here, as elsewhere, are to be read, "the units of ... are".

[2] See the reference to the work of Bowden and Hryniszak at the end of the Bibliography.

Johnson (Ref. 15) found that copper gauze, glass wool, and steel wool are unsuitable for high temperatures. Thin strips of a 70:30 copper-nickel alloy and wire gauzes of brass, of mild steel, and of stainless steel showed no deterioration or corrosion after tests at about 900°F.

For purposes of the illustrative calculations, the gauze is assumed to be made of stainless-steel wire 0.009 in. in diameter. It is supposed that the screens are of 20 mesh and are firmly packed. The basic geometric and thermal properties have been calculated by means of the relationships in Chapter 3. The results are presented in Table 5-2.

Table 5-2. Basic Geometric and Thermal Properties of the Assumed Matrix Material

Symbol	Quantity	Value	Units
D	wire diameter	0.009 0.00075	in. ft
n	mesh	20	$in.^{-1}$
β	void fraction	0.86	-
$1 - \beta$	solid fraction	0.14	-
S'''	heat transfer area per unit volume	755	ft^{-1}
α	ratio of free-flow area to facial area	0.67	-
ρ_s	density of the solid	487	lb/ft^3
$c_{p,s}$	specific heat of the solid	0.138	B/lb F
C'''	heat capacity of the matrix per unit volume	94	B/ft^3 F
D_e	equivalent diameter	0.00355	ft

5-5 Calculation of the Mean Inlet and Outlet Temperatures on the Cold and Hot Sides of the Regenerator

By definition of the regenerator effectiveness, the mean outlet temperature on the cold side of the regenerator is

$$T_A = T_2 + \eta_{Reg}(T_4 - T_2) = 1320°R$$

Similarly, the mean outlet temperature on the hot side is, practically,

$$T_B = T_4 - \eta_{Reg}(T_4 - T_2) = 871°R$$

Table 5-3 is a resume of the fluid temperatures at the regenerator inlets and outlets. Symbols employed in the thermodynamic cycle of Fig. 4-1 are related to the corresponding symbols employed in Chapter 2. Thus, $T_2 = 815°R$ while $\theta_{a,1} = T_2 - 460 = 355°F$, and so forth.

Table 5-3. Resume of Temperatures at the Regenerator Inlets and Outlets

Cold Air		Hot Gas	
in	out	in	out
$T_2 = 815°R$	$T_A = 1320°R$	$T_4 = 1376°R$	$T_B = 871°R$
$\theta_{a,1} = 355°F$	$\theta_{a,2} = 860°F$	$\theta_{g,1} = 916°F$	$\theta_{g,2} = 411°F$

5-6 Evaluation of the Mean Temperature of Each Fluid

In accordance with a recommendation of Cox and Lamb (Ref. 4), the fluid properties with the exception of the specific weight, are evaluated at a temperature which is 0.6 of the way between the average wall temperature and the bulk mean fluid temperature. This rule is used here even though Cox and Lamb worked only on flame trap matrices and Johnson correlated his data with a somewhat different definition of the mean temperature.

The bulk mean air temperature is $\theta_{a,b} \equiv (\theta_{a,1} + \theta_{a,2})/2 = 608°F$; the bulk gas temperature is $\theta_{g,b} \equiv (\theta_{g,1} + \theta_{g,2})/2 = 664°F$.

The average wall temperature $t_{s,m}$ is assumed to be midway between $\theta_{a,b}$ and $\theta_{g,b}$. Accordingly, in the illustrative example, $t_{s,m} = 636°F$.

Therefore, the temperature to be used for evaluating the fluid properties (μ, k, and c_p) on the air side is

$$\theta_{a,m} = t_{s,m} - 0.6(t_{s,m} - \theta_{a,b}) = 625°F$$

while on the gas side it is

$$\theta_{g,m} = t_{s,m} + 0.6(\theta_{g,b} - t_{s,m}) = 647°F$$

The specific weights are evaluated at the bulk mean stream temperatures under the assumptions that both the cold and the hot fluids are air and that air is a thermally perfect gas (gas constant $R = 53.3$ ft/F). The mean pressures on the air and gas sides are 8410 and 2170 lb/ft^2, respectively. Table 5-4 is a resume of the fluid property values that are employed in the calculations which follow.

Table 5-4. Values of the Fluid Properties in the Illustrative Example

Quantity Symbol	Fluid		Units
	Cold Air	Hot Gas	
γ	0.168	0.0362	lb/ft^3
c_p	0.251	0.252	B/lb F
$10^6 \cdot \mu$	20.4	20.6	lb/sec ft
k	0.0270	0.0274	B/hr ft F

5-7 Relationships Derived from the Correlation of Pressure Drop Data

From Section 3-6.2, the pressure drop of the matrix is, in a first approximation,

$$\Delta p = f \cdot \frac{L}{D_e} \cdot \frac{G^2}{\alpha^2 \cdot 2g\gamma} \qquad (5\text{-}1)$$

where, in the same approximation,

$$f = \frac{25}{\sqrt{\frac{G\,D_e}{\alpha \cdot \mu}}} \qquad (5\text{-}2)$$

Eliminating f and introducing the numerical values of g, α, and D_e,

$$\Delta p = 3200 \frac{\mu^{0.5}}{\gamma} \cdot L \cdot G^{1.5} \qquad (5\text{-}3)$$

where $[\Delta p] = lb/ft^2$, $[\mu] = lb/sec\ ft$, $[\gamma] = lb/ft^3$, $[L] = ft$, and $[G] = lb/sec\ ft^2$. With reference to Table 5-1, the allowable pressure drops on the air and gas sides are 127 and 108 lb/ft^2, respectively. Therefore, Eq. 5-3 yields the system of equations,

$$G_a = 1.475\ L^{-2/3} \qquad (5\text{-}4)$$

$$G_g = 0.418\ L^{-2/3} \qquad (5\text{-}5)$$

5-8 Calculation of the Angle Subtended by the Ducts

Since the leakage fraction and the ratio of fuel to air are small, it is assumed that $U_a = U_g = U$, in accordance with Eq. 2-25. By definition,

$$U = \frac{KGc_p}{C^m LN} \qquad (5\text{-}6)$$

Since $c_{p,a} \approx c_{p,g}$, it follows that

$$K_a G_a = K_g G_g \qquad (5\text{-}7)$$

Further,

$$K_a + K_g = 1 - K_{sls} \qquad (5\text{-}8)$$

where K_{sls} is the fraction of the circle allowed for seals, duct walls, etc. Assuming that $K_{sls} = 0.06$ (corresponding to an angle of about 22°) and eliminating G_a, G_g, and L from Eq. 5-4, -5, and -7, we obtain the set of simultaneous equations

$$K_a + K_g = 0.94 \qquad (5\text{-}9)$$

$$K_a - 0.285\ K_g = 0 \qquad (5\text{-}10)$$

The solution is $K_a = 0.21$ and $K_g = 0.73$, corresponding to angles of about 75° and 263°, respectively. Adjustments may have to be made at a later stage of the design.

5-9 Relations Derived from the Correlation of Heat Transfer Data

From Section 3-7.2, the correlation of the heat transfer data for the selected matrix is

$$\frac{\alpha \cdot h}{3600\ G\ c_p} = \frac{1.00}{\sqrt{\frac{G\ D_e}{\alpha \cdot \mu}}} \qquad (5\text{-}11)$$

Substituting the numerical values given in the preceding sections for α, D_e, μ, and c_p, we obtain the system of equations,

$$h_a = 83.5\ G_a \qquad (5\text{-}12)$$

$$h_g = 84.3\ G_g \qquad (5\text{-}13)$$

where $[h]$ = B/hr ft^2 F and $[G]$ = lb/sec ft^2. Eliminating G_a and G_g with the expressions of Eq. 5-4 and -5,

$$h_a = 101\ L^{-1/3} \qquad (5\text{-}14)$$

$$h_g = 54.6\ L^{-1/3} \qquad (5\text{-}15)$$

By definition, the reduced length is

$$\Lambda = \frac{h\ S^m\ L}{3600\ G\ c_p} \qquad (5\text{-}16)$$

Since h and G are known in terms of L, the reduced lengths may also be expressed in terms of L. Thus, employing Eq. 5-4, -5, -7, -8, and -11,

$$\Lambda_a = 57.4\ L^{4/3} \qquad (5\text{-}17)$$

$$\Lambda_g = 108\ L^{4/3} \qquad (5\text{-}18)$$

where $[L]$ = ft. Further, the harmonic mean reduced length (cf. Section 2-9.1) is

$$\Lambda_m = 75.3\, L^{4/3} \qquad (5\text{-}19)$$

The regenerator could now be uniquely determined if another relation between Λ_m and L were available. In the next section an indirect relationship is obtained: the utilization factor U is evaluated in terms of the allowable carry-over loss. Its value is all that is needed, because Λ_m, U, and η_{Reg} are related by the theory of the balanced regenerator.

5-10 Determination of the Utilization Factor in Terms of the Carry-Over

During each revolution of the matrix, cold air is carried over to the gas side and hot gas to the air side. For purposes of illustration it will be assumed that only the carry-over of the cold air need be considered, because its density is much greater than that of the hot gas. Also, it will be assumed that the leakage at the seals is so small that only the carry-over is significant; in practice this may not be the case and an estimate of the leakage at the seals would have to be made during some stage of the design or development.[1]

The rate of loss of cold air to the hot side by virtue of the carry-over equals the speed of rotation times the weight of the air contained in the total volume of the void space in the matrix. Thus,

$$\Delta m_a = 3600\, N \cdot V_{tot} \cdot \beta \cdot \gamma_a \qquad (5\text{-}20)$$

where V_{tot} is the total volume of the matrix. In terms of A_a, to a good approximation,

$$V_{tot} = AL = A_a L\left(1 + \frac{K_g}{K_a}\right) \qquad (5\text{-}21)$$

[1] An analysis of the seals may be found in the work of Bowden and Hryniszak. See the Additional References at the end of the Bibliography.

This allows for partitioning the matrix. Substituting this expression for V_{tot} into Eq. 5-20, observing that $m_a = 3600\ G_a\ A_a$, and rearranging the resultant equation,

$$\frac{G_a}{LN} = \frac{\beta\ \gamma_a\ (1 + \frac{K_g}{K_a})}{(\frac{\Delta m_a}{m_a})} \qquad (5\text{-}22)$$

The influence of $\Delta m_a/m_a$ on the power plant efficiency could be checked by employing the material in Chapter 4. This is not done here, and for the sake of brevity in the illustrative example it is assumed that a satisfactory value of $\Delta m_a/m_a$ has been found to be 1 per cent. From Fig. 4-2 it can be seen that if the leakage through the seals is also quite small, no correction is necessary for the regenerator effectiveness.

It follows that

$$\frac{G_a}{L \cdot N} = 64.5 \qquad (5\text{-}23)$$

where $[G_a]$ = lb/sec ft^2, $[L]$ = ft, and $[N]$ = sec^{-1}. The right-hand member of Eq. 5-6 is now evaluated with the result that $U = 0.036$.

5-11 Results of the Sample Calculations

Entering the theoretical curves of Fig. 2-8 for the balanced regenerator with $\eta_{Reg} = 0.90$ and $U = 0.036$, we find $\Lambda_m = 18$. (It may be observed that this is exactly the value that would have been obtained by employing Eq. 2-72, the reason being that the utilization factor in this illustrative example is very small.) Consequently, from Eq. 5-19, $L = 0.342$ ft or about 4.1 inches. Having found the value of L, we may readily obtain all other quantities of interest. The values of many of them are listed in Table 5-5.

Table 5-5. Results of the Calculations

Symbol	Air Side	Gas Side	Units
U	0.036	0.036	—
L	0.342	0.342	ft
G	3.02	0.855	lb/sec ft^2
h	145	78	B/hr ft^2 F
$N_{Re} = GD_e/(\mu \cdot \alpha)$	780	222	—
$N_{St} = h \cdot \alpha/(G\ c_p)$	0.0356	0.0658	—
f	0.86	1.61	—
Λ	13.7	25.8	—
π	0.494	0.929	—
K	0.21	0.73	—
N	0.137	0.137	rps
N	8.22	8.22	rpm

From the relationship between the rate of flow m and the mass velocity G, it is found that A_a and A_g are 12.9 and 45.8 ft^2, respectively. The area allowed for the seals being about 6 per cent of the total area, the pitch surface of the drum has a total area of 62.5 ft^2 and the volume of the drum is 21.4 ft^3. Assuming that the length of the drum is 1.5 times its pitch diameter D_d, one finds that D_d = 3.65 ft and l = 5.46 ft. The matrix screens would weigh about one ton.

5-12 Final Remarks

It has been noted that an assumption underlying the calculation procedure is that the pressure drop and the heat transfer correlations of the selected matrix material can be extended beyond the range of Johnson's tests. This would require an experimental check. In particular, the assumed friction factor on the cold side appears to be considerably lower

than a true extrapolation of the data indicates. The sample calculation could be improved by taking this difference into account.

The value 0.036 for the utilization factor is rather low. This indicates that the carry-over losses could be reduced by lowering the matrix speed without seriously impairing the effectiveness of the calculated matrix or without having to increase the matrix length considerably to retain the same effectiveness. In general, it is expected that a regenerator could be found to operate satisfactorily with a utilization factor in the order of magnitude 0.3.

The influence of conduction along the x-direction of the matrix can be calculated by means of the chart in Fig. 2-9. In the illustrative example, the conductivity of the stainless steel is $k_s = 15$ B/hr ft F, and so $(\Lambda/\Phi)_{max} \approx 0.008$. Therefore, the influence of the conduction in the x-direction is to decrease the effectiveness less than 1 per cent.

The designer may have to try a few matrix materials before he is satisfied that he has the regenerator of least weight and volume for his application. Having found a matrix to satisfy the thermal requirements, the designer may proceed to the details of the mechanical design. Finally, he can return to his calculations of the thermal performance, improving his estimates and predicting the performances at other speeds and other loads.

REFERENCES

[1] Ackermann, G. Die Theorie der Waermeaustauscher mit Waermespeicherung. Zeitschrift fur angewandte Mathematik und Mechanik, 3, 1931, pp. 192-205.

[2] Anzelius, A. Erwaermung vermittels durchstroemenden Medien. Zeitschrift fur angewandte Mathematik und Mechanik, 6, 1926, pp. 291-294.

[3] Clark, S. H. and Kays, W. M. Laminar-Flow Forced Convection in Rectangular Tubes. Transactions ASME, 75, 1953, pp. 859-866.

[4] Cox, M. and Lamb, P. S. The Regenerative Heat Exchanger for Gas Turbine Power Plant. Part IV - Performance Test on an Equal-Pressure Flame-Trap Regenerator Unit. National Gas Turbine Establishment, Rept. No. R-80, 1950.

[5] Cox, M. and Stevens, R. K. P. The Regenerative Heat Exchanger for Gas-Turbine Power-Plant. Proceedings of the Institution of Mechanical Engineers, 163, 1950, pp. 193-205.

[6] Glaser, H. Heat Transfer in Regenerators. Zeitschrift der Vereines deutscher Ingenieurs, 59, 1938, pp. 122-125.

[7] Glaser, H. Heat Transfer and Pressure Drop in Heat Exchangers with Laminar Flow. M.A.P. Volkenrode, M.A.P.-VG 96, 1947.

[8] Hahnemann, H. W. Approximate Calculation of Thermal Ratios in Heat Exchangers Including Heat Conduction in Direction of Flow. National Gas Turbine Establishment, Memo. No. M-36, 1948.

[9] Harper, D. B. and Rohsenow, W. M. Effect of Rotary Regenerator on Gas-Turbine-Plant Performance. Transactions ASME, 75, 1953, pp. 759-765.

[10] Hausen, H. On the Theory of Heat Exchange in Regenerators. Zeitschrift fur angewandte Mathematik und Mechanik, 9, 1929, pp. 173-200. R.A.E. Translation No. 126.

[11] Hausen, H. Naerungsverfahren zur Berechnung des Waermeaustausches in Regeneratoren. Zeitschrift fur angewandte Mathematik und Mechanik, 11, 1931, pp. 105-114.

[12] Hausen, H. Waermeuebertragung im Gegenstrom, Gleichstrom und Kreuzstrom, Springer-Verlag, Berlin, 1950.

[13] Iliffe, C. E. Thermal Analysis of the Contraflow Regenerative Heat Exchanger. Proceedings of the Institution of Mechanical Engineers, 159, 1948, pp. 363-372 (War Emergency Issue No. 44).

[14] Jakob, M., Kezios, S. P., and Sogin, H. H. Regenerative Heat Exchanger. Final Report to the U. S. Air Forces under Contract No. W33-038-ac-17548(17871); Illinois Institute of Technology, 1951; 191 pages.

[15] Johnson, J. E. Regenerator Heat Exchangers for Gas Turbines. ARC Reports and Memoranda No. 2630, 1952; RAE Rept. Aero. 2266, S.D. 27; 1948.

[16] Kays, W. M. Loss Coefficients for Abrupt Changes in Flow Cross Section with Low Reynolds Number Flow in Single and Multiple-Tube Systems. Transactions ASME, 72, 1950, pp. 1067-1074.

[17] Kays, W. M. and London, A. L. Heat Transfer and Flow Friction Characteristics of Some Compact Heat Exchanger Surfaces. Part I - Test System and Procedure. Part II - Design Data for Thirteen Surfaces. Transactions ASME, 72, 1950, pp. 1075-1097.

[18] Locke, G. L. Heat Transfer and Flow Friction Characteristics of Porous Solids. Technical Report No. 10 prepared under Contract N6-ONR-251 Task Order 6, for Office of Naval Research, by Department of Mechanical Engineering, Stanford University, June 1, 1950.

[19] Lubbock I. and Bowen, I. G. The Use of Rotary Regenerators in Gas Turbines. Shell Petroleum Co., Ltd., Tech. Rept. No. ICT/5.

[20] Lund, G. and Dodge, B. F. Fraenkl Regenerator Packings — Heat Transfer and Pressure Drop Characteristics. Ind. Eng. Chem., 40, 1948, pp. 1019-1032.

[21] Norris, R. H. and Streid, D. D. Laminar-Flow Heat-Transfer Coefficients for Ducts. Transactions ASME, 62, 1940, pp. 525-533.

[22] Nusselt, W. Die Theorie des Winderhitzers. Zeitschrift der Vereines deutscher Ingenieurs, 71, 1927, pp. 85-91.

[23] Nusselt, W. Der Beharrungszustand im Winderhitzers. Zeitschrift der Vereines deutscher Ingenieurs, 72, 1928, pp. 1052-1054.

[24] Romie, F. E., Ambrosio, A., Coulbert, C. D., Lipkis, R. P., and O'Brien, P. F. Heat Transfer and Pressure Drop Characteristics of Four Regenerative Heat Exchanger Matrices. BU. AER. Contract NOa(s)-8649, Department of Engineering, University of California, Los Angeles, 1948; also, ASME Paper No. 51-SA-34.

[25] Saunders, O. A. and Smoleniec, S. Heat Regenerators. Proceedings of the Seventh International Congress for Applied Mechanics, 3, 1948, pp. 91-105.

[26] Schmitt, H. E. Effect of Reheating and Heat Recovery on Gas Turbine Efficiencies and Performance. USAF Tech. Rept. 5691, 1948.

[27] Schumann, T. E. W. Heat Transfer: A Liquid Flowing Through a Porous Prism. Journal of the Franklin Institute, 208, 1929, pp. 405-416.

[28] Smith, A. G. Heat Flow in the Gas Turbine. National Gas Turbine Establishment Rept. R-39, 1948.

[29] Tipler, W. A Simple Theory of the Heat Regenerator. Shell Petroleum Co., Ltd., Tech. Rept. No. J.C.T./14, 1947.

ADDITIONAL REFERENCES

Bowden, A. T. and Hryniszak, W. The Rotary Regenerative Air Preheater for Gas Turbine. Transactions ASME, 75, 1953, pp. 767-777.

Coppage, J. E. and London, A. L. The Periodic-Flow Regenerator — A Summary of Design Theory. Transactions ASME, 75, 1953, pp. 779-787.

Appendix A

INFLUENCE OF CURVATURE IN DRUM TYPE MATRICES

Appendix A: INFLUENCE OF CURVATURE IN DRUM TYPE MATRICES

A-1 General Remarks

In this appendix it is shown that the performance of the drum type regenerator can be obtained directly from the theory of the flat regenerator (cf. Chapter 2). The demonstration is based on the assumptions of Section 2-1 and is carried out using the line of reasoning in Section 2-2.

A-2 Derivation of the Differential Equations

A drum type matrix of unit length along the axis is considered. The angular speed is ω. Heat balances are made on an element of space shown in Fig. A-1. Since the mass velocity m'' varies with the radius, it will be convenient to employ the axial interstitial velocity u, because $u \cdot r$ is a constant by continuity. Also, the matrix velocity v is a function of the radial distance, namely, $v = \omega \cdot r$.

It is sufficient to consider only one of the fluids; and it may be supposed that its channel subtends an angle $K \cdot 2\pi$ radians. The solid temperature is $t = t(r,\phi)$ and the fluid temperature $\theta = \theta(r,\phi)$.

A-2.1 Thermal Energy Conveyed by the Fluid

The energy transported per unit time by the fluid into the element of space is

$$q_r = u\rho \cdot (r\,\delta\phi \cdot 1)\,\beta\, c_p \cdot \theta \qquad \text{(A-1)}$$

A-2.2 Thermal Energy Conveyed by the Solid

Similarly, the thermal energy transported per unit time into the element of space by the solid material by virtue of its enthalpy is

$$q_{\phi,1} = \omega r \cdot (\delta r \cdot 1) \cdot C^m \cdot t \qquad \text{(A-2)}$$

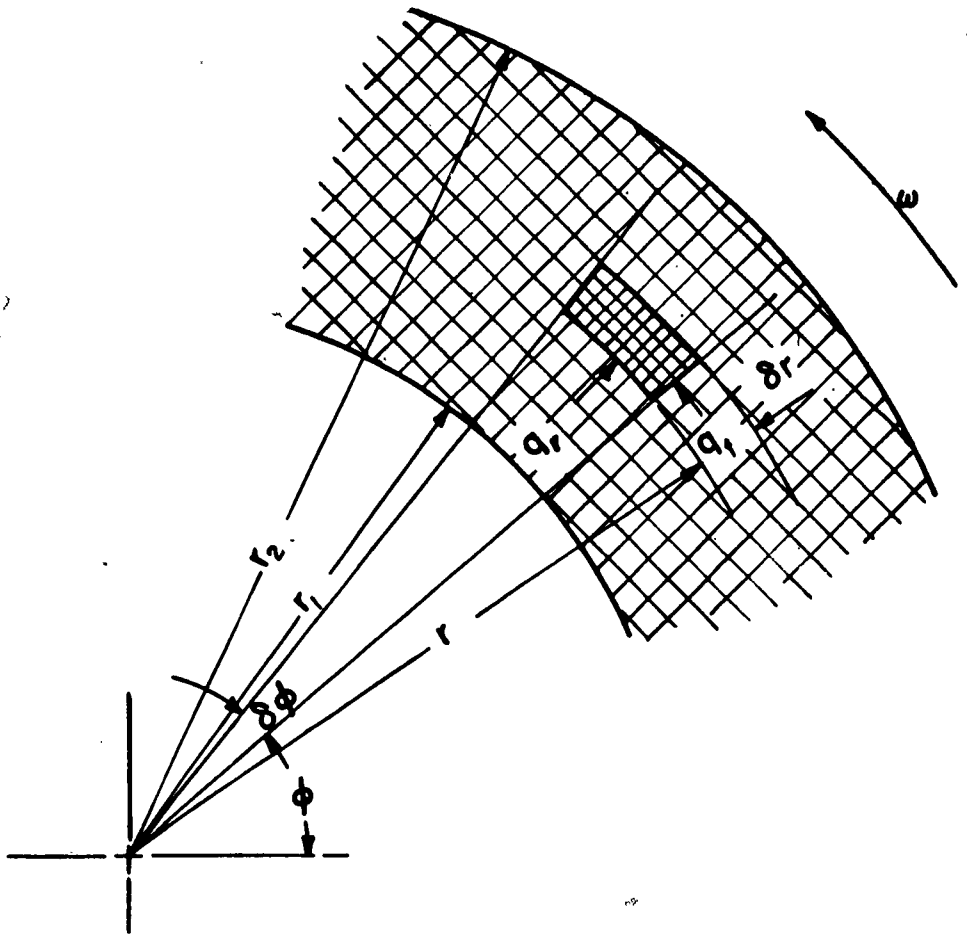

FIG. A-1 NOMENCLATURE FOR THE DRUM TYPE REGENERATOR

A-2.3 Thermal Energy in the Carry-Over

The thermal energy of the fluid carried over per unit time is

$$q_{\phi,2} = \rho \omega r \cdot (\beta \cdot \delta r \cdot 1) \cdot c_p \cdot \theta \qquad (A-3)$$

A-2.4 Balance of the Transported Thermal Energy

Applying the First Law of Thermodynamics to the elemental volume of space and observing that no heat is stored,

$$\frac{\partial q_r}{\partial r} \delta r + \frac{\partial (q_{\phi,1} + q_{\phi,2})}{\partial \phi} \delta \phi = 0 \qquad (A-4)$$

Substituting from Eq. A-1, -2, and -3 into Eq. A-4 and observing that β, ρ, c_p, and $u \cdot r$ are constants,

$$u \rho \beta c_p \frac{\partial \theta}{\partial r} + C''' \omega \frac{\partial t}{\partial \phi} + \rho \beta \omega c_p \frac{\partial \theta}{\partial \phi} = 0 \qquad (A-5)$$

A-2.5 Heat Exchange in the Elemental Volume of Space

The rate of change of the enthalpy of the matrix material is equal to the rate of heat transferred by convection in the same space element. Accordingly,

$$\frac{\partial}{\partial \phi} (C''' \omega r \cdot t \cdot \delta r) \delta \phi = h S''' \cdot (\theta - t) \cdot r \delta r \delta \phi \qquad (A-6)$$

or

$$\frac{\partial t}{\partial \phi} = \frac{h S'''}{C'''} (\theta - t) \qquad (A-7)$$

Eliminating $\partial t / \partial \phi$ from Eq. A-5 and -7,

$$u \rho \beta c_p \frac{\partial \theta}{\partial r} + \rho \beta \omega c_p \frac{\partial \theta}{\partial \phi} = h S''' (t - \theta) \qquad (A-8)$$

It is convenient to employ the rate of fluid flow per unit axial length,

$$m' = u \cdot (K \cdot 2 \pi r \cdot \beta) \qquad (A-9)$$

Then Eq. A-8 may be written,

$$\frac{2\pi K \rho \beta \omega}{m'} \frac{\partial \theta}{\partial \phi} + \frac{1}{r} \frac{\partial \theta}{\partial r} = 2\pi K \cdot \frac{hS'''}{m'c_p} (t - \theta) \qquad \text{(A-10)}$$

Equations A-7 and -10 are the basic differential equations governing the temperature of the solid and the fluid in the drum type matrix.

A-2.6 The Differential Equations in Dimensionless Space Coordinates

New coordinates are introduced:

$$\xi = \frac{hS'''}{m'c_p} \cdot 2\pi K \cdot \frac{r^2 - r_i^2}{2} \qquad \text{(A-11)}$$

and

$$\eta = \frac{hS'''}{C'''} \left(\frac{\phi}{\omega} - \frac{2\pi K \rho \beta}{m'} \cdot \frac{r^2 - r_i^2}{2}\right) \qquad \text{(A-12)}$$

where subscript i refers to the inside radius of the drum. Then considering $t = t(\xi, \eta)$ and $\theta = \theta(\xi, \eta)$, one can reduce Eq. A-7 and -10 to the simple forms obtained in discussing the flat matrix, namely,

$$\frac{\partial t}{\partial \eta} = \theta - t \qquad \text{(A-13)}$$

and

$$\frac{\partial \theta}{\partial \xi} = t - \theta \qquad \text{(A-14)}$$

A-3 Reduced Length and Reduced Period

The reduced length of the drum type matrix is

$$\Lambda = 2\pi K \frac{hS'''}{m'c_p} \frac{r_o^2 - r_1^2}{2} \qquad \text{(A-15)}$$

where r_o is the outer radius of the drum. The reduced period is

$$\Pi = \frac{hS'''}{C'''} \cdot \frac{2\pi K}{\omega} \qquad \text{(A-16)}$$

The boundary conditions expressed in terms of Λ and Π are the same for the drum type regenerator as for the flat matrix. Therefore, the solutions of the problem of the flat regenerator becomes directly applicable to the solution of the problem of the drum type regenerator.

A-4 Interpretation of the Modifications Caused by Curvature

If τ denotes the time that a point in the matrix takes to move an angle ϕ from the instant it enters the fluid, then $\phi = \omega\tau$ and, employing Eq. A-9, the definition of η becomes

$$\eta = \frac{hS'''}{C'''}\left[\tau - \frac{1}{2}\left(\frac{r}{u} - \frac{r_i}{u_i}\right)\right] \qquad \text{(A-17)}$$

where u and u_i are the radial velocities at r and r_i, respectively. It can be shown that $\frac{1}{2}(\frac{r}{u} - \frac{r_i}{u_i})$ is the time required for a particle in the fluid to move radially from r_i to r. Thus it is shown that η defined by Eq. A-12 has the same form as the η for flat matrices defined by Eq. 2-11.

Also, since $2\pi K/\omega$ represents the time that any point in the matrix is exposed to the fluid, the expression for Π in Eq. A-16 has essentially the same meaning as the expression for Π in Eq. 2-19.

Regarding ξ, one may define a mean value of the mass velocity denoted by $m''_{m,r}$ based on the arithmetic mean of the facial areas at radii r_i and r:

$$m' = m''_{m,r} \cdot 2\pi \frac{r + r_i}{2} \cdot K \qquad \text{(A-18)}$$

Then

$$\xi = \frac{h\, S'''}{m''_{m,r}\, c_p}(r - r_i) \qquad \text{(A-19)}$$

Thus, it is shown that ξ defined by Eq. A-11 has essentially the same form as the ξ for flat matrices defined by Eq. 2-10.

In particular,

$$\Lambda = \frac{hS'''}{m''_m c_p} (r_o - r_i) \qquad \text{(A-20)}$$

where m''_m is the mean facial mass velocity based on the areas at r_i and r_o. It follows that to apply the theory of the flat matrix to a drum regenerator, the reduced length must be evaluated on the basis of the mass velocity at the mean radius of the drum.

Appendix B

WORK AND THERMAL EFFICIENCY OF AN ACTUAL REGENERATIVE GAS TURBINE CYCLE

Appendix B: WORK AND THERMAL EFFICIENCY OF AN ACTUAL REGENERATIVE GAS TURBINE CYCLE

B-1 General Remarks

Expressions for evaluating the work and thermal efficiency of an actual regenerative gas turbine cycle are derived in this appendix. It is assumed that the working medium is a thermally perfect gas having constant specific heats. The expressions are developed for a pound of air entering the system at Poing 1 in Fig. 4-1. It is supposed that the compressor efficiency η_c, the turbine efficiency η_t, the regenerator effectiveness η_{Reg}, the pressure ratio $r_p = p_2/p_1$, the leakage fraction $\Delta m/m$, and the summation of the pressure losses (as well as their distribution) $\sum (\Delta p/p)$ are known.

By definition,

$$\sum \frac{\Delta p}{p} = \frac{p_2 - p_3}{p_2} + \frac{p_4 - p_1}{p_1} \tag{B-1}$$

Ratios α_1 and α_2 are defined:

$$\frac{p_4 - p_1}{p_1} = \alpha_1 \sum \frac{\Delta p}{p} \tag{B-2}$$

and

$$\frac{p_2 - p_3}{p_2} = \alpha_2 \sum \frac{\Delta p}{p} \tag{B-3}$$

Hence,

$$\alpha_1 + \alpha_2 = 1 \tag{B-4}$$

B-2 Evaluation of Temperatures T_2, T_4, and T_A

It has been mentioned in the text that Points 2' and 4' represent the ideal end states of isentropic compression and expansion, respectively. Therefore,

$$T_{2'} = T_1 \cdot r_p^{\frac{\kappa - 1}{\kappa}} \tag{B-5}$$

and

$$T_{4'} = T_3 \left(\frac{1}{r_p} \cdot \frac{1 + \alpha_1 \sum \left(\frac{\Delta p}{p}\right)}{1 - \alpha_2 \sum \left(\frac{\Delta p}{p}\right)} \right)^{\frac{\kappa - 1}{\kappa}} \tag{B-6}$$

Temperatures T_2 and T_4 are related to $T_{2'}$ and $T_{4'}$ by the compressor and turbine efficiencies:

$$T_2 = T_1 \left(1 + \frac{r_p^{\frac{\kappa - 1}{\kappa}} - 1}{\eta_c} \right) \tag{B-7}$$

and

$$T_4 = T_3 \left\{ 1 + \eta_t \left[\left(\frac{1}{r_p} \cdot \frac{1 + \alpha_1 \sum \left(\frac{\Delta p}{p}\right)}{1 - \alpha_2 \sum \left(\frac{\Delta p}{p}\right)} \right)^{\frac{\kappa - 1}{\kappa}} - 1 \right] \right\} \tag{B-8}$$

Now, the regenerator's effectiveness by definition is, with reference to Fig. 4-1,

$$\eta_{Reg} \equiv \frac{T_A - T_2}{T_4 - T_2} \tag{B-9}$$

Consequently, the intermediate temperature T_A, that is, the temperature of the cold air leaving the regenerator, may be expressed in terms of T_1 and T_3:

$$T_A = T_1 \left\{ \frac{1 - \eta_{Reg}}{\eta_c} \left(\eta_c + r_p^{\frac{\kappa - 1}{\kappa}} - 1 \right) \right\} + T_3 \cdot \left\{ \eta_{Reg} \left[1 - \eta_t + \eta_t \left(\frac{1}{r_p} \cdot \frac{1 + \alpha_1 \sum \left(\frac{\Delta p}{p}\right)}{1 - \alpha_2 \sum \left(\frac{\Delta p}{p}\right)} \right)^{\frac{\kappa - 1}{\kappa}} \right] \right\} \tag{B-10}$$

Having found T_2, T_4, and T_A in terms of the given quantities, one may now calculate the heat added Q_a to the cycle and the net work W of the cycle, as shown below.

B-3 Evaluation of the Heat Added to the Cycle

The heat input Q_a per pound of air entering the system at Point 1 is the heat required to raise the temperature of $(1 - \frac{\Delta m}{m})$ pound of the air from Point A to Point 3. Hence,

$$Q_a = c_p (1 - \frac{\Delta m}{m})(T_3 - T_A) \tag{B-11}$$

B-4 Net Work of the Cycle

The net work of the cycle per pound of air at Point 1 is the difference between the work done by the turbine, namely,

$$W_t = (1 - \frac{\Delta m}{m})(h_3 - h_4) = (1 - \frac{\Delta m}{m})\, c_p(T_3 - T_4) \tag{B-12}$$

and the work done by the compressor, namely,

$$W_c = h_2 - h_1 = c_p(T_2 - T_1) \tag{B-13}$$

Hence,

$$W = c_p \left[(1 - \frac{\Delta m}{m})(T_3 - T_4) - (T_2 - T_1)\right] \tag{B-14}$$

B-5 Maximum Thermal Efficiency

In general, the thermal efficiency of the cycle is

$$\eta_{th} \equiv \frac{W}{Q_a} \tag{B-15}$$

From the preceding sections of this appendix it is evident that η_{th} depends upon T_1, T_3, η_c, η_t, η_{Reg}, α_1, $\sum (\Delta p/p)$, $\Delta m/m$, and r_p. For any practical values of the first eight quantities, which must be given or calculated, there is a value of the pressure ratio r_p which gives the maximum thermal efficiency $\eta_{th,max}$ (cf. Fig. 1-3). This value may be found by the elementary processes of maximizing η_{th} by means of the

differential calculus. Or, it can be found more simply by plotting η_{th} as a function of r_p.

The maximum work of the cycle per pound of air may be found in similar ways.